Sedimentology and sequence stratigraphy of uplifted Quaternary marine terraces at the southern margin of the Corinth Rift, Greece

By

Sandra Eriksson

Master Thesis in Basin and Reservoir Studies

Department of Earth Science

University of Bergen

November 2018

Abstract

The purpose of this study is to identify the sedimentology and stratigraphic sequence of the uplifted, Quaternary marine terraces in the Corinth Rift, Greece. The area of study is located south of Xylokastro and, as opposed to previous work, this project focused on small-scale mapping and logging, rather than determining the large-scale morphology of the area, resulting in a more detailed map of the area in terms of deposits and their extent. A comparison is then made to conclude whether the method used to map the area still holds strong in comparison to detailed fieldwork.

There is a lot of lateral variation between terraces, sometimes they are depositional and in other areas they may be dominantly erosional, and a total of 13 different terrace levels were mapped, some with sub-levels. It was found that marine terraces remain highly laterally continuous despite large distances unlike their fluvial counterparts. The deposits are the stratigraphically youngest, marine terraces, which were deposited between 0.7-0.45 Ma to present. Six marine terrace facies were observed in the area, of which they are all consisting of beachface facies, with some shoreface deposits present.

Cross-sections were made in order to create trajectories, which were then used when considering sea-level variations and a general vertical succession. With the detail of the study, it has been observed that within terrace levels there are small-scale transgressions present as well as across terrace-levels, suggesting the need to include changes by transgression into the previous interpretation of terraces, which was generated by uplift alone. A correlation between the elevation of the terraces (given by age constraints) and a glacio-eustatic sea-level curve suggest an uplift rate of 1.3 mm/year is more likely than 1.6 mm/year. However, neither provided a perfect fit, therefore the best fit may more likely lie in-between or alternatively the use of a non-linear uplift rate.

Key words: Marine terraces; Quaternary; Sequence stratigraphy; Sedimentology; Uplift.

Acknowledgements

This thesis is the final product of a master's project in Basin and Reservoir Studies at the Department of Earth Science, University of Bergen. I would like to express my appreciation towards the university and its staff for their advice and lectures throughout the degree as well as the funding provided by the university making this project a possibility.

I would like to start by first and foremost expressing my sincerest gratitude to my main supervisor, Martin Muravchik, and my co-supervisors Rob Gawthorpe and Gijs Henstra. They provided me with invaluable guidance through inspirational discussions and critique. I would especially like to thank Martin for taking the time to meet and go through parts of this thesis, giving feedback and helping with the processing of the data as well as aiding in obtaining data.

Additionally, I would like to thank Rob Gawthorpe, Martin Muravchik, Gijs Henstra, Gauti Trygvason Eliassen and Anders Hågenvik for the times out in the field. It was a pleasure sharing ideas, observations and to learn from your knowledge in the field as well as the discussions at the 'five brothers' in the evenings. Anders deserves a special thanks for the collaboration both in the field and in the computer lab 'Grotten'. Furthermore, I would also like to thank the Hotel Segas for being so accommodating and a special thanks to Aris for helping me with my laptop when it almost broke.

Also, Emilie Randeberg deserves a special mention and my gratitude for taking the time to talk to me and help me whenever I struggled.

Last but not least, I would like to thank my supportive group of friends who kept encouraging me despite hardships along the way, especially Cy, Emma and sister Minna who proofread my thesis. My dog Odd also deserves a mention as the hero who got me through this despite breaking my computer and eating my drafts.

Contents

Table of Contents

1. Introduction

1.1. Background and rationale for thesis

The study area is localised in the Gulf of Corinth, south of Xylokastro (figure 1). The area is localised on two ridges, Ridge 1 and Ridge 2. Ridge 1 is localised west of Ridge 2 and also nearer Xylokastro, Ridge 2 is closer to Sykia and further to the east, extending towards Melissi, although never reaching that far. These two ridges should be perfect for studying the lateral variations and the sequence stratigraphy of terraces as there should be no major fault intercepting this area. The maximum elevation studied is at just above 500 m and the lowest studied terrace level is at roughly 50 m above sea-level.

Largely studies in the area have focused on the rifting as it is a perfect example for studying early rifting as well as uplift (e.g. McNeill & Collier, 2004; Bell *et al.*, 2009; Turner *et al.*, 2010; Taylor *et al.*, 2011; Nixon *et al.*, 2016). The syn-rift sedimentation has also been studied greatly (e.g. Ford *et al.*, 2013; Pechlivanidou *et al.*, 2017; Gawthorpe *et al.*, 2017) Thusly, the terraces have only been studied for the purpose of determining uplift rates in the area and therefore the sedimentology was not so much of importance as the presence of corals and dateable fossils. A few studies have been made regarding the sedimentology and lateral continuity of the terraces, however, not in this study area. The only data in this area has been inferred from previous studies performed in other areas in the region (Sébrier, 1977; Dufaure & Zamanis, 1980; Keraudren & Sorel, 1987; Doutsos & Piper, 1990). The overall morphology of the area and the terraces have been inferred from SPOT imagery by Armijo *et al.* (1996) and with a 2 m-resolution Digital Surface Model (DSM) by De Gelder *et al.* (2018), however no fieldwork has been done in the area around the terraces south of Xylokastro. From previous research it is clear the terraces follow parallel to the shoreline.

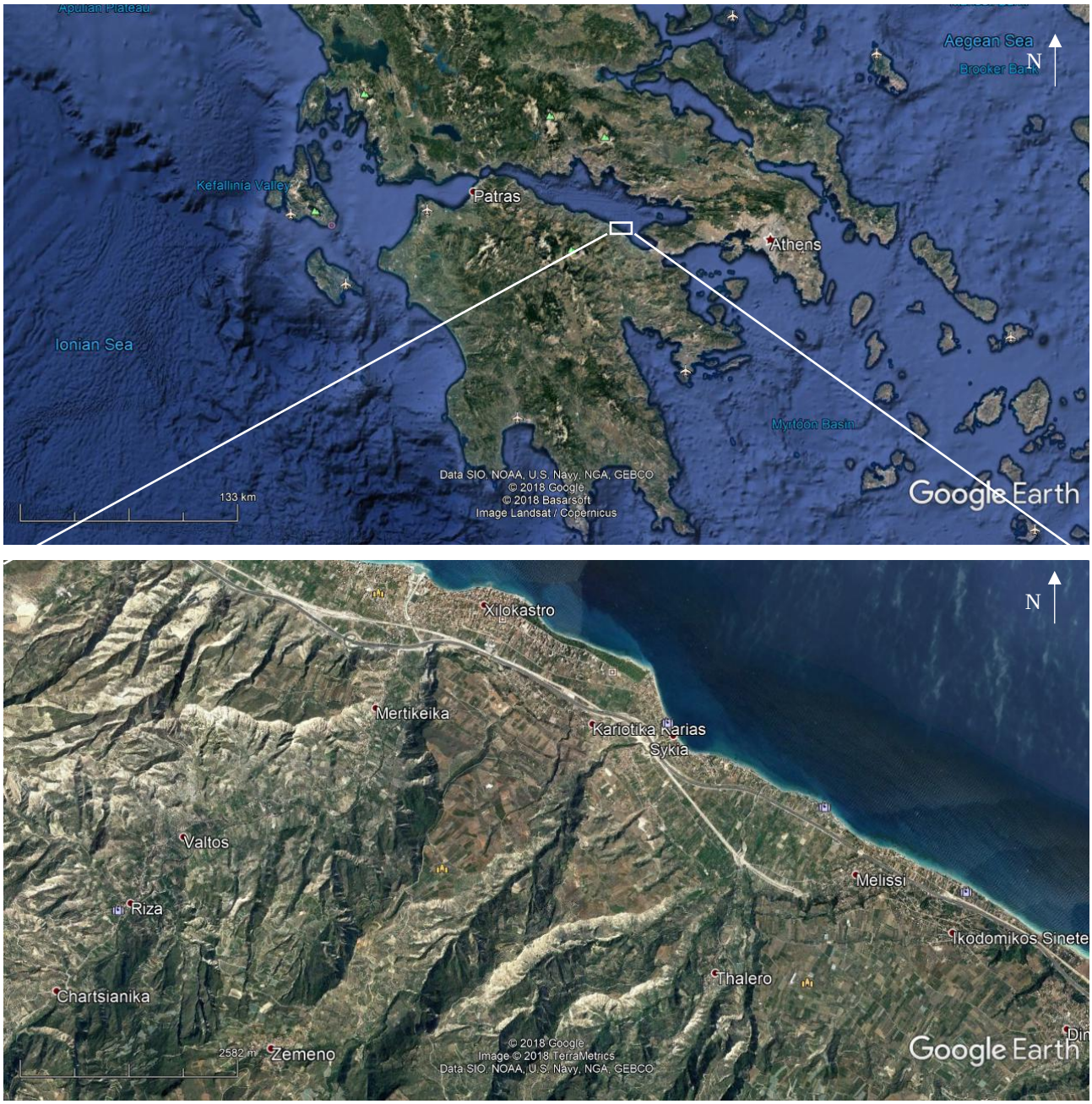

Figure 1. Maps obtained from Google Earth of the area present day, an overview map with a white box, which is zoomed in in the underlying image of the study area.

Apart from bringing in new knowledge and data about the sedimentology of the marine terraces, which will provide an insight to the sequence stratigraphy, this thesis will also compare uplift rates to terraces mapped in order to determine the best fit when assuming a constant rate of uplift. The sedimentological detail and sequence stratigraphy on its own as well as lateral continuity is knowledge which is vital when looking for natural resources and reservoir properties. This can be applied to other known areas which have experienced rifting and uplift in the past.

1.2. Aims and objectives

The purpose of this study is to investigate the sedimentology of the marine terraces in Corinth, as well as the sequence stratigraphy. Analysis of the data gathered in the field will be used to determine whether the previous mapping method done by Armijo *et al.* (1996) is still a valid technique for small-scale mapping and to determine how accurate it is. It should be stressed that Armijo *et al.* (1996) did not focus on the sedimentology of the terraces, only the large-scale geometry and extent of them.

I. Description of facies and facies associations of terrace deposits as well as surfaces found in the area.
II. Map the geometry and extent of the terraces.
III. Generate a shoreline trajectory, by using the maps, logs and cross-sections.
IV. Analyse all gathered data and compare it to that of Armijo *et al.* (1996) and determine whether the method previously used to map terraces still holds or whether detailed field mapping reveals a different geological story.
V. Compare the terrace levels with a sea-level curve to determine uplift rates.

1.3. Outline of thesis

Chapter 1, as seen above, is a brief introduction to the background and purpose of this thesis. It is followed by chapter 2, which presents the geological setting of the Corinth Rift on a regional and a more local scale. The more local scale focuses on the terraces and the uplift, whilst the more regional scale focuses on the rifting. As this thesis focuses on the terraces, chapter 3 will emphasise previous research and the theoretical background of terraces. Chapter 4 presents the methodology used in order to produce this thesis. It presents the different phases of the research and the different programs used in order to produce the maps and models created. This chapter is then followed by chapter 5, in which the results of data acquisition and subsequent analysis is presented. It is subdivided into three main parts: Facies and facies associations, new terraces model, and sequence stratigraphy. The first part uses logs and field observations to present the sedimentology of the terraces and the nature of the surfaces between underlying beds. Maps created from field mapping in ArcMap are used to present the new model of terraces, additionally, this part contains a comparison of my own terrace model to that of Armijo *et al.* (1996). Finally, in this section, the sequence stratigraphy is presented with a general vertical succession, a shoreline trajectory, and a sea-level curve. Chapter 6 discusses the results presented in chapter 5 and argues whether or not the model by Armijo *et al.* (1996) is accurate

on small-scale and large-scale and, additionally, discusses uplift rates. The thesis is concluded by chapter 7, which contains a summary of the thesis and suggestions for further research which could be undertaken.

2. Geological setting

This chapter is subdivided into subsections, starting with 2.1. Tectonic setting, which dominantly focuses on the regional tectonic setting. The second subdivision, 2.2. Syn-rift stratigraphy and sedimentology, briefly presents the phases of sedimentation. Lastly, 2.3. Uplift, a subsection of great relevance to the terrace formations is presented.

2.1. Tectonic setting

The study area is located in the Corinth Rift, which is one of the youngest, most active extensional structures in the Aegean Region, eastern Mediterranean (Nixon *et al.*, 2016). The area is subjected to fault activity and uplift, forming a rather unique combination of structures discussed below. The rift itself forms an asymmetric half-graben and it has a set of prominent uplifted marine terraces onshore. Regionally, the area is connected to a triple junction by the westward propagation of the North Anatolian Fault. The Aegean microplate (Kahle *et al.*, 1998) is part of a triple junction, Karliova occurs where the Arabian, Anatolian and Eurasian plate meet, see figure 2a (Armijo *et al.*, 1999). To the south, there is the Hellenic subduction zone where Anatolia meets the African plate (figure 2b). The Corinth Rift is located in the back-arc region of the Hellenic subduction zone, part of the Hellenic mountain belt, which has an NNW-SSE trend. The pre-rift basement of Corinth is composed of a nappe complex of Mesozoic age (Rohais *et al.*, 2007a; Skourtsos & Kranis, 2009; Taylor *et al.*, 2011; Ford *et al.*, 2013). None of the nappes are exposed in the study area. Rifting in the Corinth was initiated less than 5 Ma (Ori, 1989), however, an exact timing has yet to be established. The rift has a WNW-ESE strike orientation (Jackson *et al.*, 1982) and is extending at a vast rate of 10 to 16 mm/year (Bernard *et al.*, 2006; Briole *et al.*, 2000; Clarke *et al.*, 1998). Normal faulting is the dominant type of deformation and surface rupture in the Gulf of Corinth and generally extends in a north to south orientation (Bell *et al.*, 2008; Jackson *et al.*, 1982; Taylor *et al.*, 2011). The rift is currently more than 100 km in length and less than 30 km wide (Armijo *et al.*, 1996; Bell *et al.*, 2006; Doutsos *et al.*, 2006). Based on syn-sedimentary deposits it is now widely agreed upon that multi-phase rifting occurred in the area (Ford *et al.*, 2013; Ori, 1989).

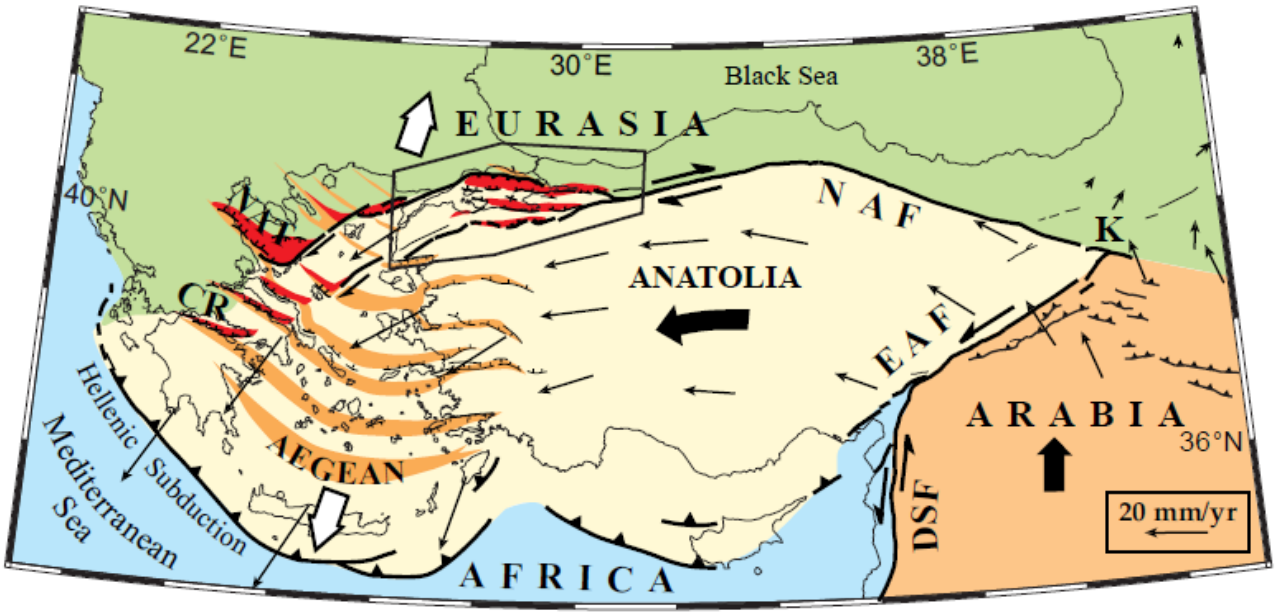

Figure 2a. Structural map showing the interactions of the Anatolian plate with surrounding plates. (Armijo et al., 1999)

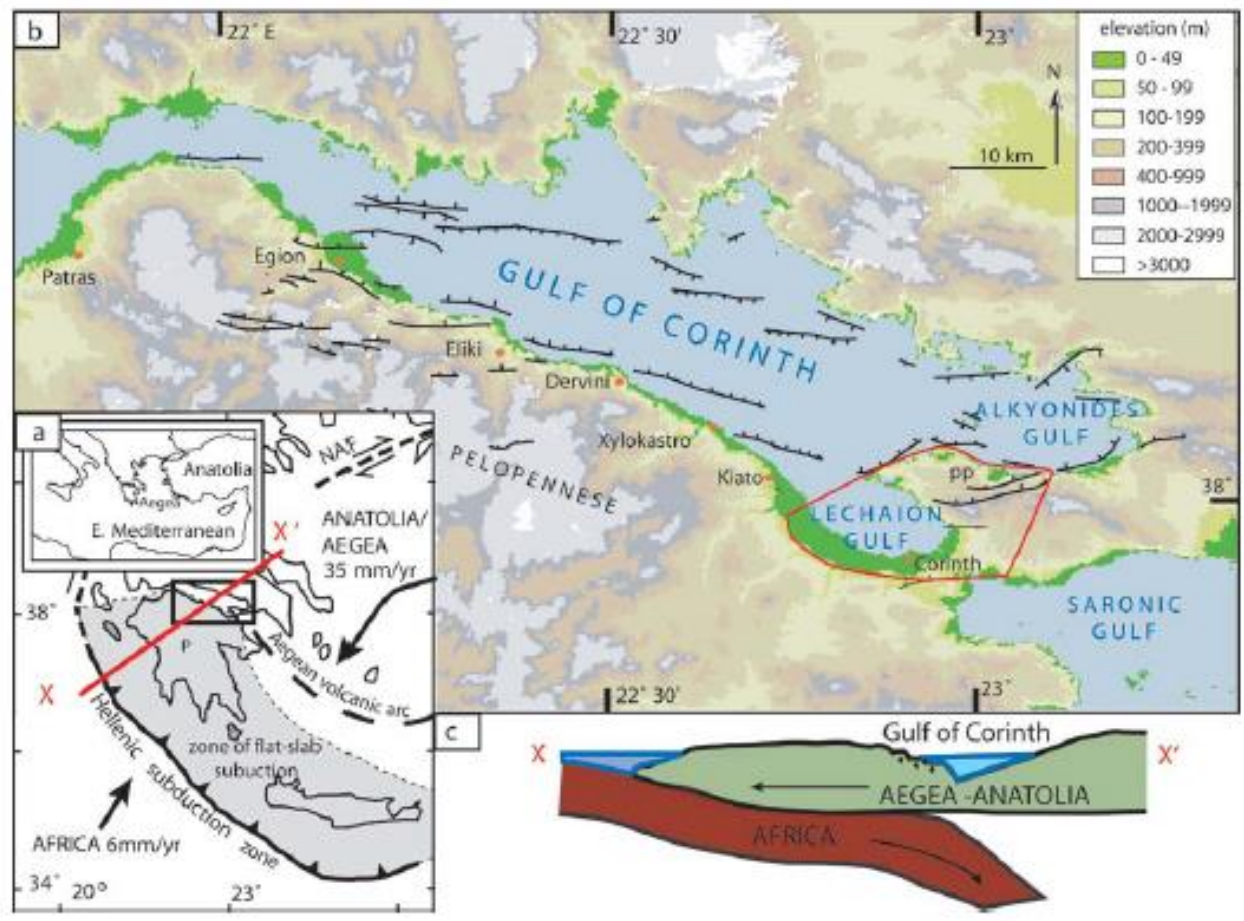

Figure 2b. Structural map zoomed in on the Gulf of Corinth, highlighting faults and a cross-section showing the plate movements (Turner et al., 2010).

2.2. Syn-rift stratigraphy and sedimentation

There have been many studies both onshore and offshore regarding syn-rift deposits in the Corinth rift. This subchapter will focus on the onshore studies as the terraces studied for this thesis are currently onshore. The sediments of the former basin are generally referred to as the Corinth Marls, which are dominantly freshwater lacustrine to brackish facies, of potentially Plio-Pleistocene age (Freyberg, 1973; Sébrier, 1977; Collier, 1990), with interbedded marine marls as well as shoreface sands and conglomerates (Kerauden & Sorel, 1987). It is generally accepted that there are four events in the evolution of the rift sedimentation. The initial stage of rifting is interpreted by fluvio-lacustrine sediments with faults, which were subsiding at slow rates (overall extension rates are less than 1 mm/year) (Ford *et al.*, 2013). This is followed by an increase in extension rate (2 to 2.5 mm/year) and subsidence (fault slip rates 1 to 2 mm/year) and during this time alluvial fans moved forwards into Gilbert-type prograding deltas (Demoulin *et al.*, 2015; Rohais *et al.*, 2007a). The third phase is characterized by a further increase in extension (3.4 to 4.8 mm/year) with further delta progradation and uplift (Ford *et al.*, 2013). Finally, the most recent phase which is dominantly based on uplift as well as increase in extension rates from less than 5 mm/year in the east to 16 mm/year to the western part of the rift (Avallone *et al.*, 2004; Bernard *et al.*, 2006; Nyst & Thatcher, 2004). These different events create syn-rift sediments referred to as the Lower Group, Middle Group and Upper Group (Nixon *et al.*, 2016). Onshore, the lower group has an estimated time of deposition of circa 4-3.6 to 2.5-1.8 Ma (Rohais *et al.*, 2007a), the middle from circa 2.5-1.8 to 0.7-0.45 Ma (Ford *et al.*, 2013; Leeder *et al.*, 2012), and the upper group from 0.7-0.45 Ma to present (Ford *et al.*, 2013; Rohais *et al.*, 2007a). The upper group is the one which is of interest for this study and is dominantly made up of reworked middle group sediments (Rohais *et al.*, 2007b).

The Lower Group is dominated by facies ranging from alluvial fan to shallow-water lacustrine depositional environments (Ori, 1989; Doutsos & Piper, 1990) and can in itself be subdivided into three formations: Exochi Formation, Valimi Formation, and Aiges Formation (Rohais *et al.*, 2007b). Exochi Formation (between 50 to roughly 600 m in thickness) is dominated by alluvial deposits and the most proximal one of the three formations. Valimi (ranging from 50 to 800 m thick) corresponds to fluvio-lacustrine sediments and are overall finer than those of the Exochi Formation. Aiges Formation (10 m to more than 1000 m thick), is the most distal of the three and represents the distal fan delta and turbiditic depositional system (Rohais *et al.*, 2007b). These deposits are overlain by the Middle Group conglomerates, either conformably or unconformably. The Middle Group has been interpreted to have been deposited in large and thick alluvial fans in the south and fining northwards into fine-grained turbidites (Doutsos *et al.*, 1988; Doutsos & Piper, 1990; Poulimenos, 1993; Zelilidis

& Kontopoulos, 1996) and has a thickness ranging from 500 to more than 1000 m, mean thickness being ca. 800 m (Rohais *et al.*, 2007b). Similarly to the Middle Group, the Upper Group either conformably or unconformably superpose the underlying group. Facies of this group range from fluvial to marine environments and they are deposited on perched terraces or alternatively form carbonate reefs (Schrøder, 1975; Keraudren & Sorel, 1987; Pirazzoli *et al.*, 2004; Kershaw *et al.*, 2005). The Upper group is slightly different from the underlying ones as it drapes incised palaeomorphology (incision from 1 m to more than 80 m) and also consists of red palaeosoils (up to 5 m in thickness) and consolidated slope breccias of reworked Middle Group sediments. On a more local scale, the Upper Group corresponds to small terraces representing coastlines of the past and present (Rohais *et al.*, 2007b).

2.3. Uplift

Palaeoshorelines present in the area have been used as reference markers for coastal landmass displacement (Armijo *et al.*, 1996; Turner *et al.*, 2010). Armijo *et al*. (1996) focused on using three levels, which were interpreted as corresponding to Marine Isotope Stage (MIS) 9c, 7e and 5e and tracing them parallel to the shoreline in order to examine the uplift variations. The ages were obtained by dating of corals (Collier, 1990; Collier *et al.*, 1992) and molluscs (Sébrier, 1977). The basinward migration of north-dipping fault systems has created downstepping marine terraces and shoreline features from the current coastline up to an elevation of around 800 m (Armijo *et al*., 1996; McNeill & Collier, 2004). The uplift rate of the Late Pleistocene to Holocene vary from around 0.8 mm/year in the far west to 2.0 mm/year in the centre and circa 0.3 mm/year in the east (see figure 3). Furthest to the east lies the Lechaion Gulf, not considered part of the active rift, however, terraces are present along the Gulf shoreline and this is due to isostatic adjustment rather than fault slip (Turner *et al*., 2010) and this area also shows the lowest uplift rates in the area.

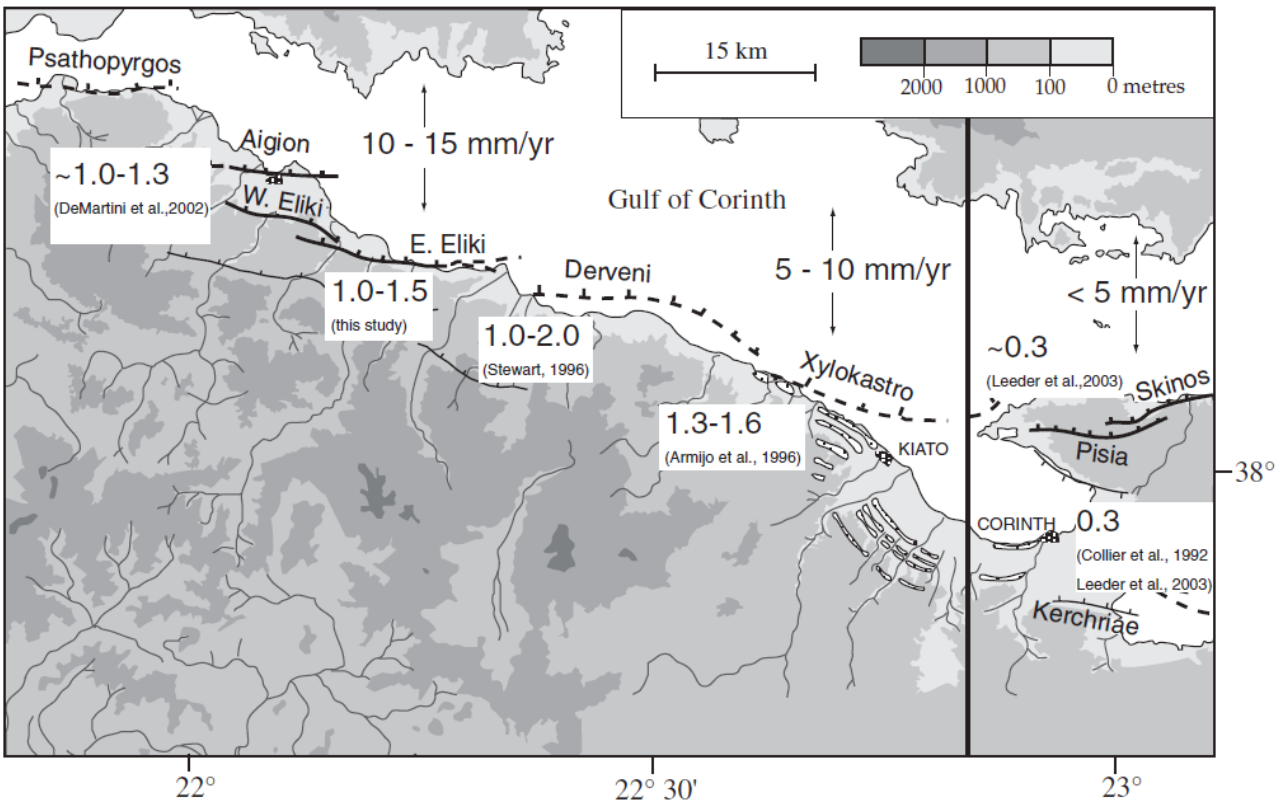

Figure 3. Map of uplift rates and extension rates across the Gulf of Corinth, furthest to the east by Corinth is the minimum uplift of 0.3 mm/year, considered to be unrelated to faulting (McNeill & Collier, 2004).

3. Terrace theory and previous work

In this subchapter, terrace formation, as well as some previous work, will be discussed in order to better understand chapter 5. Firstly, some theory and terminology will be presented, followed by a subsection discussing previous work, introducing amongst others that of Armijo *et al.* (1996), as it is a major paper discussing the terraces studied and will be used for comparison in section 6, the discussion. Some more recent studies will also be included, although most base their terraces of the study by Armijo *et al.* (1996).

3.1. Theory and terminology

Terraces can form in either a lake or marine environment as it is the result of fluctuating eustatic sea level as well as tectonic uplift (e.g. Chappell 1974; Lajoie 1986; Anderson *et al.*, 1999). There are two types of terraces, depositional and erosional (McNeill & Collier, 2004). The depositional terraces form by the growth of coral reefs or by progradation of deltas. The latter is formed when, during a

highstand, a fan-delta may aggrade and prograde basinward depending on the subsidence rate and sediment flux, consequently forming a gently basinward dipping surface. A break in the slope of the sub-aerial delta top occurs between the fluvial topset and the beachface/shoreface. In this case, in the Corinth, the break is likely between 5 to 10 m below sea-level. This is inferred to be close to the terrace outer edge.

The second type of terrace, the predominantly erosional terraces, are formed when there is a low input of sediment, for example between deltas (see figure 4). These terraces are the ones of most interest for the purpose of this thesis. They are formed by wave erosion, which moves the shoreline landward, see figure 5 (Anderson *et al.*, 1999). This created a planar or gently basinward-dipping surface where a thin deposit may be left. The base of the former seacliff/shoreline is represented by the inner edge and is considered an accurate proxy for determining the paleo-water level (McNeill & Collier, 2004). In this paper, the inner edge is referred to as the back-end of the terrace.

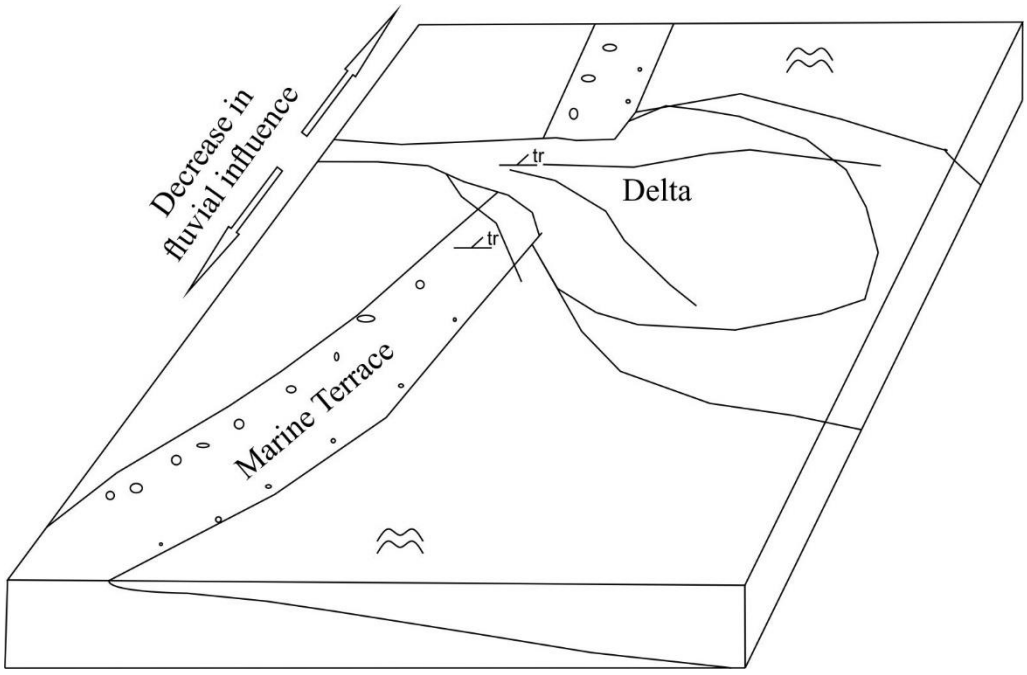

Figure 4. A diagram generated for this study to demonstrate where marine terraces are generated in a setting where deltas are present.

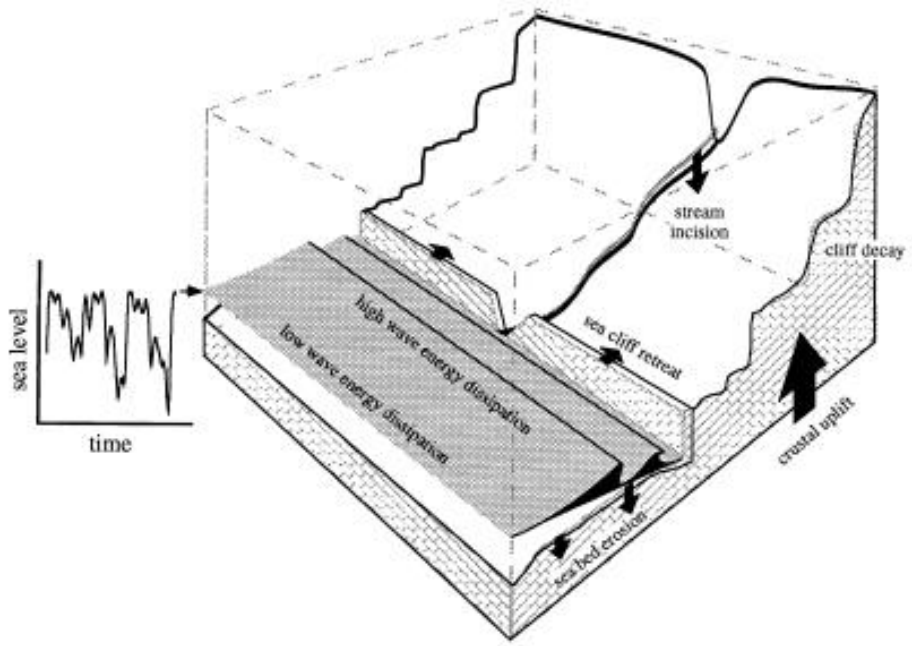

Figure 5. Diagram of terrace formation, the waves cut into the cliff-face and uplift creates a step-like pattern, alternating sea-level on its own can also create terraces (Anderson et al., 1999

3.2. Previous studies

The terraces in the Gulf of Lechaio and Corinth have been studied for over a hundred years (Depéret, 1913), although it is only more recently that they have become of more interest rather than a side-study alongside faulting and uplift. Sébrier (1977) described six terraces south of Corinth and differentiated between them based on the variety of marine fauna and degrees of weathering. The terraces consist of an erosion-resistant 2 to 6 m thick caprock, dominantly well-cemented sandstone and conglomerates (Sébrier, 1977). Detailed sedimentological descriptions of the terrace edges as well as space correlations were made by Dufaure & Zamanis (1980), resulting in the first map of terraces. A schematic map by Keraudren & Sorel (1987), slightly modified the space correlations made by Dufaure & Zamanis (1980). A sedimentological description and surface morphology interpretation was made by Doutsos & Piper (1990), with the conclusion that the terraces are a result of a complex interaction between active normal faulting and sedimentary processes. Six marine transgressive cycles were described in the Corinth Canal as well as *Acropora sp.* coral samples were dated (Collier, 1990; Collier *et al.*, 1992). The dates were interpreted to correlate with interglacial isotope stages 5, 7 and 9 of the marine record and from this, a minimum average uplift of 0.3 mm/year for the Corinth Isthmus was deduced. Furthermore, Armijo *et al.* (1996), used SPOT satellite high resolution panchromatic imagery to extend the terraces previously correlated and mapped. This study

used contour lines (4 m) to follow the terraces and ensure their consistency, the result is presented as a map, see figure 6. However, it did not take into account the sedimentology of the terraces which is the purpose of this paper as some of the terraces are topsets, some truncated foresets and some marine terrace deposits.

Further to the west, the Eliki fault area has been studied (McNeill & Collier, 2004) and terrace dating has been attempted using corals and shells (Stewart, 1996). The conclusion of the study was that an increase in extension rates may have taken place between the late Pleistocene, early Holocene and present time (McNeill & Collier, 2004). Furthermore, the elastic geodetic rates over short time periods may not be comparable to those of cumulative rates over periods of hundreds of thousands of years, especially not when taking into consideration earthquake recurrence intervals (Collier *et al.*, 1998).

Furthest to the southeast, the Lechaion Gulf, where the Corinth Canal is situated, this area is not considered to be part of the active rifting, but still presents terraces due to uplift (Turner *et al.*, 2010). Uplift rates since MIS 7 on the north coast of Lechaion Gulf can be explained by footwall fault displacement, however, the south coast presents evidence of isostatic uplift, where the isostatic uplift rates increase westward in the Corinth Canal where it meets the modern rift, Corinth Gulf (Turner *et al*., 2010).

De Gelder *et al.* (2018) used high-resolution topography in order to create a three-dimensional analysis of the sequence geometry of the marine terraces mapped by Armijo *et al.* (1996). This refined analysis may change the dating of some terraces, previously considered to be part of MIS 11c (Temple II) to be part of MIS 9e, which has previously been debated due to the poor age constraint. Based on their analysis, what Armijo *et al.* (1996) mapped as Laliotis in the area of this study, may be considered Temple II by De Gelder *et al.* (2018).

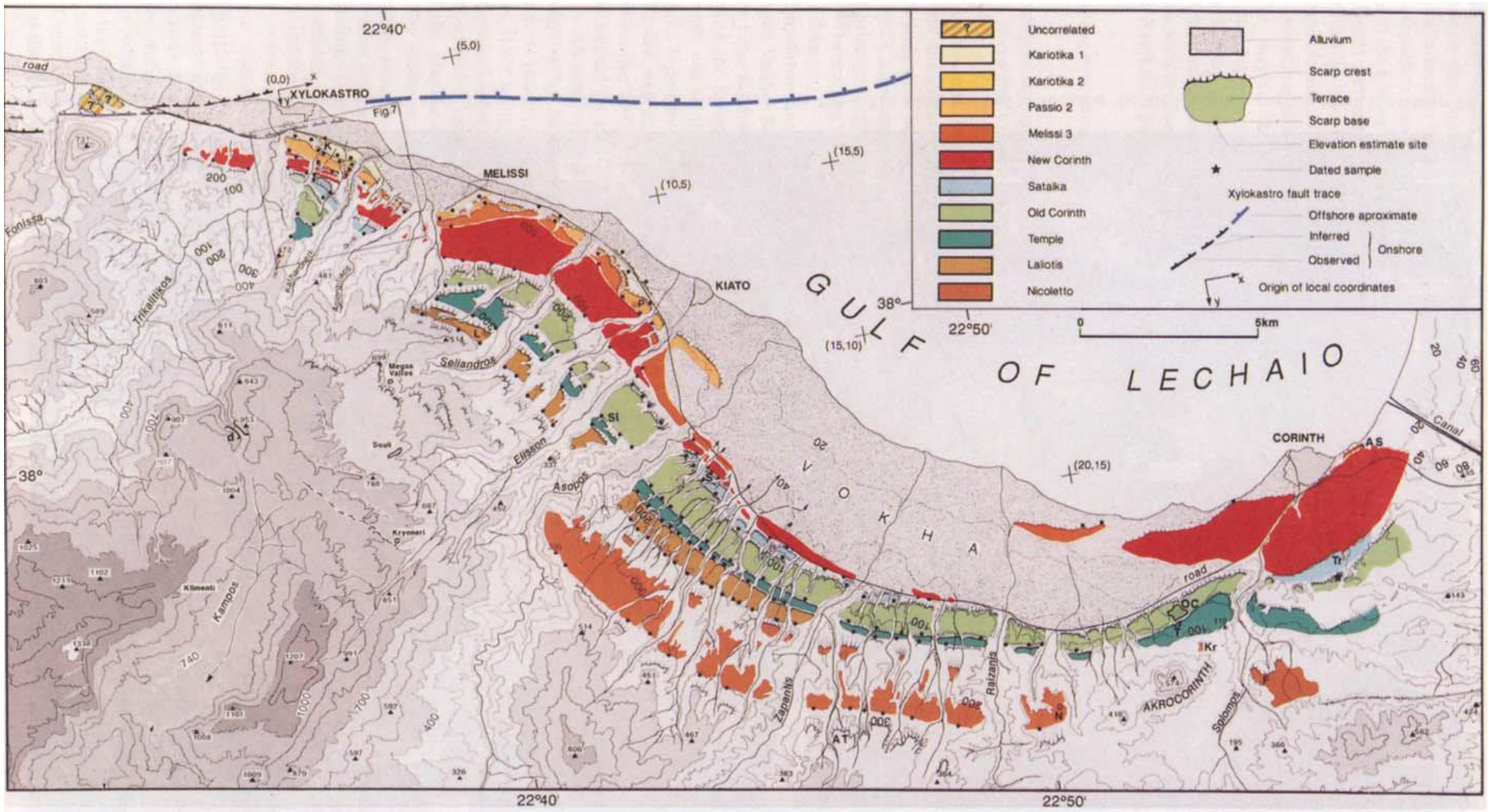

Figure 6. Map of the marine terraces between Xylokastro and Corinth. The oldest terraces are found further inland, away from the coast and the youngest are found alone the coastline. It is based on interpretation of the SPOT images and aerial photographs and different elevations are shown with different shades of grey (darkest shade between 1000-1300 m, medium shade 700-1000 m, and lightest shade 400-700 m) (Armijo et al., 1996).

4. Method

The process for producing this thesis can be divided up into two main categories; fieldwork and data analysis. Fieldwork is necessary in order to gain all the data needed to produce new maps and to test hypotheses. It was split into two field seasons, one in May 2017 (14/05-29/05) and one in October 2017 (04/10-24/10), a total of 36 field days. Some days were cut short due to the weather during the first field season, which was significantly rainier than the second one. A fellow student, Anders Hågenvik, was working on the delta deposits in the area and we worked very closely on all deposits in the area as the mapping and measure-taking often overlapped.

4.1. Pre-field work

Prior to the first field season, multiple maps were made of the area using ArcMap and ArcCatalog (further description of software in section 4.3.3.). The most zoomed in ones were of the scale 1:5000 and these were used for detailed mapping of boundaries and outcrops. Two main sets of maps were made, ones with contour lines and ones with Google Earth Image. Another main set of maps made were four different overview maps at a crude scale of 1:26 000. They all had the same base of a Google Earth map, overlain with either a slope map generated in ArcMap, a contour map, assumed terrace deposits based on initial analysis of generated slope maps, as well as a map with outlined flat surfaces. In the appendix the slope map, contour map, as well as the map draped over Google Earth can be found as there were used during the process of data analysis and in the field. The ones in the Appendix contain the final map version and not the previous ones which were proven to be wrong in terms of terraces boundaries.

4.2. Field work

The purpose of the field work was to gain knowledge and data of the area's geometry and sedimentology. In order to do this logs, bed thicknesses, strike-dip measurements, boundaries, as well as terrace lateral geometries, were thoroughly mapped and notes were taken. Equipment used to obtain the data were a geological hammer, compass-clinometer, GPS, binoculars, tape-measurer, brush, University of Leicester grain size chart, hand-lens, mapping board and a DSLR-camera (Canon 60D). A laser range-finder was borrowed from Dr Martin Muravchik, who also lent a telescope and flew a drone to gather data and images of one of the main ridge faces (Cross-section F). Most of the

areas were accessible by either car or walking, however, some were fenced off or inaccessible due to complications.

The first field season was dominantly used for reconnaissance and to get an overall understanding of the geology of the area as well as the complications present to reach certain outcrops. A few logs were made as well as some mapping. Complications discovered were those of sediment wash-over, steep cliffs, loose blocks and sediment, scorpions, and thorny vegetation.

During the second field season, most of the data collection was done such as strike-dip measurements of deposits (Map in Appendix), multiple logs were made (see Appendix), and traditional mapping of outcrops in order to map the extent of terraces. In order to study steep to vertical cliffs, a telescope was used as well as binoculars and for one ridge (Cross-section F), photos and film were taken with the aid of a drone. This footage was then processed by Dr Martin Muravchik and given back as a file which could be uploaded onto CloudCompare (see section 4.3.2.), where the cliff face could be analysed in a 3-D view and measurements could be taken.

4.3. Computer modelling and data analysis

Before being able to write the final thesis and discuss the data, it all had to be digitalised and then analysed. The modelling is divided up into separate subsections based on method and software used. In order to create the maps in ArcMap, data from digital elevation models (DEM's) were imported as well as coordinate points taken in the field of outcrops and their features. In some cases, the only way to correlate logs and terrace outcrops is based on the altitude and contour lines. The terrace deposits do extend laterally, however individual beds tend to change and vary in thickness so the only way to correlate logs is based on the altitude and the general pattern, which in some terraces is a reverse grading pattern and in others, it is just alternating beds of granules and conglomerates. Logs and measurements were added and suitable profiles were chosen for cross-sections. LiDAR, CloudCompare were used to get features and their geometrical data correctly transferred into the model which was digitalised using CorelDraw.

4.3.1. LiDAR (Light Detection And Radar)

LiDAR which was obtained by Dr. Martin Muravchik and his collaborators for their projects partially covered the area of interest for this thesis, the eastern cliff-face of the Sythas Valley. LiDAR, being a remote sensing tool, is commonly attached to a plane and measures the properties of reflected and scattered light to determine information about a target, in this case, precise surface measurements of

the area to build a three-dimensional model. The exact distance of the target is obtained by measuring the two-way travel time of the laser pulses (Karp & Stotts, 2013). The data from the Sythas Valley was useful for this thesis' purpose in order to get precise geometrical relationships between different surfaces.

4.3.2. Photometry and CloudCompare

As previously mentioned in section 4.2., a drone was used to take footage of the easternmost cliff-face on Ridge 2. Dr. Martin Muravchik created a virtual outcrop model which could be imported and analysed in CloudCompare. The software allowed for dip measurements and bed thicknesses to be taken on the vertical surface which was not possible to do in the field. This was all used to build a cross-section of the section (Cross-section F). Photographs taken with the drone added detail to the relationships between beds later discussed in chapter 5.

4.3.3. ArcGIS

High resolution Pleiades DEM's were imported to ArcCatalog and then to ArcMap where layers of data were added. The Pleiades DEM's quality greatly improved the terrace interpretation where data was lacking from the field by following elevation patterns (De Gelder *et al.*, 2015). Data from the field was added as points based on outcrop coordinates sourced from GPS locations. Polygons were generated from the points and were compared to the terraces interpreted by Armijo *et al.* (1996). Polylines were created where cross-sections for interpretation purposes were most suitable in terms of terrace coverage and quality of data. In ArcMap, however, the polylines can only show elevation based on the DEM's and so in order to get a correct horizontal to vertical scale (1:1), it needs further processing, see section 4.3.4.

4.3.4. Adobe Illustrator and CorelDraw

For the purpose of digitalising logs, CorelDraw was used, the majority were digitalised at a scale of 1:10, except for logs 1 and 21 which were digitalised at a scale of 1:20. CorelDraw was chosen for its versatility and ease of editing. It was also used to create diagrams such as the general vertical succession of the area. Cross-sections were first created in Adobe Illustrator by importing a polyline from ArcMap with the corresponding Digital Elevation Map (DEM) to create a profile with the correct horizontal versus vertical scale. Vertically exaggerated versions of the profiles were created

due to the thinness of the terrace deposits. These were later imported as PDF's into CorelDraw where digitalisation of outcrops and structures were created based on field sketches, photographs and the model created in CloudCompare. It should be noted that the scale of the logs first follows the Udden-Wentworth sedimentary grain-size scale (mud, silt, very fine sand etc.). When reaching granule-sized sediment, the scale is adapted for ease of observing variations in conglomerates after Blair and McPherson (1999) and their classification of coarse sediments.

5. Results

The results have been divided up into subsections, where firstly the facies and facies associations will be presented and interpreted based on field observations. These are partly the basis for the other results, being the new map of terraces (and deltas), which in turn is established from field data acquired and analysis of logs. Thirdly to be presented is the sequence stratigraphy of the area. This will be a combination of data from cross-sections (based on mapping) creating a sea-level trajectory, looking at small sea-level changes within terrace levels and large-scale sea-level changes from one level to another. Note this thesis focuses on the marine terraces, deltaic sediments will briefly be presented in chapter 5.1 in order to be able to distinguish the differences between the topsets and the marine terraces as they can appear similar. A brief description of the foresets is also included as it is present at the base of some logs which are used for the interpretations of the sequence stratigraphy. As this thesis focuses mainly on the terraces and their deposits, the delta deposits are only briefly described in a broader spectrum, for detailed descriptions and analysis please see Hågenvik (2018).

5.1. Facies and Facies Associations

The facies vary a lot in geometry which is why there are two tables, one for deposits and one for surfaces. The surfaces are not facies per se, but they are vital to distinguish marine terraces from other facies associations which can be similar, in this case predominantly the topsets of the deltas. Additionally, included in the surface table is "Lag deposit" for the reason that it can be present beneath other strata than just the marine terraces, also it does not always necessarily leave behind a deposit, sometimes it is just an irregular surface with some (often larger) clasts. The facies association and facies model are comparable to what can be observed in the Corinth Rift at the present day. This is due to the fact that the studied deposits are younger than 450,000 years (Keraudren & Sorel, 1987), given by dating of corals. Considering the Mediterranean was always closed off from the Atlantic,

this explains the lack of tidal influence on the coastline, which has always been wave or river dominated. In the Corinth case, the long straight coasts and lack of sediment supply from any rivers create a wave-dominated coastline. Any large sediment influx will be due to flash floods and heavy rainfall during winter. Additional seasonal changes in sediment deposits are the sand-contents. During summer seasons when the weather is calmer, sand is more likely to be deposited causing matrix-supported conglomerates. Whereas during winter season storms and higher wave action segregate sediments better, creating clast-supported and open-work conglomerates (Horrillo-Caraballo & Reeve, 2010).

The subdivision of facies of units is based upon logs produced in the field and therefore a fairly objective data source. They are described in table 1, where data is divided into two columns; lithology/structure and dimensions/geometry. In the lithology/structure column it is first stated what kind of facie is being described (e.g. sandstone), this is followed by information about grain size if sandstone, then sphericity, roundness and sorting of clasts/grains. After which clasts are described in the same order, then intraclasts if present and matrix. Lastly, structures are described. Whenever clasts are described as ‘a (parallel)’, it means the a-axis (long axis) of the clasts follow parallel to the flow. The column for dimensions/geometry uses geometry definitions based on Tucker (2011) (Figure 7), where small-scale bed units refer to units on metre-scale up to tens of metres. The large-scale geometries refer to sediment bodies on a regional or kilometre scale. The final column states potential processes which could create the described unit and if possible, an interpretation of the depositional environment given the logs and the background knowledge of the area. Table 2 describes and interprets surfaces rather than deposits. Instead of having a description of the beds, there is a description of the relationship between beds and between which beds the surface can be found.

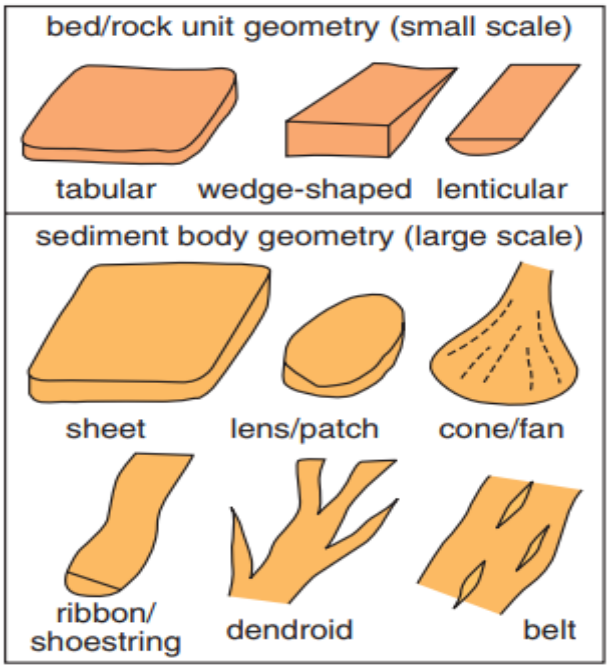

Figure 7. Diagram demonstrating the definition of sedimentary body geometries used to describe features seen in the field (Tucker, 2011).

5.1.1. Facies and surfaces

The area is dominated by multiple types of conglomerates. However, the composition of the conglomerates is mostly the same, although in some locations it varies – lack of intraclasts, or lack of e.g. phyllite. The composition is dominantly quartz, quartzite, chert, phyllite, sandstone, micrite, limestone, marl and older metamorphosed basin rocks of various compositions. Intraclasts are often coarse sandstone or conglomeritic in composition, containing the same or similar clast compositions as the bed. Commonly in a bed, there is one type of intraclast, although in some beds there are up to three different types of intraclasts (sandstone and two different conglomeritic intraclasts, one being a dark intraclast and the other a lighter coloured one containing intraclasts within itself. Dominantly these are intraclasts of conglomeritic underlying units (topsets or foresets of deltas), but occasionally some marl or sandstone clasts. In terms of clast size, intraclasts are often larger than the average clasts in the units. Generally, fine sediments are rare and only found in thin mm to cm laminae in the units of interest for this study. Carbonate cement bands sometimes appear as well as most of the matrix contains little carbonate cement.

Facies Association	Facies Name	Lithology & Structure	Dimensions & Geometry	Sedimentary Processes & Interpretation
Marine terraces	MT.1.1	Conglomerate: low sphericity, sub-rounded, poorly to well sorted, clast supported/openwork. Clasts: max 5 cm, min 0.2 cm, av 0.5 to 0.8 cm Matrix: little to none. Reverse and normal grading, borings in clasts. For image see figure 8A.	Tabular, 8 to 30 cm thick beds.	**Beachface (Swash/Backwash):** Swash/backwash from waves causing grading. Borings indicate a non-fluvial environment. (Hart & Plint, 1995; Jennings & Shulmeister, 2002)
	MT.1.2	Very coarse grained sandstone to small pebbly conglomerate: a(parallel) and a(imbrication), low sphericity, sub-angular to rounded, moderately to well sorted, clast-supported/openwork, occasionally matrix-supported. Matrix: little to no cement. Planar parallel lamination (PPL) and cross-bedding. For image see figure 8B.	Tabular geometry of beds. 0.5 to 10 cm thick.	**Lower Beachface:** Cross-bedding and planar parallel lamination common for beach. (Hart & Plint, 1995; Reading & Collinson, 1996)
	MT.2.1	Conglomerate: clast to matrix supported, rarely openwork (dominantly clast supported)	Tabular, 10 to 70 cm thick beds.	**Plunge-step (Lower Foreshore):** Borings indicate a non-fluvial

		Matrix: Fine to coarse grained, low sphericity, sub-angular to sub-rounded, poorly to moderately sorted. Little cement present. Clasts: max 15 cm, min 0.3 cm, av 1 to 4 cm Intraclast max 25 cm, min 2.5 cm, av 7 cm All clasts: low sphericity, sub-rounded to rounded, poorly to very poorly sorted. Structureless, some bored clasts. For image see figure 8C.		environment. Matrix present could suggest a rather low wave-energy as it is not able to completely segregate the sediments by size. Coarsest clasts can be found deposited at the breaker point between shoreface and foreshore or the upper surf, also where there is almost instant deposition causing the lack of structure or lack of well-developed structure. (Maejima, 1982; Dupré *et al.*, 1980; Kirk, 1980; Short, 1984; Bardaji *et al.*, 1990; Reading & Collinson, 1996)
	MT.2.2	Conglomerate: oblate-shaped clasts, low sphericity, sub-rounded, moderately to well sorted, clast to matrix supported. Clasts: max 2 to 3 cm, min 0.2 to 0.5 cm, av 0.5 to 1 cm Matrix: fine to coarse grained sandstone, low sphericity, sub-angular to sub-rounded, poorly to well sorted, little cement. Inclined bedding, imbricated clasts. For image see figure 8D.	Tabular, sometimes wedge-shaped. 5 to 25 cm thick.	**Upper Foreshore (Berm):** Inclined beds and imbrication indicate berm accretion in the foreshore (Bardaji *et al*., 1990; Hart & Plint; 1995), or transitional Lower beachface as it is possible to create inclined bedding and imbricated clasts in such an environment as well with the aid of breaking waves (Massari & Parea, 1988).

	MT.3	Coarse grained to small pebbly conglomerate: a(parallel) and a(imbrication), low sphericity, sub-rounded to rounded, moderately to well sorted, clast-supported/openwork. Matrix: little to no cement. Symmetrical ripples, wavy bedding. For image see figure 8E.	Tabular, laterally vary in thickness and on 10s of metres scale, occasionally pinch out in a wedge-shaped manner. 1 to 10 cm thick.	**Shoreface:** Oscillation creating symmetrical ripples. Lack of cement due to segregation of grains during wave process. (Hart & Plint, 1995; Reading & Collinson, 1996)
	MT.4	Very fine to fine grained sandstone: high sphericity, sub-rounded, moderately sorted Very few pebbles, max 1 cm clasts, low sphericity, sub-angular to rounded. Symmetrical ripples: wavelength 10 cm, amplitude 0.5 cm, burrows. For image see figure 8F.	Tabular, 2 to 10 cm thick.	**Storm deposit:** Oscillation, not necessarily within fair-weather wave base, due to the finer grained sediments being segregated and moved offshore. (Massari & Parea, 1988; Reading & Collinson, 1996)
Silt-fine sand	SF	Silt to fine grained sand, occasionally gravel. Very varied maturity of grains, silt and sand: mixed sphericity, sub-rounded, well to very well sorted. Gravel is more varied, low sphericity, angular to sub-rounded, moderately sorted. Parallel lamination, wavy lamination. See figure 9A.	Tabular, 1.5 m to possibly up to 20 m where thickest.	Unconsolidated sand and silt fall out of suspension during floods or during still water, where local flow velocities have been reduced (El-Hames & Richards, 1994). Wavy lamination may be due to water escape.

Corals	C	Combination of marl and fine to very fine sandstone, high sphericity, subrounded, moderately to well sorted. Corals either present in colonies or as separate tubes. The individual coral tubes are up to 0.7 cm in diameter, averaging in 0.5 cm. See figure 9B	Tabular, but appears in patches as it is not laterally extensive. 1 to 2 m exposed.	Corals interpreted as *Acropora sp.* (Collier *et al.*, 1993). Good example is log 12. Sandy wavy/silty sediments with burrows as well as corals are good indicators of a transgression. (Collier, 1990)
Delta topset	DT.1	Conglomerate: low sphericity, angular to sub-rounded, poorly sorted, clast to matrix supported. Clasts: max 15 cm, av 1 to 3 cm, min 0.2 cm Intraclasts: max 14 cm (a few 30 to 70 cm found in log 5) Matrix: medium to coarse sand, low sphericity, angular to sub-angular, poorly sorted, little to no cement. Poorly developed internal structure, sometimes inclined or horizontal planar bedding, figure 10A.	30 to 300 cm, tabular on small scale.	Tractional deposition of gravel in braided stream channel (Gobo *et al*., 2015) and the lack of well-developed structures indicate a high flow regime. (Backert *et al.*, 2010)
	DT.2	Sandstone-conglomerate: fine grained to large pebbly conglomerate, low sphericity, sub-angular to sub-rounded, moderately sorted Granules and pebbles: low sphericity, angular to sub-angular, poorly sorted. Inclined lamination in varying orientations. See figure 10B	Tabular to wedge-shaped. 5 to 55 cm thick.	Tractional deposition of sandy longitudinal bars forming the inclined lamination, orientation depending on the orientation of the bar in the river. (Gobo *et al.*, 2015)

	DT.3	Sandstone-conglomerate mix: very fine to gravel sized grains, low sphericity, sub-angular to sub-rounded, moderately to well sorted. Few pebbles: max 3 cm, av 3 mm to 1 cm, little carbonate cement. Trough cross-bedding, wavy bedding, occasionally normal grading. Vertical burrows. For image see figure 10C.	Mix of lenticular and wedge-shaped on small scale. Each bed 2 to 30 cm.	Trough cross-bedding due to wave reworking but also small unidirectional flows from distributary channel outlet. Vertical burrows suggesting a high energy environment and the normal grading indicating change in flow energy, possibly seasonal changes. (Backert *et al.*, 2010; Gobo *et al.*, 2015; Reading & Collinson, 1996)
Delta foreset	DF.1	Sandstone: silt to very coarse grained, low sphericity, sub-angular to sub-rounded, moderately to poorly sorted, carbonate cement, bivalves Pebbles: rounded, < 1 cm, low sphericity. Planar parallel lamination. See figure 10D.	Generally the thinnest bed of clinoforms, 2 to 15 cm, tabular.	Tb (Turbidity flow in Lowe sequence), found between beds of DF.2. High energy planar parallel lamination. (Backert *et al.*, 2010; Lowe, 1982)
	DF.2.1	Conglomerate: low sphericity, sub-rounded, moderately sorted, max 4 cm, min 0.3 cm, av 0.7-2 cm Matrix: same as DF.1 sandstone. Often mix of clast to matrix supported, oblate shaped clasts. Normal grading. For example see figure 10 E	Cone shaped on large scale and tabular on small scale, 10 to 50 cm thick.	High density flow creating grading in conglomerate, could be Ta (Turbidity flow in Lowe sequence, where Ta stands for traction and ‘a’ stands for first bed aka coarsest), non-cohesive. (Lowe, 1982; Gobo *et al.*, 2015)

	DF.2.2	Conglomerate: low sphericity, rounded, poorly sorted, clast-supported Clasts: max 13 cm, min 0.3 cm, av 1cm, oblate shaped, intraclasts present, < 3 cm, shell fragments. Sometimes a(p) for small clasts, no small-scale structures visible, large-scale bedding. See figure 10F for example.	20 to 100 cm thick beds, cone-shaped and tabular geometry.	Structureless suggest bedload transport in high flow regimes. (Backert *et al.*, 2010) The imbrication of clasts could be due to sheet floods. (Rohais *et al.*, 2008)
Delta toe-set	DB.1	Sandstone: silt to coarse grained, high sphericity, sub-angular to sub-rounded, moderately sorting, silt laminae, planar parallel lamination. For image see figure 10G.	Each bed 2 to 10 cm thick and each set of alternating beds is between 0.5 to 1 m. Wedge to tabular shaped.	Silt laminae and planar parallel suggesting the most distal part of the deltas relative to DB.2 and foresets. Deposits of low density flow. (Gobo *et al*., 2014)
	DB.2	Conglomerate: low sphericity, sub-rounded to rounded, poorly sorted, min 0.2 cm, av 0.5 to 1 cm, max 2 cm, Matrix: coarse sand and little cement some faint parallel, very gently inclined lamination, sometimes a(parallel) clasts Clasts from underlying bed of Corinth Marls < 15 cm, low sphericity, sub-angular. Figure 10H.	Up to 50 cm thick beds. Tabular to wedge-shaped.	Debris flow, non-cohesive, sometimes listric shears (the inclined “lamination”). (Gobo *et al*., 2014)

Table 1. Table of all facies logged and described in the area, special emphasize on marine facies.

Surface type	Name	Relationships/Geometry	Processes/Interpretation
Transgressive	Lag	Thin sediments deposited at base of bed. Can also show as irregular surface. Lag max 30 cm thick and not very extensive. Often thinner or barely present. See figure 11A for field example.	Uneven surface of variously sized clasts presenting a lag deposit likely created during a transgressive event. (Johnson & Baldwin, 1996; Tucker, 2011)
Erosive	Scour	Irregular surface between sediments, often hard to distinguish due to coarse sediments. For image see figure 11B.	Erosive event where current is strong enough to erode into underlying sediment. (Johnson & Baldwin, 1996; Tucker, 2011)
Unconformity	U.1	Angular unconformity between Rehti-Dendro Formation and terraces/deltas. Very clear and throughout the area as the Corinth Marls have been faulted and therefore the dip is often steeper or in a different direction than the terraces and deltas. See figure 11C.	Angular unconformity due to the irregular surface and the underlying bed having a distinct dip difference. Likely a distinct time period and erosion of the Corinth Marls before deposition of the terraces/delta deposits. (Armijo *et al.*, 1996; Gawthorpe *et al.*, 2017)
	U.2	Disconformity between topsets and terraces. Beds parallel, but laterally lower beds turn into sigmoidal clinoforms beneath and overlying beds remains finely bedded. See figure 11D.	Transgressive disconformity or ravinement surface occasionally overlain by a lag deposit and this is a result of sea level rise, marking shoreface retreat (Massari and Parea, 1988)

Table 2. Table of surfaces found in the study area.

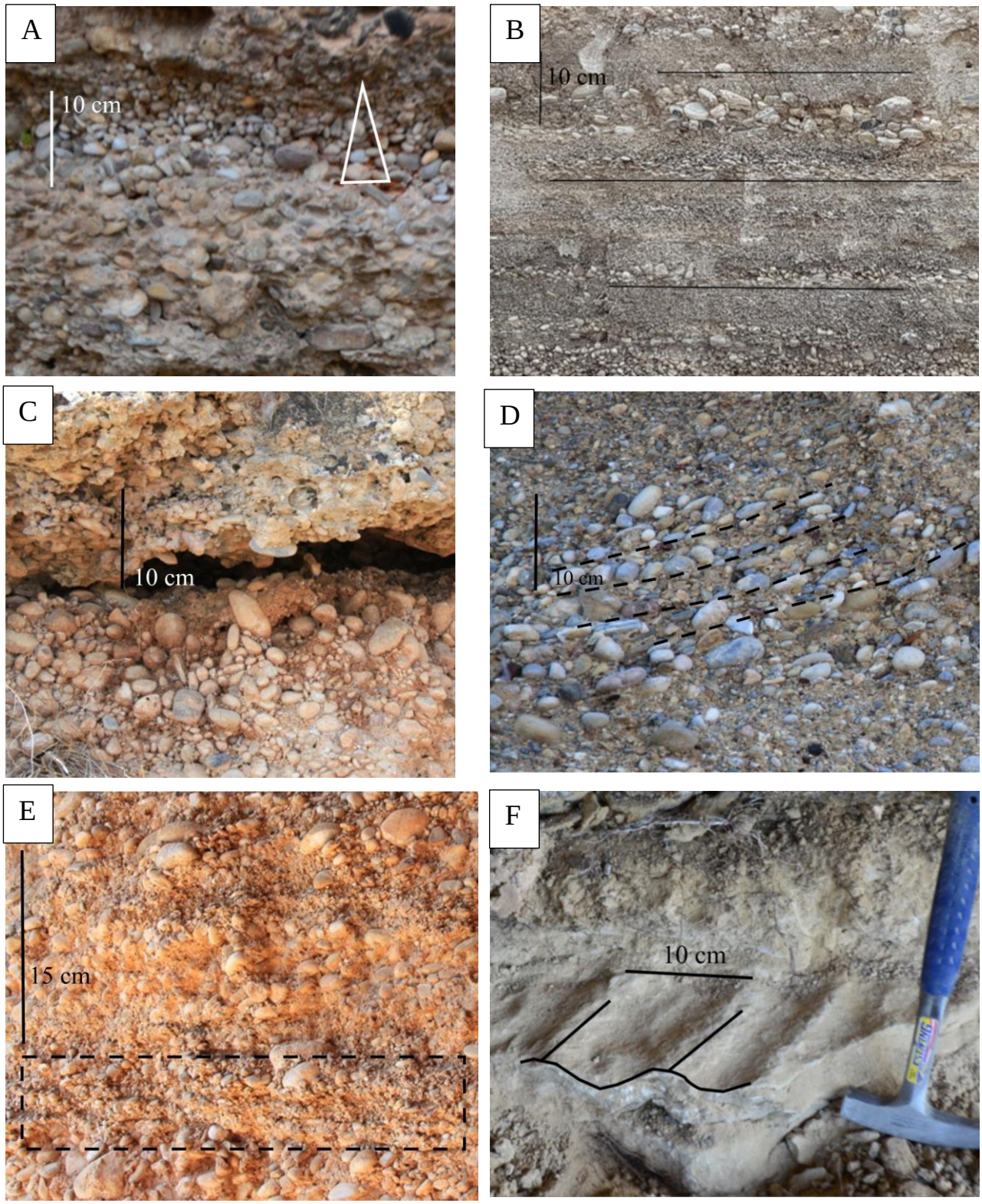

Figure 8. Marine facies: A) MT.1.1, triangle represents normal grading; B) MT.1.2, parallel lines to highlight some of the planar parallel lamination, most left unmarked for reader to be able to distinguish them; C) MT.2.1, generally poor structure and can be considered structureless; D) MT.2.2, inclined bedding and some imbrication of clasts highlighted by dashed lines; E) MT.3, within the dashed box is gravel ripples, can be difficult to distinguish but clear waves are visible; F) MT.4, ripples in sand.

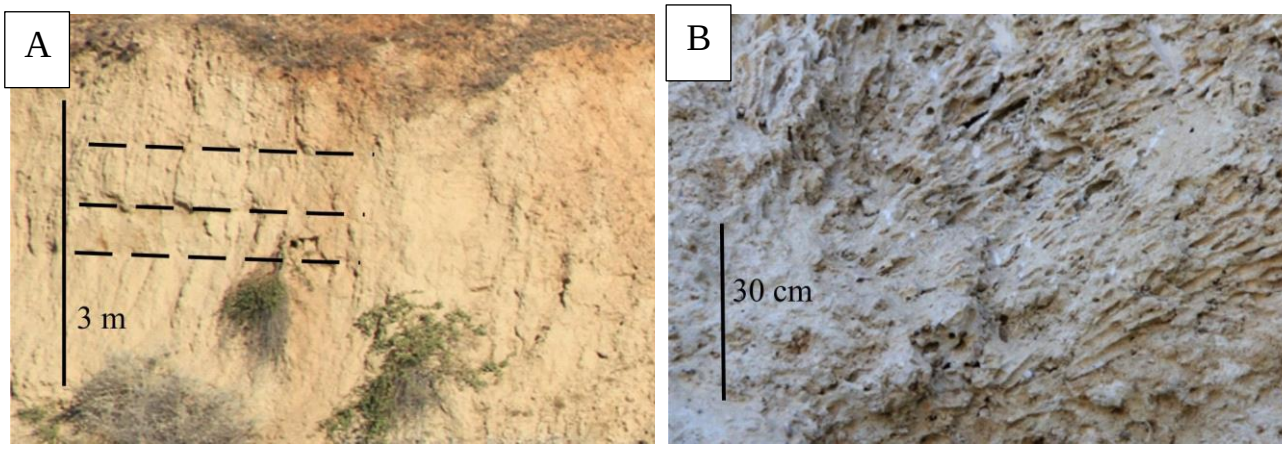

Figure 9. A) Dashed lines highlighting the near-horizontal bedding of the silt-fine grained unit; B) Remnants of a coral colony.

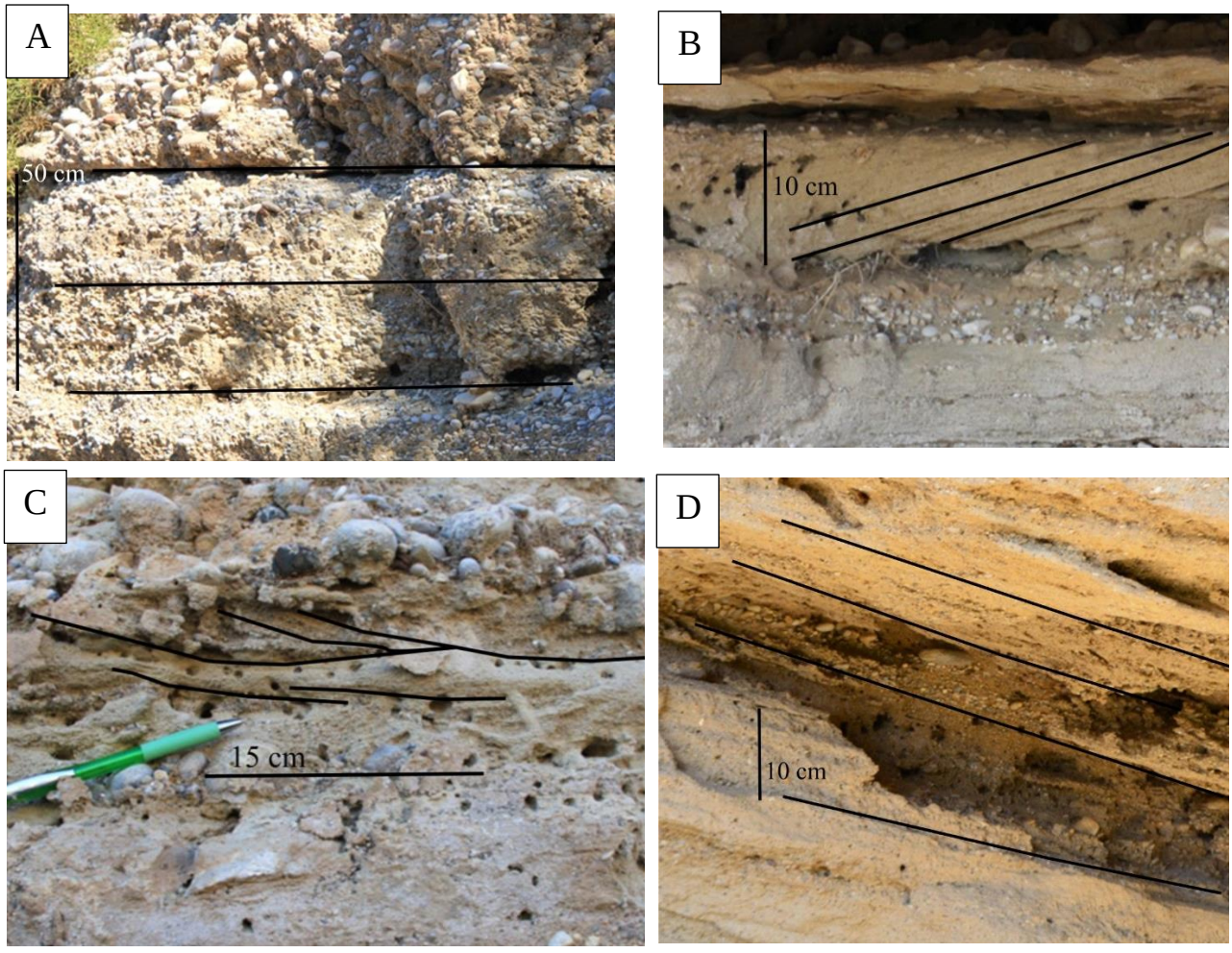

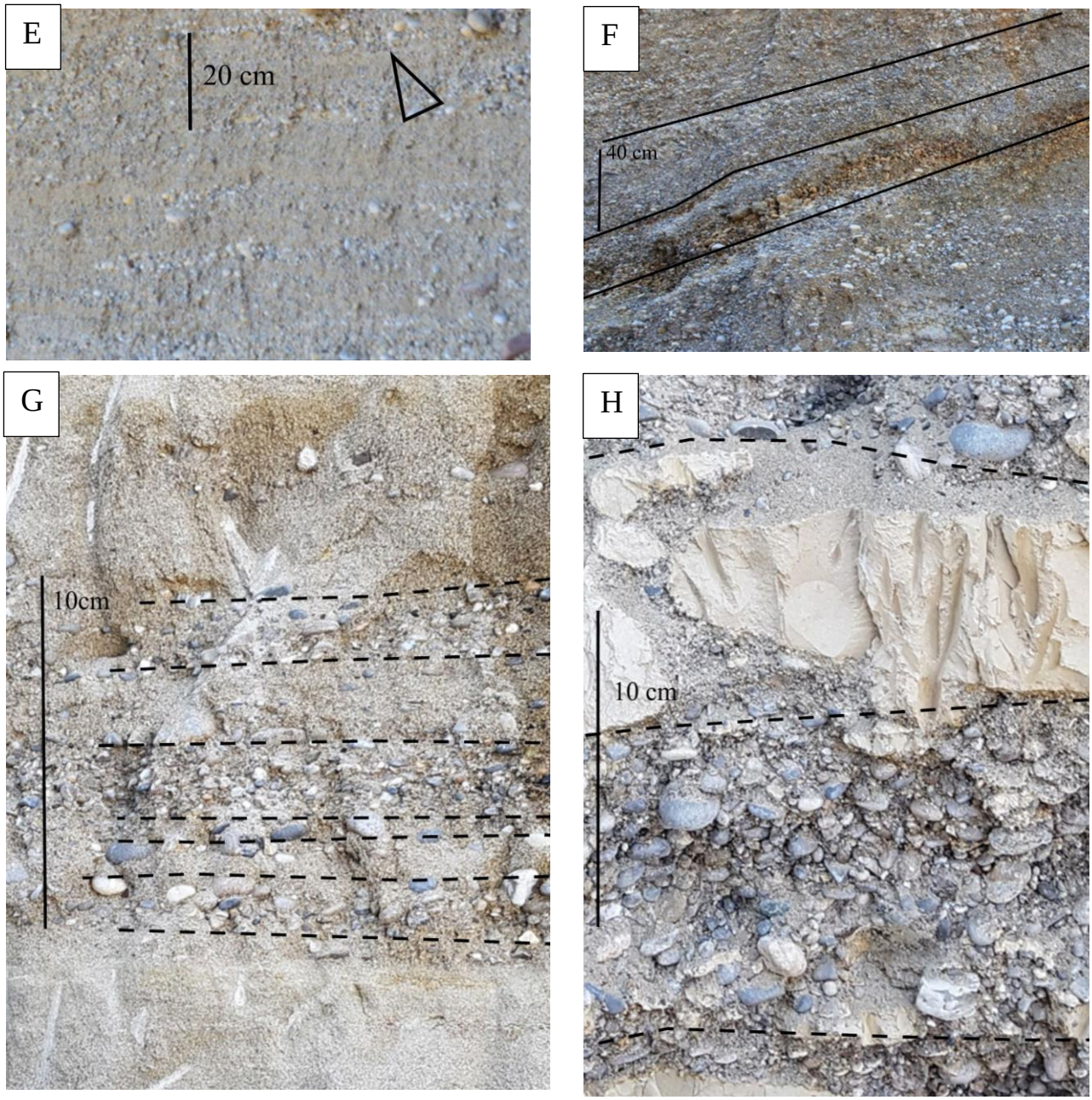

Figure 10. Fluvial facies: A) DT.1, large scale planar bedding shown in black lines, often structureless within; B) DT.2, inclined bedding demonstrated by black lines; C) DT.3, black lines highlighting small troughs which have been burrowed, can also be found in a marine environment if unidirectional flow is present; D) DF.1, planar laminated shown with black lines; E) DF.2.1, normal grading highlighted by a triangle; F) DF.2.2 Large scale beds with no internal structures; G) DB.1, dashed lines highlighting the lamination which is a bit crude due to the poor sorting; H) DB.2, dashed lines highlighting bedding.

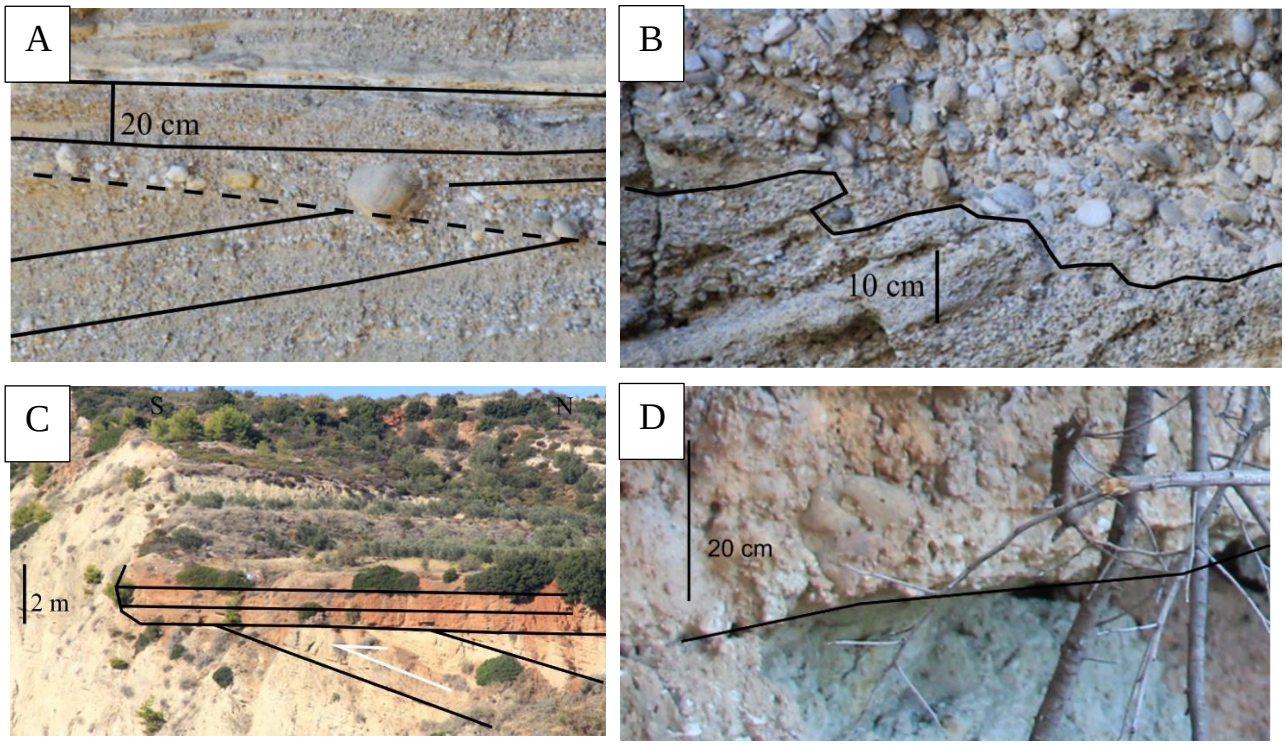

Figure 11. Surfaces: A) Lag shown with dashed lines of large clasts; B) Scour with infill of poorly sorted conglomerate highlighted by a black line following the scour; C) Angular unconformity between Rehti-Dendro Formation and a marine terrace highlighter by black lines; D) Disconformity between a marine terrace and a topset shown with a black line.

5.1.2. Facies Association

This study looks at the deposits above the faulted and distorted Corinth Marls, with a particular focus on the marine terraces. Other facies associations are briefly discussed for the purpose of understanding the overall geology in order to create a sea-level trajectory and a general vertical succession. Composition-wise terrace deposits and topsets are similar, however, generally terraces have better-defined beds as well as better sorting (see facies table for details). When referring to younger and older terraces, older terraces are generally considered T1 to T6, T7 to T13 are considered younger. This definition is mostly based on the quality of outcrops, weathering and how laterally extensive the deposits are.

Marine Terrace (deposits)

Description

The thickness of the deposits vary from 50 cm to 5 m but are frequently around 1 to 3 m thick. The terrace deposits do extend laterally, however individual beds tend to change and vary in thickness as well as pinch out laterally, for example, follow T12 on the map (figure 14). T12 forms a thick clear

terrace in locality of log 2 but pinches out to what appears to be only truncated foresets at the northwesternmost point of ridge 2 (just east across the valley of log 5). The back-end of terraces, best presented in the cross-sections in chapter 5.3, show which terraces have a pinch-out back-end and which have a more concave back-end. Generally, the younger terraces superposing deltas tend to pinch out, and the older terraces tend to have a more concave back-end if the back-end is visible. In some cases, e.g. T1 (log 21), the back-end is not visible as the terrace is the only outcrop still remaining at that elevation.

The marine terrace beds are distinguished by their alternating granule-conglomeratic beds, with a lot of small clast size variations. Also, the clasts are commonly semi-mature and oblate-shaped. In good fresh exposures, it is often possible to see organisation such as imbrication or parallel a-axis in clasts and often the alternating beds change orientation and are of mm to cm in size. Borings are found in clasts in beds (see table x1, MT.2.1) and in the matrix, and burrows are generally found in the sandstone beds. The beds are overall horizontal to near horizontal (< 5 º dip) and the dip direction can vary from northwest to northeast (see map in Appendix with strike/dip data). Facie DT.3, despite being considered a topset facie, does appear on occasion in marine terraces as a marine facie, see log 1.

Interpretation

It is difficult to determine the depth at which the facies were deposited (specifically MT.3 and MT.4), but based on grain size and burrows the relative depth to one another can be interpreted, see figure 13. In coarse-grained beaches, wave action may cause smaller sediments (e.g. sand) to move further offshore, however when the wave energy is very low the different grain sizes may not be as well segregated and matrix supported conglomerates will be more prominent (Emery, 1955; Clifton, 1973; Hart & Plint, 1995). Open framework and clast-supported conglomerates are formed during high energy action. The sorting of clasts is generally better in shoreline deposits than in fluvial deposits, which furthermore indicate that the well-sorted conglomerates are of nearshore marine origin (Zenkovitch, 1967; Hart & Plint, 1995). Cross-bedding found may be a product of the influence of fluvial currents or alternatively, asymmetrical wave motion, rip current, longshore current or tidal currents. Given the presence of deltas it is quite likely to have an impact on the beach structures (Dupré *et al.*, 1980; Massari & Parea, 1988).

Gravel ripples found in facie MT.3 are a typical nearly shore parallel feature, although it can be found in deeper water (Leckie & Walker, 1982; Hart & Plint, 1995). It is always hard to determine whether the sand in the conglomerates was deposited after or at the same time as the clasts. According to Hart & Plint (1995), if there is no sand matrix in the granule-sized to large clast conglomerate then it was

likely deposited later. A combination is also possible where the terrace deposits thin landwards until there is just a truncation or lag left.

Based on the morphology of the terrace beds, the beaches used to be a combination of what Jennings & Shulmeister (2002) referred to as Mixed sand-and-gravel beaches and Composite beaches, with a combination of sand and gravel, where gravel is found higher in the beach face and sand is found in the shoreface or up to lower foreshore, see figure 12. It can be considered a combination due to the high segregation in some beds, however when matrix-supported conglomerates with a relatively high sand content are common, this could potentially be seasonal changes, changing the dynamics of the beaches. In this case, the higher energy and better-segregated beds would occur during winter and the poorly sorted beds occur during the summer periods (Jennings & Shulmeister, 2002; Komar, 2005). To offer an interpretation of the terrace back-ends, pinch-outs represent a gentler sea-level change and a more concave back-end indicate a more abrupt change in sea-level.

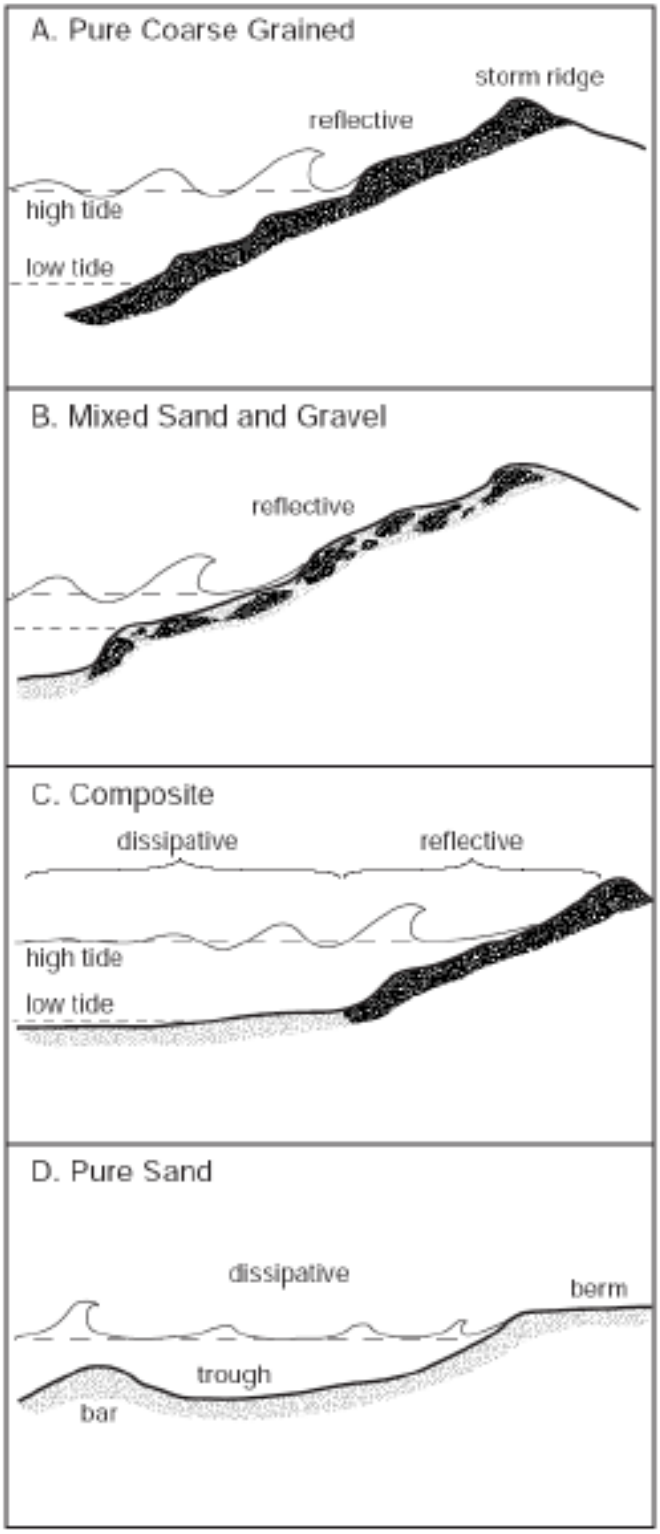

Figure 12. Four different types of beaches described by Jennings & Shulmeister (2002), one of particular interest is type B. Mixed Sand and Gravel.

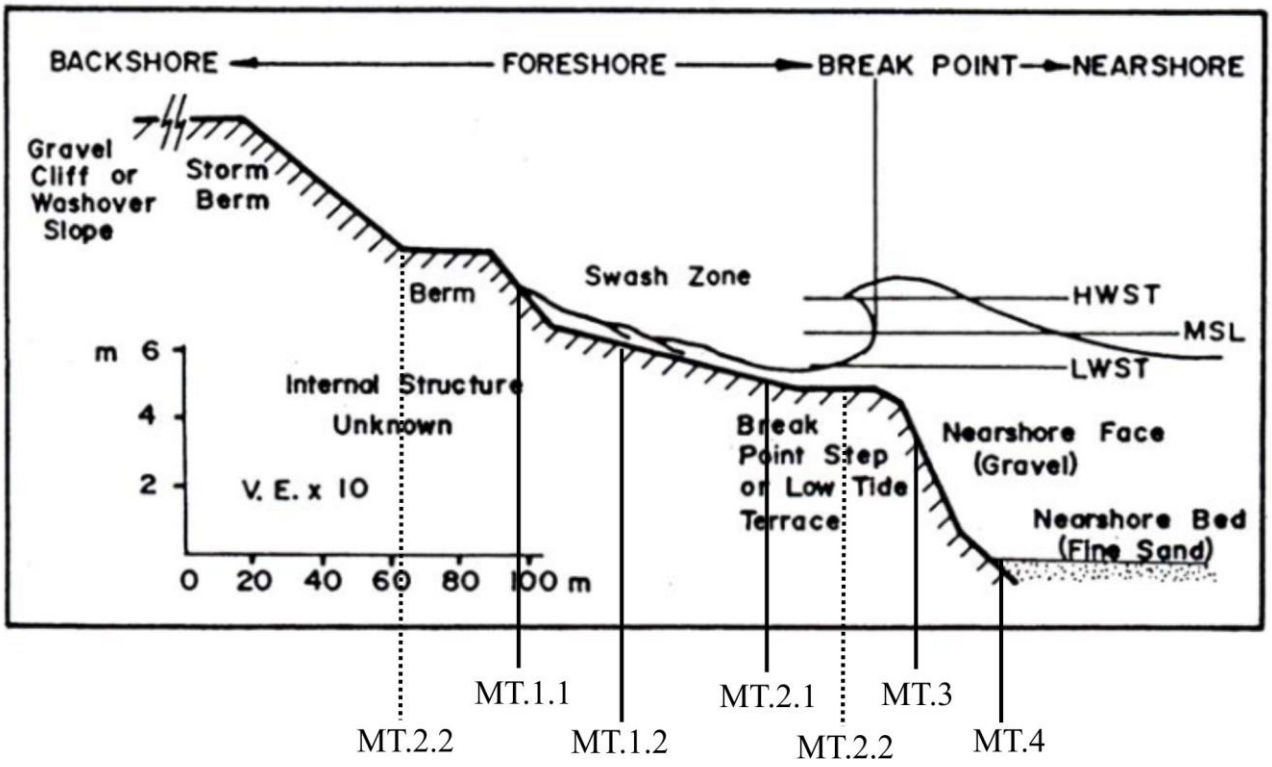

Figure 13. Diagram placing the marine terrace facies relative to one another, note how MT2.2 vary in location depending on which interpretation is used, see Table 1, MT.2.2 (Edited figure by Kirk, 1980).

Silt-fine sand

Description

These deposits are the finest grained deposits in the study area. Dominantly silt to very fine sand, with a few occasional clasts. The deposit may appear tabular where it is at its thickest, but laterally pinches out in lenses and often very localised. Parallel and wavy lamination is frequently present.

Interpretation

The deposits have been interpreted as suspension fall-out due to the nature of the sediment (Backert *et al.*, 2010). Given the present day coastline, it is likely to have been deposited in a more protected environment covered by a cusp. Also, the thickness of the deposit suggests a deeper marine/lake environment.

Corals

Description

A coral colony (figure 9B) is only found in one locality, a few metres from log 12. Otherwise, it is only sediment with individual loose coral tubes. Individual tubes are generally of better quality than the coral colony. The carbonate has mostly been replaced and the remnants were not dateable in either coral colony or tubes.

Interpretation

There is a temporary break in clastic supply or alternatively no clastic supply reaching this area as it is not laterally extensive. The ones found in this particular area were unfortunately not dateable, however, the dating of the corals by Armijo *et al.* (1996) can be used as a correlation since the bed has been inferred to be of the same terrace level. This corresponds to the Middle to Late Pleistocene, interglacial stage 5e (Armijo *et al*., 1996). This would further match up with terraces and corals dated in Cyprus, where corals dated at the same interglacial stage were found (Siddall *et al.*, 2003; Frébourg *et al*., 2012).

Delta Topset

Description

Structures found are highly variable from structureless to trough cross-beddings, occasionally channel bodies are present. These deposits are laterally not very extensive or similar, or in other words, they change in thickness or feature. Log 3 and Log 4 are very typical topsets where trough cross-bedding is not present, but in these cases, the topsets can be traced to clinoforms. Log 12 has a lot of vertical burrows, however, the top metres of the topset have a clear channel feature of roughly 6 m across, potentially larger but hard to determine under the vegetation and angle of exposure. The facies are dominantly conglomerates with a few sandstone beds. There is not much in terms of bioturbation, but 1 cm thick vertical burrows are present in some sandstone beds. Individual beds vary from 0.05 to 1 m in thickness and the overall topsets vary from 1 to 5 m in thickness. The strike of beds is that of the foresets, but with near horizontal dip (< 5 º) and the dip direction range from north to east, northeast being the most prominent dip direction, same as foresets.

Interpretation

Log 12 is interpreted as a topset with marine influence hence the bioturbation. The normal-graded trough cross-bedding (log 12) suggests unidirectional flow and the observed structure could be the result of migration and accretion of bars in a braided distributary channel (Massari and Parea, 1990; Breda *et al.*, 2007). The tabular conglomeritic topsets are interpreted as an indication of interaction of fluvial and wave processes (Leithold & Bourgeois, 1984), generally referred to as the transition zone (Backert *et al.*, 2010).

Delta Foreset

Description

There are two main types of clinothems found in the area: sigmoidal and oblique, of which the latter is the dominant one, especially in larger clinoforms. In this area, sigmoidal clinoforms are commonly

in thinner sets compared to the oblique ones. The exact thickness of the foresets is rarely possible to make out as the base and top are rarely both present, but it is in the 10 to nearly 100 m scale and the individual beds are 10 to 100 cm thick. Fossils found in this unit are large oyster shells, occasionally whole 7 cm shells and other times undistinguishable fragments. Sediments found are generally conglomeratic, with a few thin sandier beds. The sandier beds are either sandstone with pebbles or silt- to sand-stone. The more intact shells are frequently found in the sandstone beds. The conglomerate clinothems are dipping northeast in general, although there is a variety of dip directions from north to east. Dip variations range from 7 to 36 º, average being around 15 to 25 º.

Interpretation

The majority of the foresets are very small. Of the six deltas analysed (see general vertical succession and Hågenvik (2018) for more details), only two are on the 100 m or larger scale. Delta 1, 4, 5 and 6 are all less than 50 m in thickness. Some foresets show alternating sigmoidal and oblique geometries and these likely represent varying stages: sigmoids being deposited when there is more sediment and more accommodation space available (sea-level rise) and oblique (sea-level stand-still or fall) clinoforms when there is progradation, but not as much accommodation space (Helland-Hansen & Martinsen, 1996; Gobo *et al.*, 2015).

Delta Toe-set

Description

The base and the top are not visible and individual beds are 10 to 100 cm thick. Beds are alternating between finer and coarser beds. Toe-set deposits are very rare throughout the area, but where present they were mapped and logged Only one good example of a good toe-set exposure was accessible and describable in the Sythas Valley (see photos figure 10G and 10H). There are no fossils or burrows found in these beds and the dip is nearly horizontal. Slumping and scour features are relatively common.

Interpretation

The toe-sets are partially interpreted as toe-sets due to the large-scale clinoforms they are part of, which can be seen in cross-section A-A', where clinoforms descend into toe-sets. Also, they are finer grained than the overall foresets or topsets and have a more horizontal bedding. Furthermore, the change of flow and the slumping indicate a transitional deposit into toe-set (Postma and Roep, 1985; Leszczyński and Nemec, 2014).

Surfaces

Description

Lag is found throughout the area, either above an angular unconformity, disconformity or even in scours-fills. Scour and fill are a bit trickier to recognise in the coarse sediment, but are clearly present (see picture for example). Generally, they are quite small (less than 10 cm), but sometimes they are large and clearly visible. There is a large angular unconformity between the Rehti-Dendro formation and the deltaic deposits or terraces, as well as angular unconformities between foresets and terrace deposits. Disconformity is rather rare and only found where both topset and marine terrace are present. There are only a few good examples of this, log 6 is one where the sigmoidal clinoforms, topsets and marine terraces are visible, albeit log 6 only show the uppermost of the topset and the marine terrace as the purpose of this thesis is to analyse the marine terraces.

Interpretation

Scour can be a result of various factors, though due to the nature of the beds of interest it is likely to be wave erosion in the terrace case. Reworking of sediment may leave a lag deposit behind followed by a marine or terrace deposit (Bergman & Walker, 1987). The unconformity between the Rehti-Dendro formation and the younger deltaic units and terraces is interpreted as a longer period of break in deposition, uplift and erosion due to the difference in dip angles as a result of faulting (Armijo *et al.*, 1996; Gawthorpe *et al.*, 2017). The disconformity between terraces and topsets is due to shoreface retreat and formation of terraces, which are shoreline parallel, nearly the same strike as the average topset. Depending on the delta the strike is different but whenever both are present it is nearly impossible to distinguish the difference without the clear lag surface or topsets turning sigmoidal (Massari and Parea, 1988).

5.2. Geometry of marine terraces

This subchapter presents the final map of revised terraces in the area. The differences from that of Armijo *et al.* (1996) will be discussed in section 6. Given my subdivision of terraces is slightly different, they have been given simplified names and their equivalent according to Armijo *et al.* (1996) can be found in table 3. The area is mainly divided into two ridges, Ridge 1 being the northern-western ridge covered by cross-sections A-A', B-B' and C-C'. Ridge 2 is further east and covered by cross-sections D-D', E-E' and F-F'.

5.2.1. Extension of marine terraces

The purpose of this subchapter is to present the revised model of the area, the differences from the previous model will be discussed in section 6. Some ‘flat’ areas which have previously been considered terrace deposits have shown to be either truncated foresets or topsets after fieldwork in the area. Also presented in this subchapter is a table which explains which Armijo *et al.* (1996) terrace is referred to when using the system used to subdivide them for the purpose of this thesis. Furthermore, composition and division of marine terraces will be presented as they have slightly different compositions and structures.

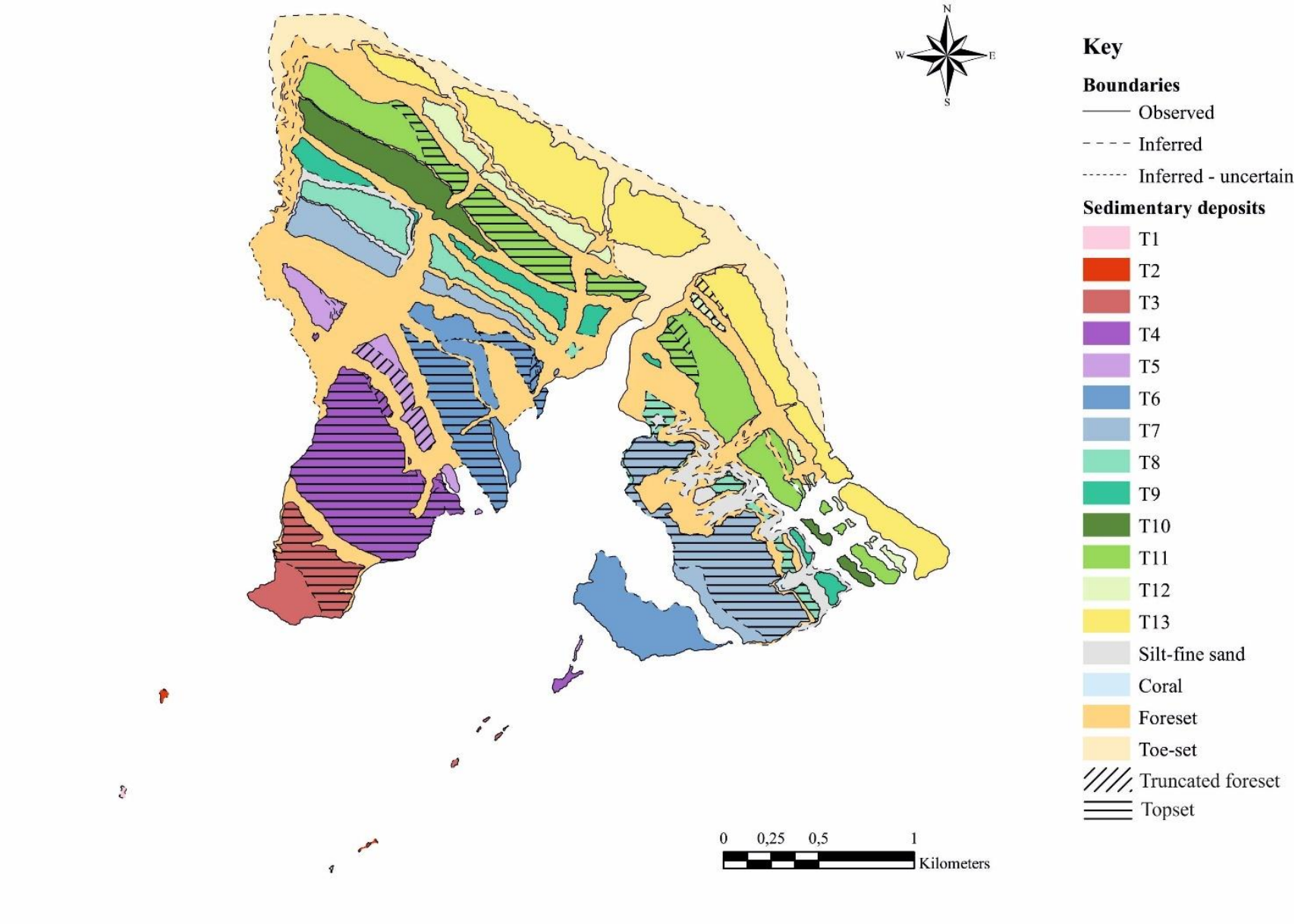

Figure 14. Generated map with key from field data. The Rehti-Dendro Formation has not been marked out, but essentially covers the background area not highlighted in colour.

Terrace name used in this paper	Equivalent terrace used by Armijo *et al.*
T1	Nicoletto*
T2	Laliotis
T3	Temple
T4	Old Corinth
T5	Old Corinth
T6	Sataika
T7	New Corinth
T8	New Corinth
T9	Melissi 5
T10	Passio 2
T11	Passio 2
T12	Kariotika 2
T13	Kariotika 1

Table 3. Table of terraces mapped for the purpose of this paper in comparison with equivalent terrace names used by Armijo et al. (1996).

**T1 has been referred to as the Nicoletto terrace even though Armijo did not map terraces that far inland in this particular area. But as Nicoletto is the following terrace in the succession nearer the Corinth Canal, it may be inferred to extend as far as to this area mapped.*

5.2.2. Terrace composition and features

Not all terraces have individual logs due to poor outcrop quality or inaccessibility, however they were defined as terrace deposits either with the aid of telescopes or based on description and geometry of the bed as well as a lack of evidence indicating the presence of deltaic beds (T1 to T12 on Ridge 1 and T1 to T7 on Ridge 2). Attempts for logs were always made, however, in some cases, the outcrop was simply too weathered to make out good structures. All 21 logs can be found in the Appendix. Laterally, some terraces are grouped together despite having a slight elevation difference (generally no more than 6 m elevation difference), e.g. T11 at location of log 6 on Ridge 2. Additionally, on the map, when highlighting truncated foresets, it refers to a relatively horizontal surface with a truncation of foresets rather than a slope. This could potentially be a period where terrace deposits could have occurred but were not preserved or occurred elsewhere.

T1: Only small raised outcrops remain of T1 (see log 21). Intraclasts found are dominantly sandy or marly. The outcrop of T1 on ridge 1 is more of a grass-covered mound, with a few small exposures of terrace deposits.

T2: Very small and poor outcrops, on Ridge 2 there is T2a and T2b, of which T2a is a clear outcrop *in situ*, where the log 21 was made, it also lines up perfectly with T2 on Ridge 1. T2b is composed of large loose terrace blocks which may or may not be *in situ*, but show distinct terrace features such as similar to those of log 2 and log 16. Overall, T2b demonstrate a more typical terrace deposit and has been grouped as T2 due to the overall slopey-ness of the whole older section.

T3: T3 is also divided up into a and b, similarly to T2. On Ridge 1, T3b is only present as one consistent deposit, superposing a delta (cross-section A & C later presented), however, laterally on Ridge 2, T3a and T3b are both present. The topmost subsection could potentially be what is referred to as Temple 2 by De Gelder *et al.* (2018). However, due to the two outcrops being either above or below the elevation of T3 on Ridge 1, they were grouped together as one terrace. On Ridge 2, the lower part of the terrace has two subdivisions, which are at level with the delta and represent a period of erosion into Rehti-Dendro Formation, followed by sea-level rise causing erosion of the existing terrace (see figure 15 zoomed photo from the terraces from Ridge 2, cross-section E).

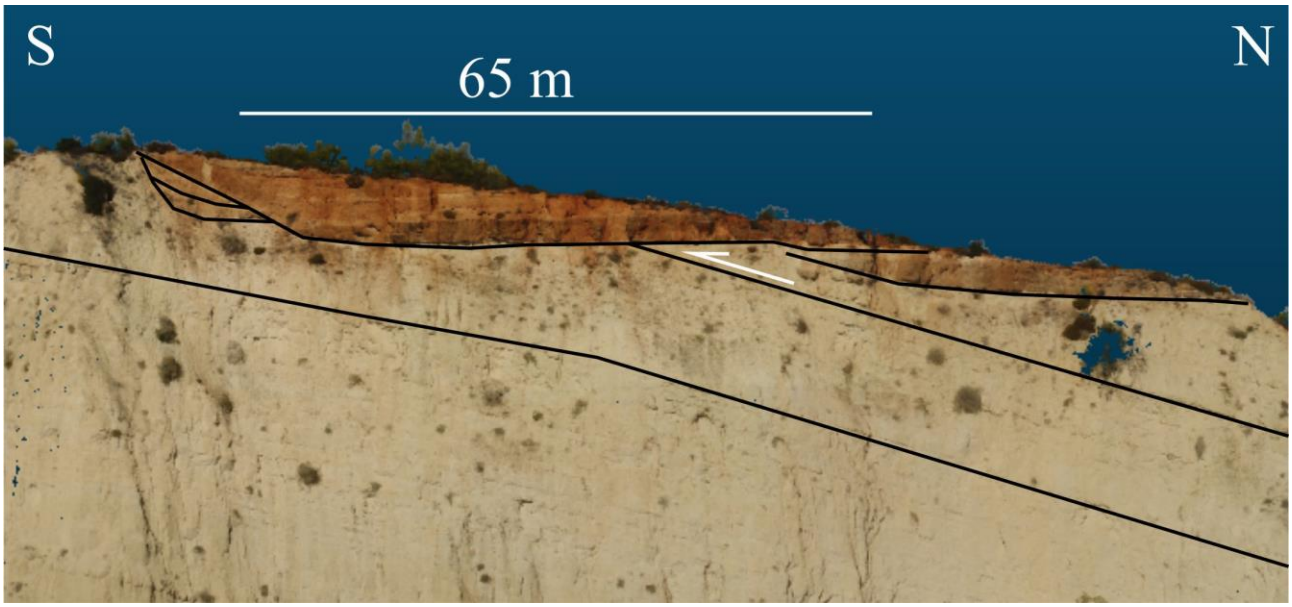

Figure 15. Image from CloudCompare of T3b, where the older underlying part of the terrace has been eroded away and replaced further landward by a newer terrace.

T4: This terrace has a lot of lateral variations due to delta build-out on Ridge 1. Terrace exposures are thin and small on Ridge 1 (log 19 and 20) as it is dominated by topsets, whilst on Ridge 2 they are slightly wider.

T5: Slightly below T4 is T5 (log 18), which is not always present as a terrace deposit, but sometimes just a flat surface of truncated foresets. T5 is also a more sloped terrace than say T3 or T4.

T6: It forms a clear and extensive terrace deposit on Ridge 2, however, on Ridge 1 it is very 'slopey' and lacks good outcrop exposure besides the locality where log 17 was generated. It does not extend all the way to Sythas, however, as seen on cross-section A, there is a break in the foresets where T6 is to be expected and resedimentation of a foreset is present. This terrace could potentially be sub-divided into two after how De Gelder *et al.* (2018), who divided it up so that the lower one is Sataika 1 and the upper part is Sataika 2. Nevertheless, due to the overall sloping nature of the whole bed, it was decided that it would remain as one bed instead of two as there is no clear step.

T7: The lateral thickness of T7 varies a lot and is not always present at all, though at log 16, it is one of the best terrace exposures in the area. The lack of T7 on Ridge 2 may be due to delta build-out, only a small lag at the back-end of the topsets is marked as marine terrace T7 on Ridge 2.

T8: Similarly to T7, a small exposure of T8 can be located on Ridge 2, traced as T8 with contour lines. A better outcrop of T8 was logged on Ridge 1 (log 14), log 15 is also from this terrace, although not the best outcrop.

T9: This is one of the more interesting terrace deposits as it has a lot of lateral variation depending on the presence of deltas. The thickest marine deposit found and logged is log 9, however, log 10 and 11 allow for a good idea of lateral variety. Log 10 is based on a small heavily weathered outcrop, but overall they all have similar patterns. Both log 9 and 11 start with a shoreface facie which gradually shallows upwards until beachface, and locality of log 10 remain somewhat in the middle of transition between these two logs.

T10: T10 and T11 were previously grouped together but given the clear distinction found between them on Ridge 2 and a clear small drop between them found on Ridge 1 they have been split into two separate terraces, although the change was likely minor. Laterally T10 is very broken up and only

present at the easternmost and westernmost side and anything in between is topset or an extended T11.

T11: Subdivided into two smaller terraces on Ridge 2, with minor elevation differences of max 6 m difference, often less than 3 m. Likely a smaller sea level fall which is more prominent on ridge 2 than Ridge 1 due to the underlying material being softer to erode than the delta-build out found on Ridge 1, giving a more step-like formation on Ridge 2, whereas it is more 'slopey' on Ridge 1. T11 is also, just like T10, not laterally extensive throughout the area as there is a topset building out on the eastern flank of Ridge 1, extending slightly onto Ridge 2. See log 6 for an example of terrace superposing a small topset and delta.

T12: Subdivided into two smaller terraces on ridge 2, with minor elevation differences of max 6 m, often less than 3 m. This is likely due to a smaller sea level fall. Log 2 is one of the best terrace exposures, as well as a very thick and well-preserved terrace (see figure 16). As seen in the figure there is what can be interpreted as a small rise in sea-level, given that MT.3 becomes the dominant facies with its ripples. Each terrace is different as some coarsen upwards and some fine upwards. Other logs were made on Ridge 2, log 7 and 8. Occasionally, a terrace deposit is not present but can be laterally inferred over a flat surface where truncated foresets are exposed, see westernmost side of Ridge 2 on map. Log 7 and 8 are very similar to the lower part of log 2, potentially the upper part of log 2 was not preserved in localities of log 7 and 8.

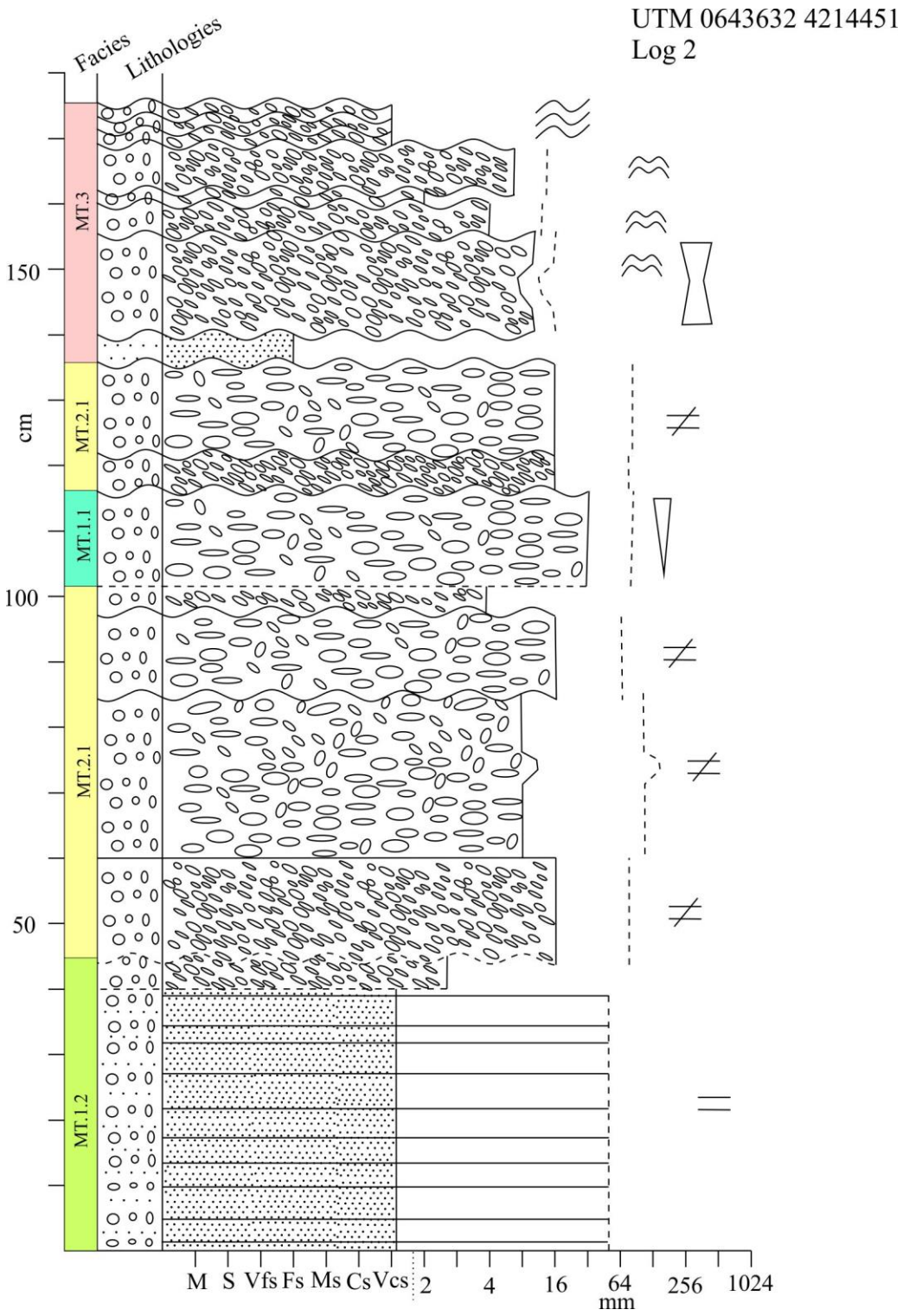

Figure 16. Typical marine terrace log with many alternating (often thin) beds with varying structures.

T13: Youngest terrace mapped in the area and also most laterally extensive, without breaks of topsets or foresets. Log 1 was made where the best exposure was present and as previously mentioned this is one case where DT.3 is considered a marine facie with deltaic influence, likely a small distributary channel influencing the shoreline (see figure 4 and 10C, as well as Appendix for log).

5.2.3. Cross-sections

A total of six cross-sections were made, three on Ridge 1 (A-A', B-B' and C-C') and three on Ridge 2 (D-D', E-E' and F-F'). The B and E cross-sections are of the older terraces without delta build-outs and the A, C, D and F cross-sections are of either side of both ridges. It was easier to split it into 6 to get better details as the terrace deposits are thin. This is why each cross-section has an additional cross-section with a vertical exaggeration of 3x.

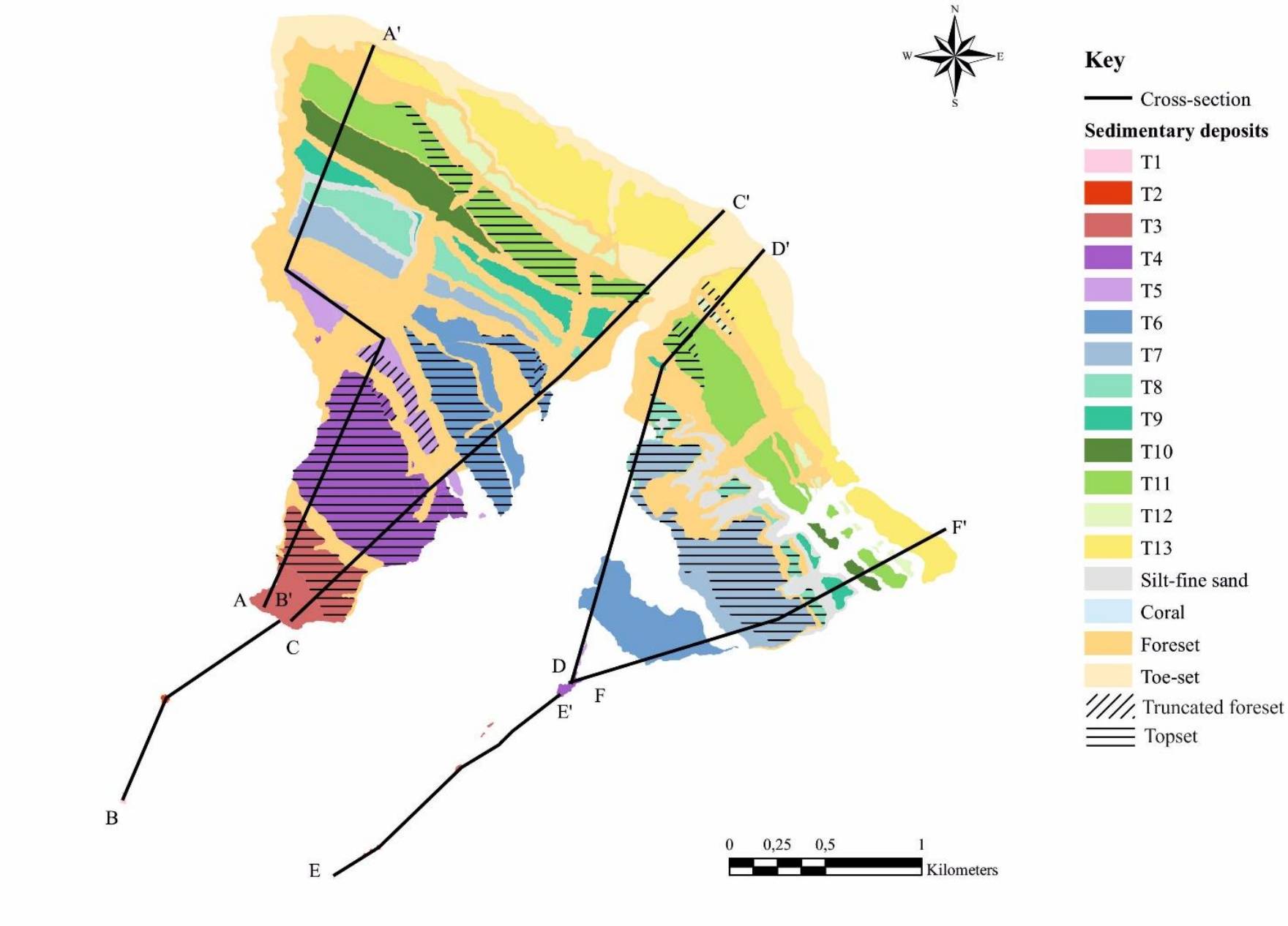
A'
C'
D'
F'
A
B'
C
B
D
F
E'
E
N
W
E
S
0
0,25
0,5
1
Kilometers
Key
Cross-section
Sedimentary deposits
T1
T2
T3
T4
T5
T6
T7
T8
T9
T10
T11
T12
T13
Silt-fine sand
Coral
Foreset
Toe-set
Truncated foreset
Topset

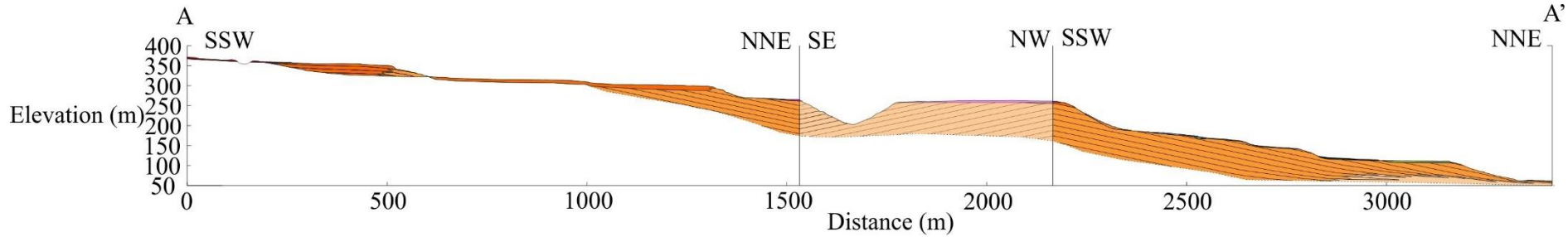
A
SSW
NNE
SE
NW
SSW
NNE
A'
Elevation (m)
400
350
300
250
200
150
100
50
0
500
1000
1500
2000
2500
3000
Distance (m)

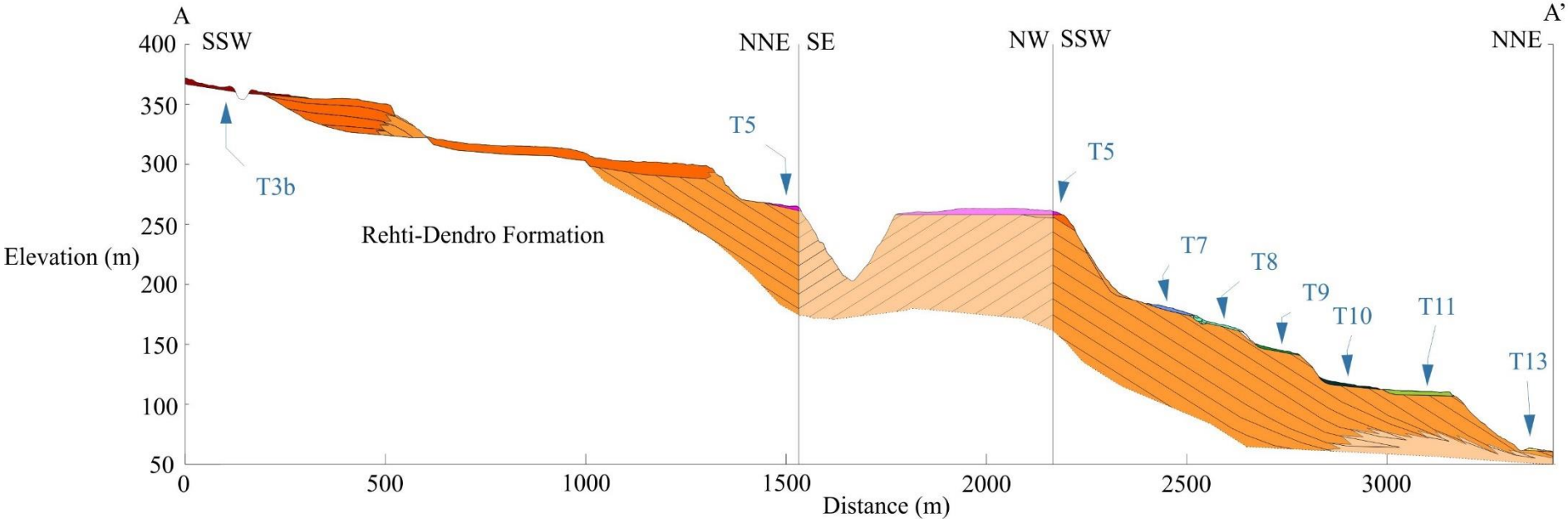
A
SSW
NNE
SE
NW
SSW
NNE
A'
T3b
T5
T5
T7
T8
T9
T10
T11
T13
Rehti-Dendro Formation
Elevation (m)
400
350
300
250
200
150
100
50
0
500
1000
1500
2000
2500
3000
Distance (m)

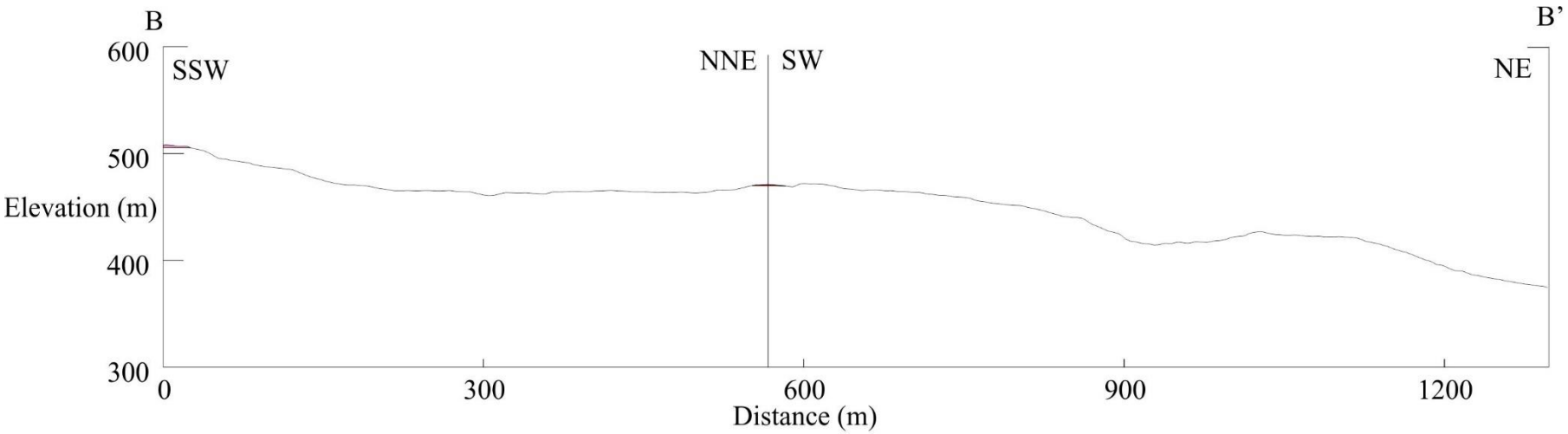
B
B'
SSW
NNE
SW
NE
600
500
400
300
Elevation (m)
0
300
600
900
1200
Distance (m)

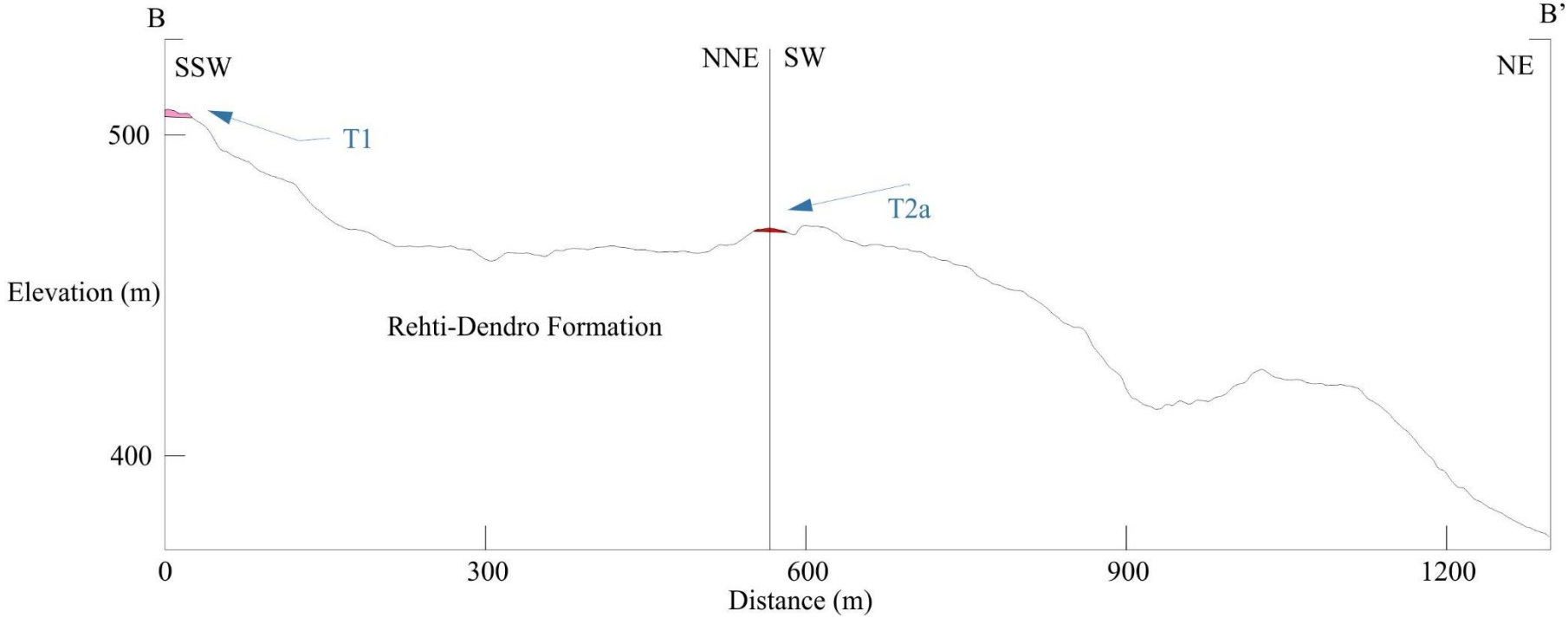
B
B'
SSW
NNE
SW
NE
T1
T2a
500
400
Elevation (m)
Rehti-Dendro Formation
0
300
600
900
1200
Distance (m)

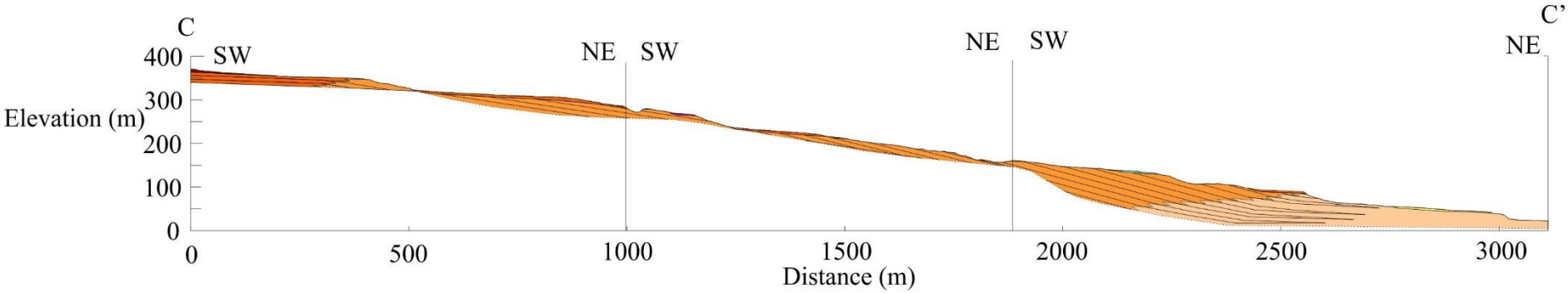
C
C'
SW
NE
SW
NE
SW
NE
Elevation (m)
400
300
200
100
0
0
500
1000
1500
2000
2500
3000
Distance (m)

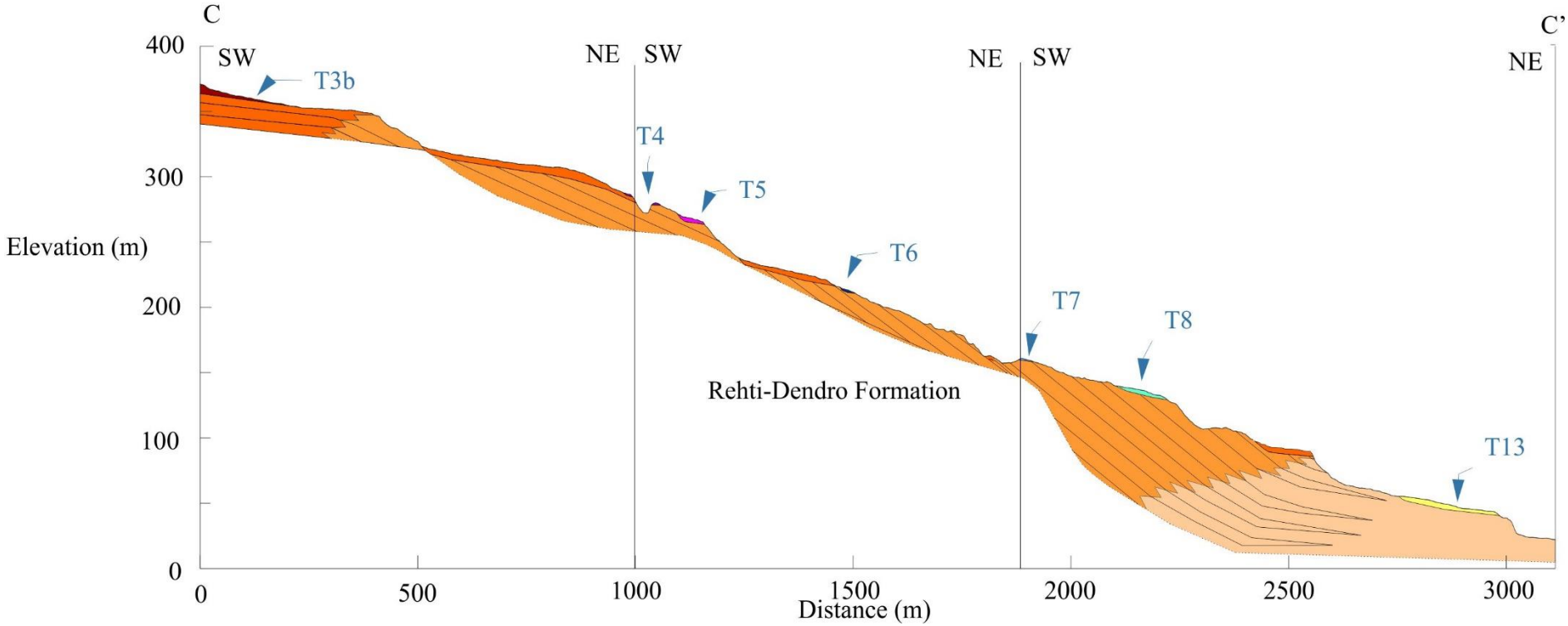
C
C'
SW
NE
SW
NE
SW
NE
T3b
T4
T5
T6
T7
T8
T13
Rehti-Dendro Formation
Elevation (m)
400
300
200
100
0
0
500
1000
1500
2000
2500
3000
Distance (m)

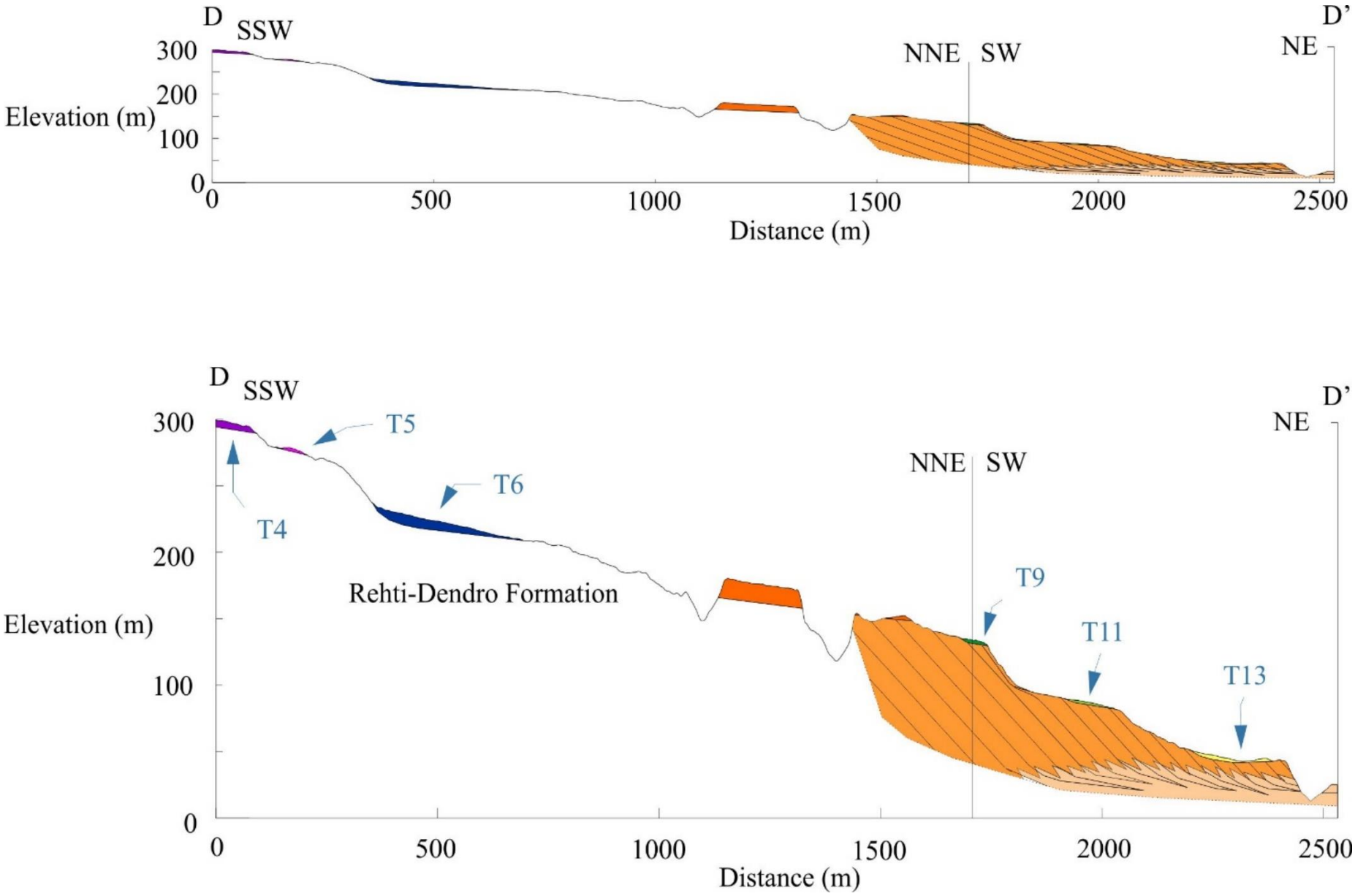
D
SSW
D'
NE
NNE
SW
300
200
100
0
Elevation (m)
0
500
1000
1500
2000
2500
Distance (m)
T5
T6
T4
T9
T11
T13
Rehti-Dendro Formation

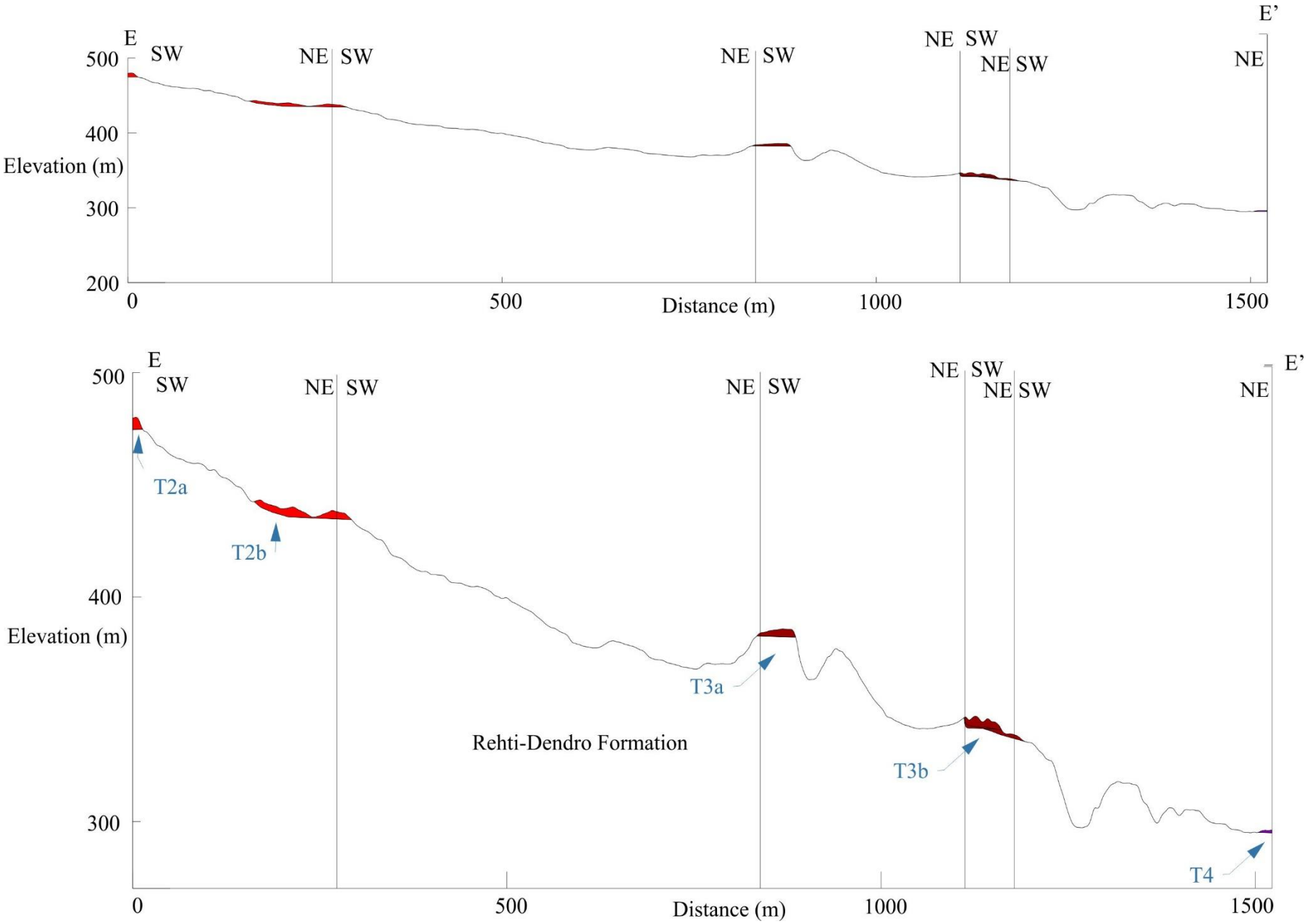
E
E'
SW
NE
SW
NE
SW
NE
SW
NE
SW
NE
500
400
300
200
Elevation (m)
0
500
1000
1500
Distance (m)
T2a
T2b
T3a
T3b
T4
Rehti-Dendro Formation

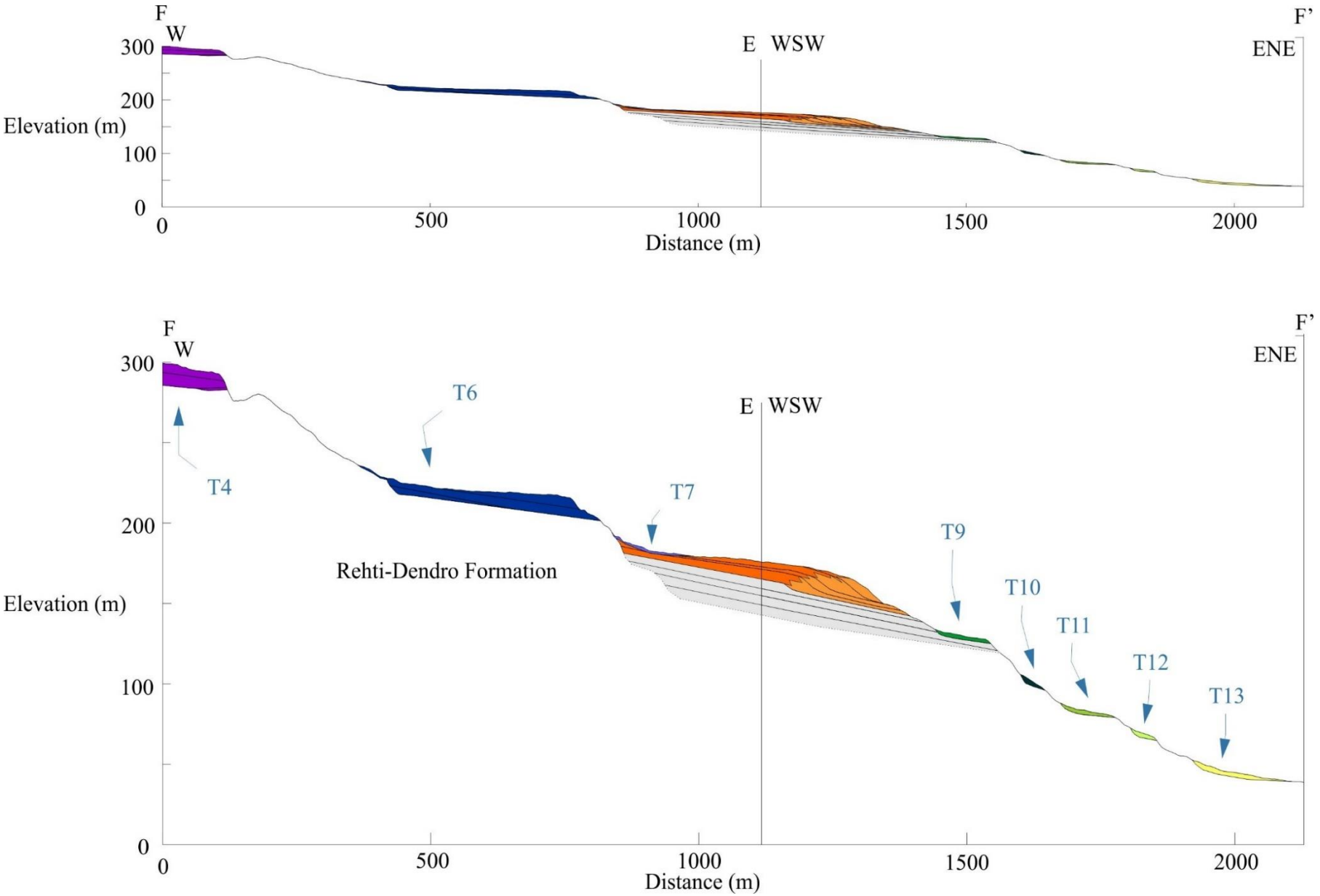

Figure 17. Map of cross-sections followed by cross-sections alphabetic order (A to F), also follows the order from west to east, with exception for the older terraces.

5.3. Sequence stratigraphy

This subchapter presents the interpretations of data presented in subsection 5.2.3 in forms of a sea-level trajectory and a general vertical succession. Each cross-section (figure 17) has a trajectory and each trajectory has highlighted points. Each point is firstly named based on the terrace they are associated with and then followed by subsequent points explaining sea-level variations. In a few cases there is an alternative explanation given for the terrace formation, marked by a dashed line and this dashed line is a cumulative interpretation of all trajectories rather than a separate analysis of each trajectory. Lateral variations are common due to the local variations, such as small delta build-outs.

5.3.1. Trajectory

The following subsection presents all the trajectories, then goes through each terrace level and their corresponding points.

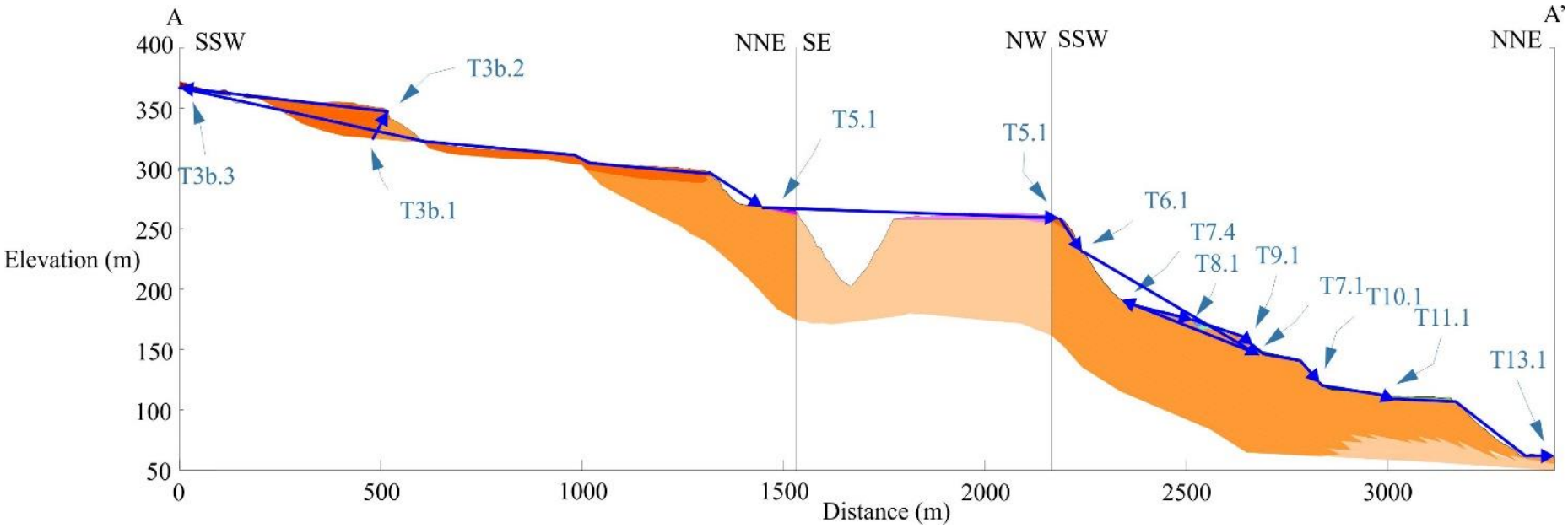
A
SSW
NNE
SE
NW
SSW
NNE
A'
T3b.2
T3b.3
T3b.1
T5.1
T5.1
T6.1
T7.4
T8.1
T9.1
T7.1
T10.1
T11.1
T13.1
Elevation (m)
400
350
300
250
200
150
100
50
0
500
1000
1500
2000
2500
3000
Distance (m)

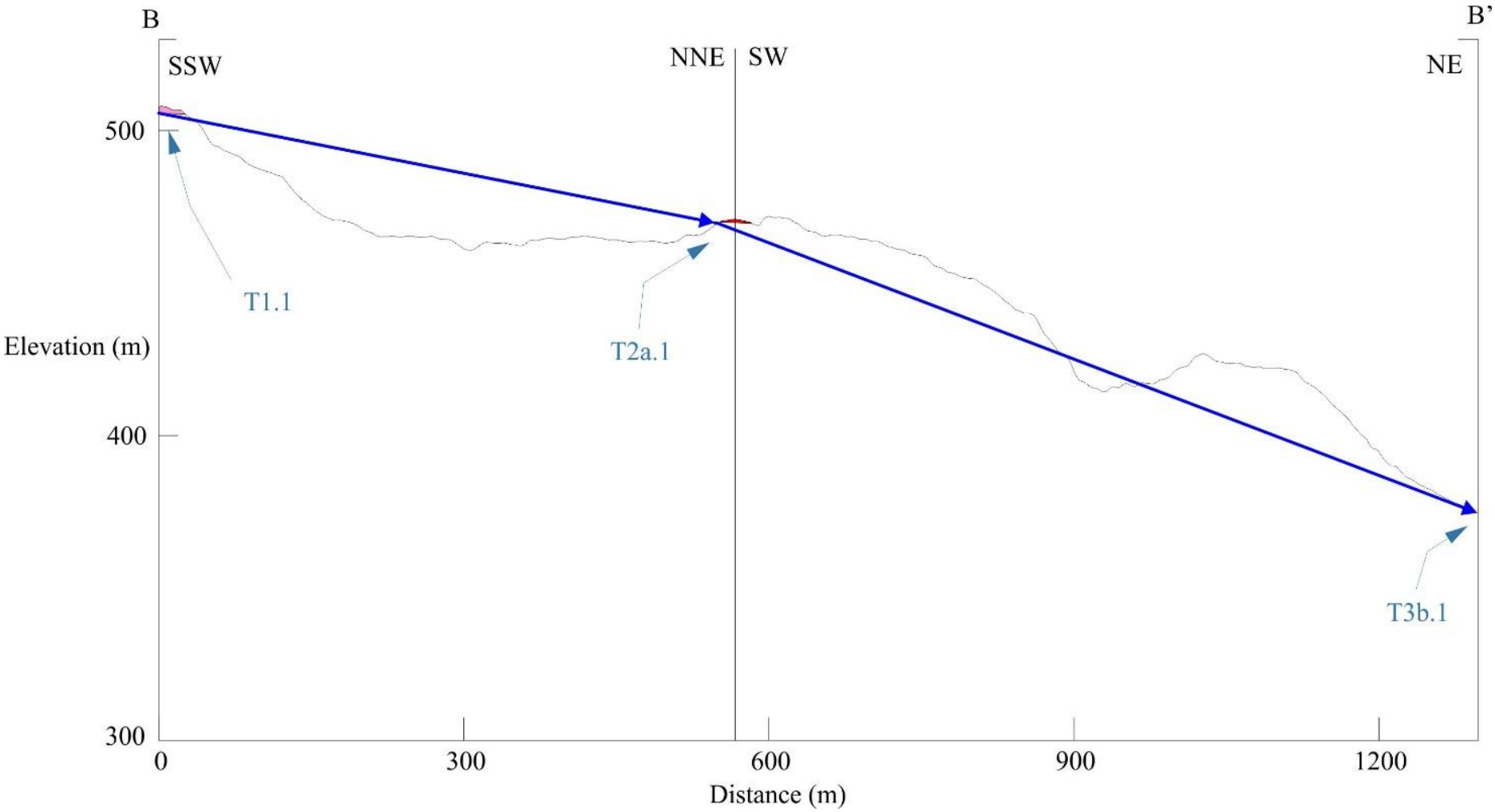
B
B'
SSW
NNE
SW
NE
500
400
300
Elevation (m)
T1.1
T2a.1
T3b.1
0
300
600
900
1200
Distance (m)

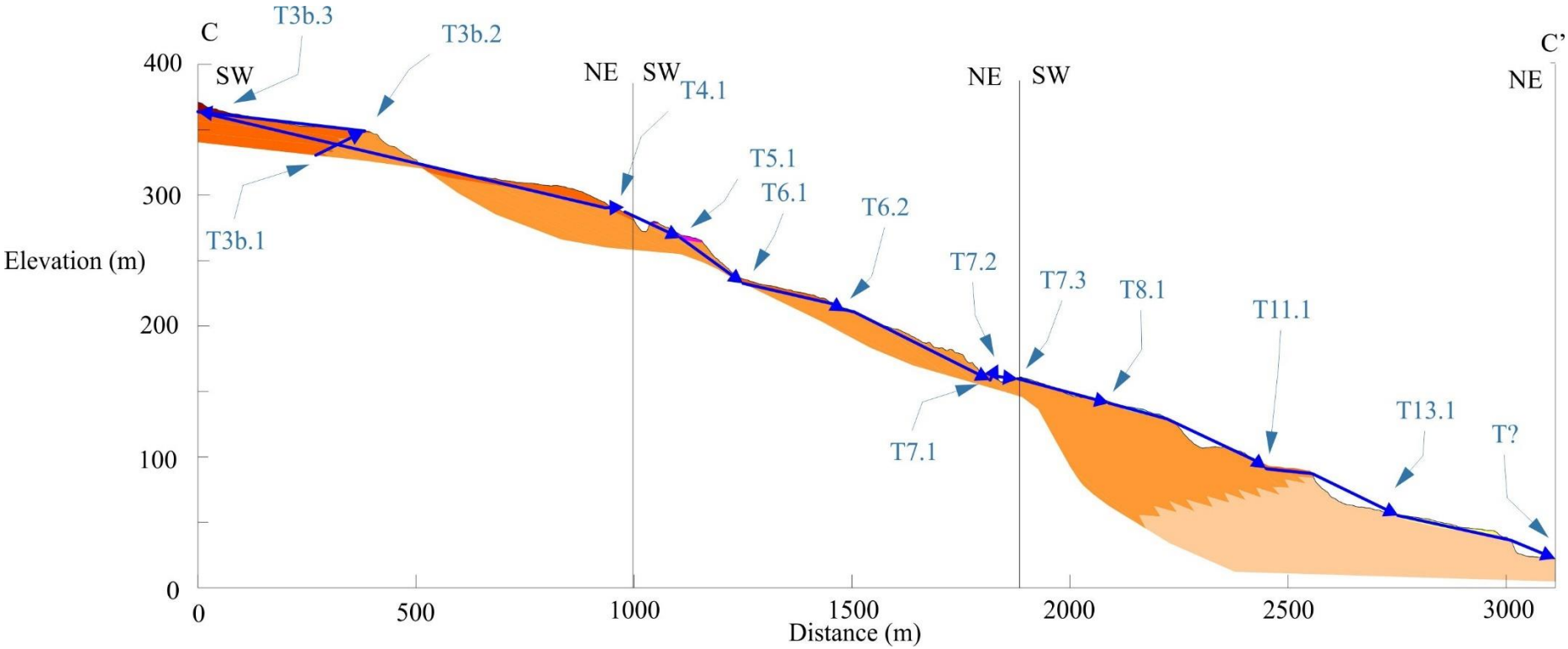
C
C'
SW
NE
SW
NE
SW
NE
T3b.3
T3b.2
T4.1
T5.1
T6.1
T6.2
T7.2
T7.3
T8.1
T11.1
T13.1
T?
T3b.1
T7.1
Elevation (m)
400
300
200
100
0
0
500
1000
1500
2000
2500
3000
Distance (m)

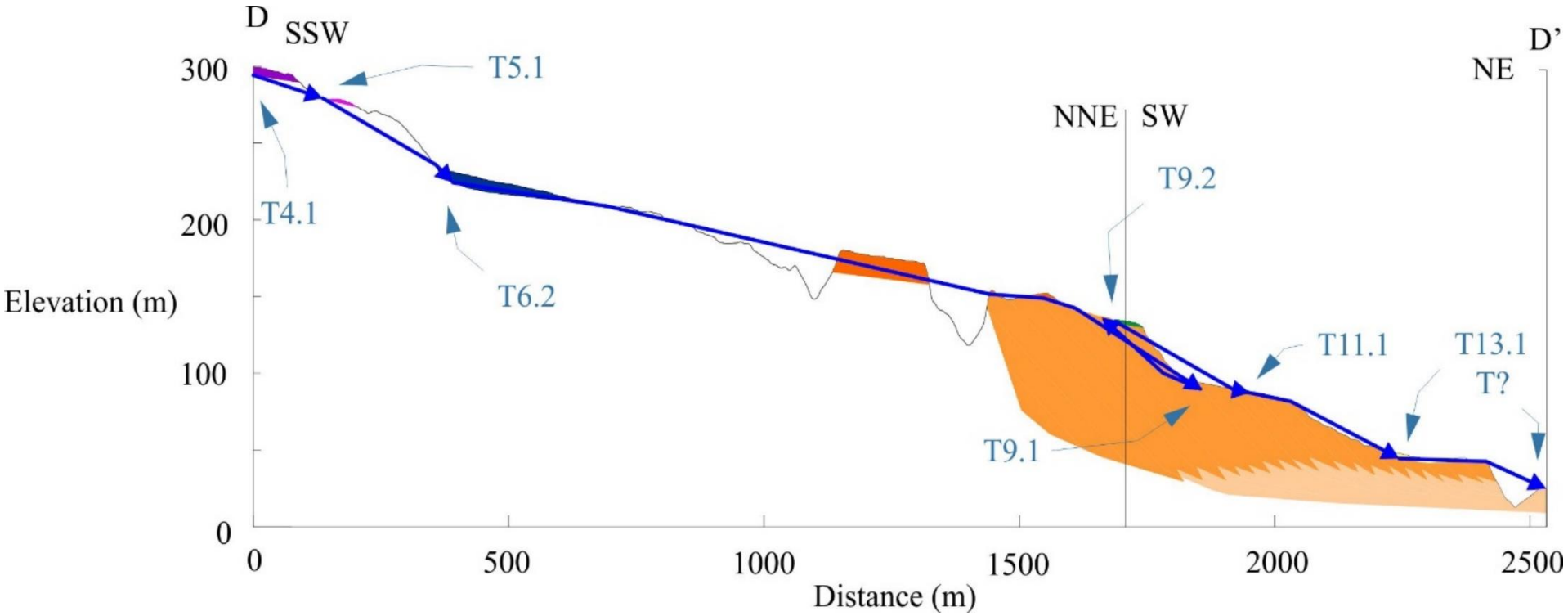
D
SSW
D'
NE
NNE
SW
T5.1
T4.1
T6.2
T9.2
T11.1
T13.1
T?
T9.1
Elevation (m)
300
200
100
0
0
500
1000
1500
2000
2500
Distance (m)

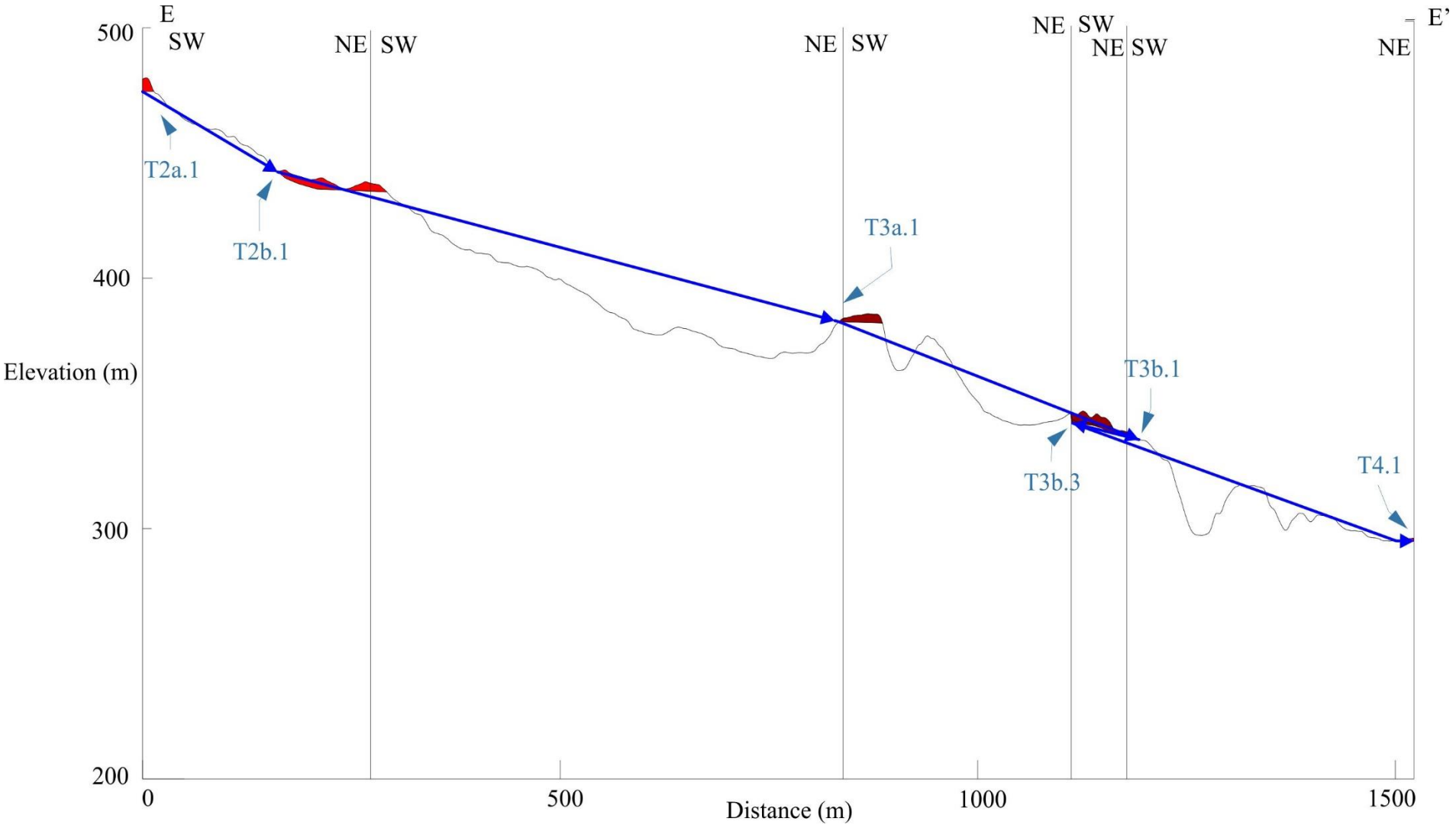
E
SW
NE
SW
NE
SW
NE
SW
NE
SW
NE
E'
500
400
300
200
Elevation (m)
T2a.1
T2b.1
T3a.1
T3b.1
T3b.3
T4.1
0
500
1000
1500
Distance (m)

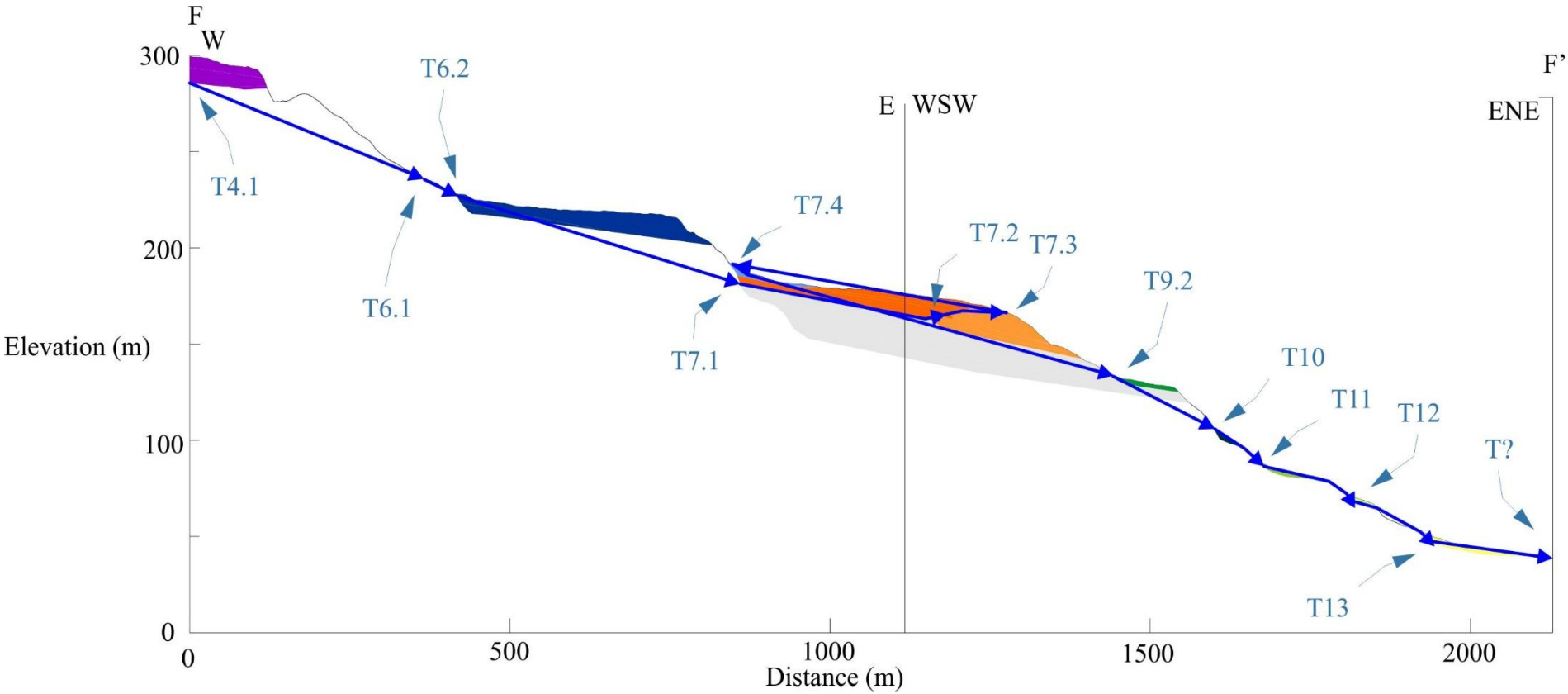

Figure 18. Trajectories of cross-sections in alphabetic order A to F. Profiles are the same as cross-sections, see map in figure 17 for details.

T1: The point T1.1 found on both ridges represent the formation of the oldest terrace, T1. This is followed by sea-level fall either due to uplift and/or eustatic sea-level change.

T2: Point T2a.1 represent the back-end of T2 deposits and this is followed by a further drop in sea-level until T2b.1.

T3: T3a.1 is only present in Ridge 2, followed by a sea-level fall. On Ridge 1, T3b.1 is represented by progradation and aggradation of sigmoidal clinoforms until point T3b.2 where there is a small transgression creating the back-end of T3b, T3b.3. On Ridge 2, due to the lack of delta build-out, there is a small terrace forming prior to that of T3b.3, likely during the phase of T3b.1 until T3b.2. See figure 15 for details of T3b.

T4: On Ridge 1, T4 is dominated by gently sloping topsets up until point T4.1, which represents the back-end of a small pinch-out marine terrace deposit. On Ridge 2, T4 is superposing the Rehti-Dendro Formation.

T5: The point T5.1 represent the back-end of the terrace and is present on Ridge 1 as either a marine deposit superposing foresets or present as truncated foresets. On Ridge 2 it is present as a marine terrace overlying the Rehti-Dendro Formation.

T6: Sea-level fall to point 6.1 represent the first phase of the terrace formation, either generating a marine terrace deposit, a topset or a break in an existing foreset (Figure 19 and 20). This is further followed by another sea-level drop continuing the marine terrace formation, or in other cases creating the back-end for T6 marine terrace, depending on locality in the area. The SF facies found in two areas (see map) could potentially have been deposited during this interval as it is older than T7, and most likely deposited in either protected shallow or deep marine/lake environment given the grain size and features present.

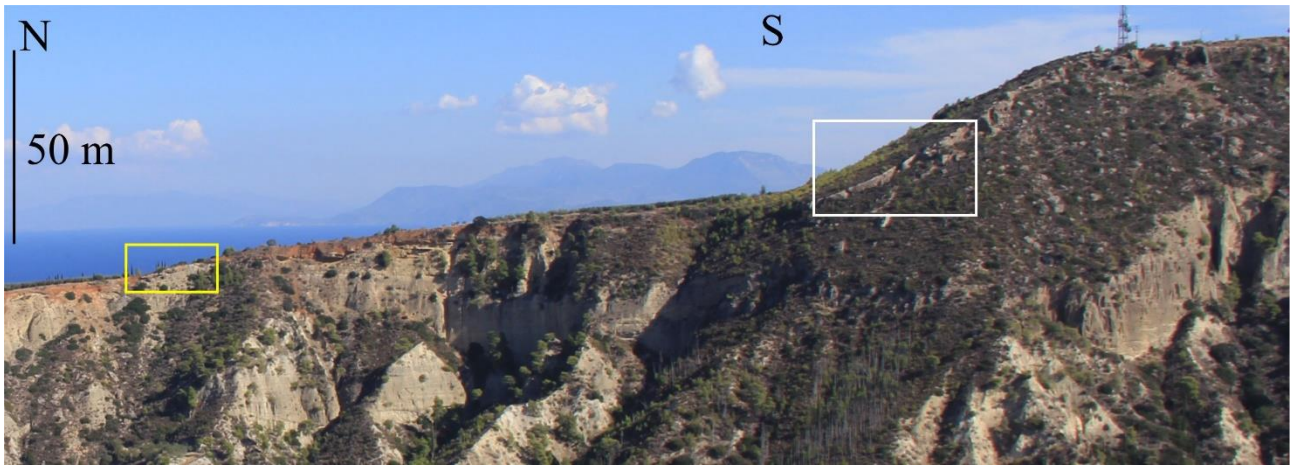

Figure 19. Figure from across Sythas Valley looking to the east, the white box is zoomed in in figure 20 and the yellow box is zoomed in in figure 23.

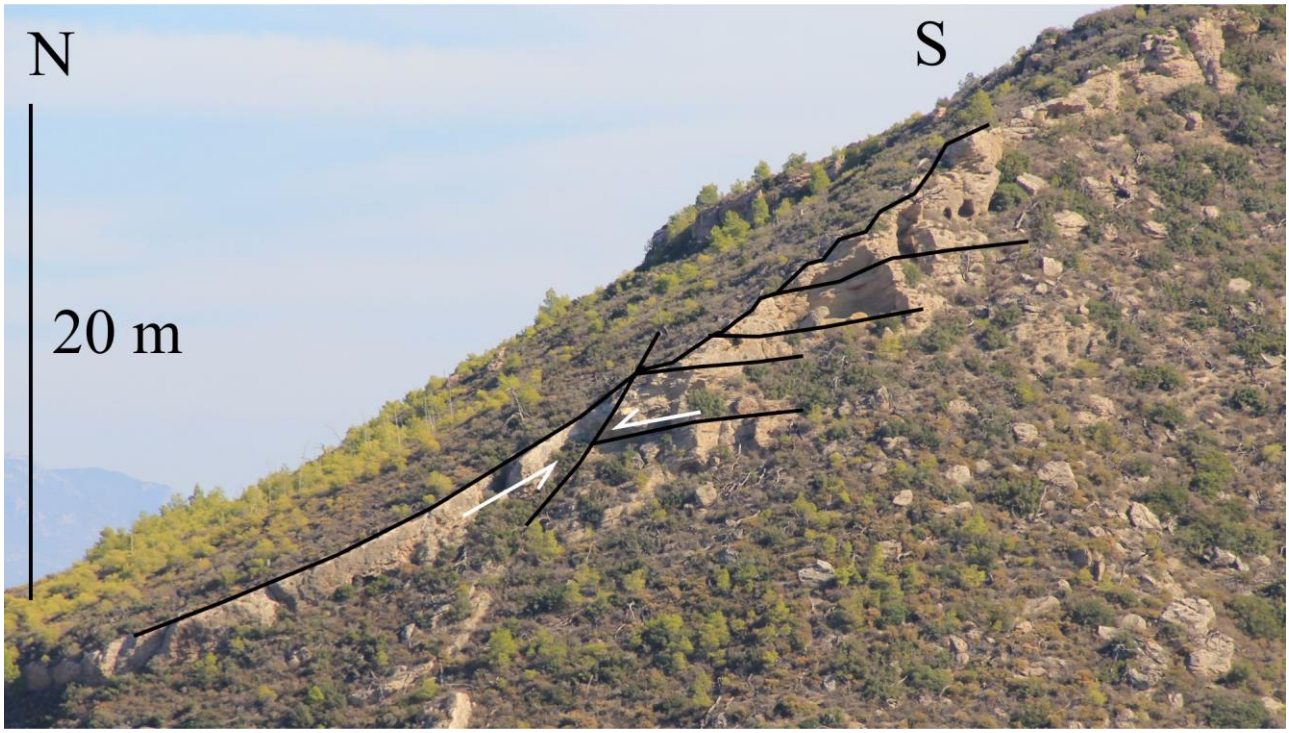

Figure 20. White box from Figure 19 zoomed in to show the foresets which are cut and eroded. The break is laterally continuous with T6. Figure 18A, point T6.1.

T7: Point T7.1 represent a drop in sea-level, with a gentle basinward sloping build-out of topset deposits until point 7.2. This is followed by a progradation and aggradation of delta build-out until it reaches its peak at T7.3, which is then followed by a transgression and formation of a marine terrace T7.4. See Figure 21 for details of delta overlying the silt-fine sand facie.

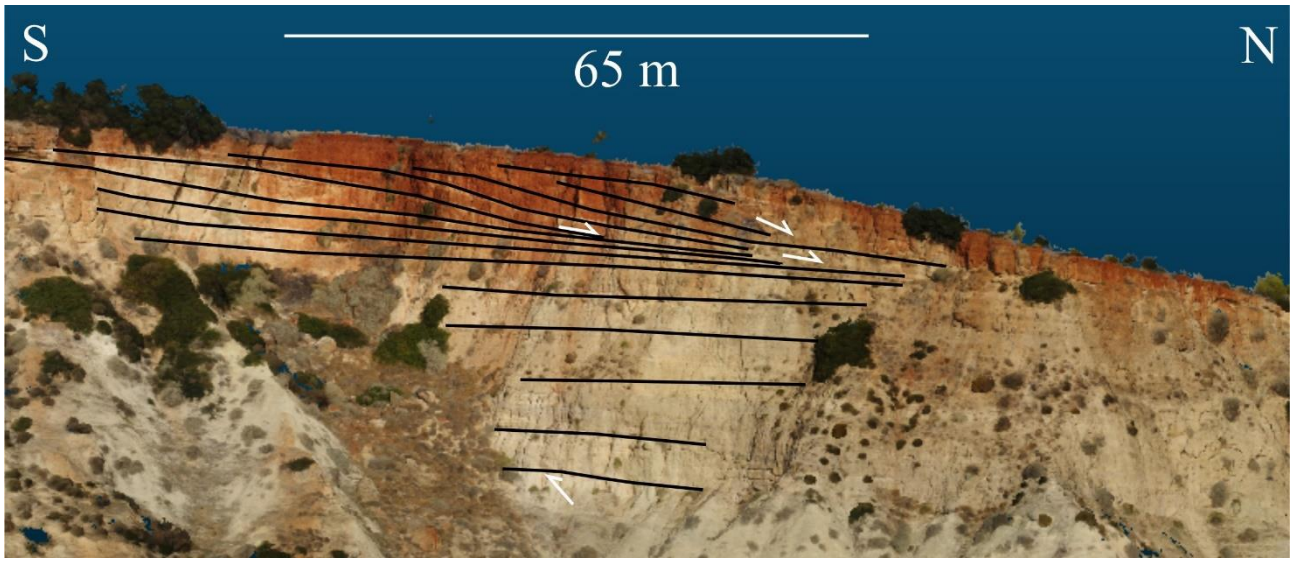

Figure 21. Image from CloudCompare of delta beneath T7 on Ridge 2. white arrow beneath the lowest back line indicate the boundary between the Rehti-Dendro Formation.

T8: Point T8.1 indicate the back-end of T8 after a small sea-level drop from T7. On the western-most part of the area, the back-end of T8 appear intertwined with the front of T7. T8 only being a short sea-level drop from T7 creating a small concave back-end. See figure 22 for details of features.

Figure 22. Boundary between T7 (red deposit to the right) and T8 (thin red deposit to the left) where the thin silt-fine sand facie is present. the surface appears reworked or oddly laminated before the deposition of T8. Figure 18A, point T8.1.

T9: T9.1 indicate a sea-level drop without much impact on the overall sedimentary deposition of the area, except one clear downlap (Figure 23) created at cross-section D. This is followed by point T9.2, which represent the back-end of T9 and laterally vary a lot in terms of what unit it is overlying. In the far east it is superposing silt-fine sand, in the centre where present foresets are found below and in

the far west a combination of both, thin silt-fine sand at the back-end and below the overall bed are delta foresets. The extent of the silt-fine sand to this level from T7.1 suggests that there is a large sea-level drop to first deposit the silt-fine sand, followed by a sea-level rise. The silt-fine sand deposit itself is most likely a more localised deposit and not a laterally continuous deposit like the marine terraces.

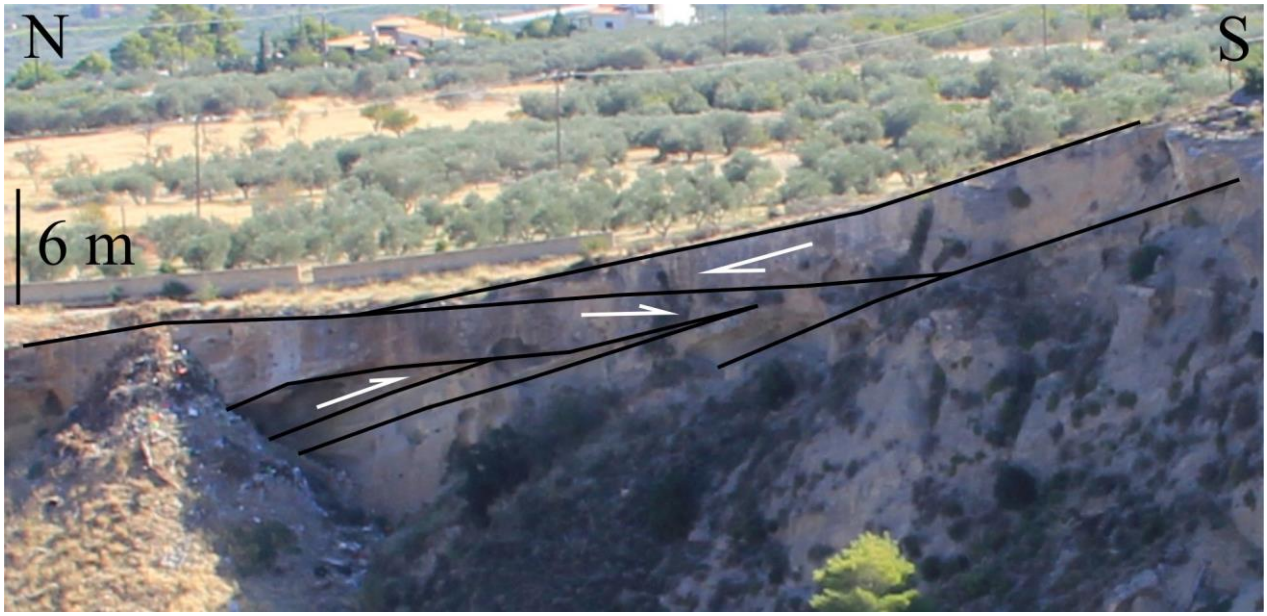

Figure 23. Downlap onto a sigmoidal clinoform, figure 18D, point T9.1.

T10: Point T10.1 represent the back-end of T10, a fairly steep sea-level drop from previous terraces.

T11: A small sea-level drop followed T10.1 to point T11.1, which indicate the back-end of T11. Laterally the marine terrace is replaced by a topset.

T12: Point T12.1 represent the back-end of the T12, which is a thin, laterally discontinuous marine terrace.

T13: Point T13.1 indicate the back-end of the youngest studied marine terrace T13.

T?: Represent sea-level fall to a lower level which has not been studied.

5.3.2. General vertical succession

With the aid of the cross-sections a general vertical succession was generated in order to place the terraces and deltas in order of relative age to one another. For a lot of terraces there is a lack of time constraints as they superpose the Rehti-Dendro Formation and do not interact with other terrace deposits laterally. In these cases, the generally accepted idea of constant uplift and regression is applied.

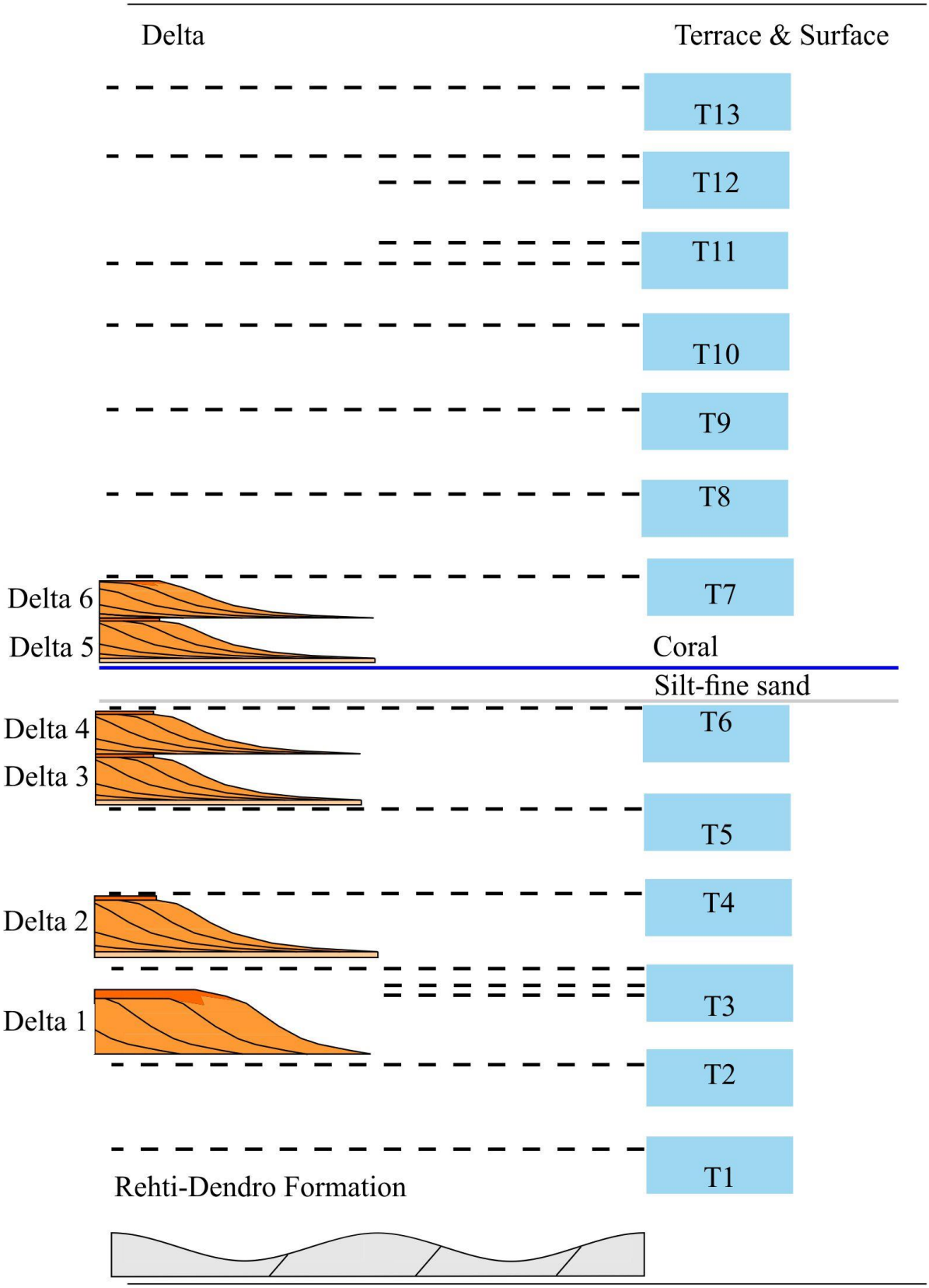

Figure 24. A general vertical succession of the formations in the study area. the dashed lines represent the terrace extent as laterally some marine terraces are found above deltas as well as laterally continuous and other times, they are only present on one ridge (commonly Ridge 2 as it has not nearly as many deltas or as big deltas as Ridge 1). For example, T3 has arguably 3 terrace parts on Ridge 2, whilst on Ridge only one is present due to the underlying delta.

The general vertical succession generated is not vertically accurate, e.g. Delta 2 is the largest one in the area and Delta 1 is closer to one tenth in size (figure 24). The reasoning for the scaling used is as the focus is on the marine terrace deposits and the exact ages between each deposit is not currently known and therefore they are evenly spaced as of now. T1, being the oldest formation is at the base and the succession is younging upwards. Given that the most recent sediments are greatly impacted by uplift and forced regression, without evidence of transgressions (e.g. within T3 on Ridge 2), they are presumed to be downstepping. It is completely possible that e.g. T13 is older than T12 as they never overlap or interact in any way, making it impossible to determine relative age. The relative time of deposition for the silt-fine sandstone found on both ridges, which due to being deposited on the same elevation is considered the same deposit, just not a laterally continuous one. Therefore, the SF deposits is considered to be younger than delta 2, even though on Ridge 2, the thickness gives the impression of a deep marine/lake environment. It is older than T7, potentially younger than T6 or deposited at a similar time as T6.1 was deposited, when there is an overall reworking of sediments across the area. These localised areas of protected water, potentially by a cusp (look at present-day shoreline and how similar it is to the terrace morphology, can be assumed to have been similar in the past).

6. Discussion

This chapter will discuss the data presented and analysed in chapter 5 and compare it with previous research and models. The first subsection will present correlations of logs in various localities of the area to discuss the lateral continuity as well as variations in a response to one of the key aims of the thesis - to determine the sedimentology of the marine terraces. This knowledge may be vital for anyone working offshore when having identified terraces in a seismic section. Secondly, a comparison will be made between the division of terraces used in this thesis and the division made by Armijo *et al.* (1996), whose interpretation is still widely used as a base when interpreting terrace levels (e.g. De Gelder *et al.*, 2018). As previously mentioned, and continuously stressed, it should be highlighted that the paper by Armijo *et al.* (1996) focused on large-scale aerial mapping, not localised field mapping and the sedimentological division of units into marine and fluvial deposits. The section will mainly focus on the additional detail field mapping found and provide insight to how the sedimentology and the local detail may prove beneficial to the overall interpretation of the sea-level variations through time. This is done by discussing the revised sea-level trajectory, previously only considered to be uplift and regression/forced regression to now also include periods of transgression.

Lastly, the marine terraces will be used in an attempted correlation with an interglacial sea-level curve of the past 800 Ma (by Spratt & Lisiecki, 2016) in order to tie the marine terrace formation to highstands. The elevation at present time can then be used in order to determine uplift rates and variation through time.

6.1. Sedimentology of terraces and lateral variations

In general, wave-worked gravels tend to be more laterally continuous than fluvial, which are more lenticular than sheet-like (Clifton, 1973; Leithold & Bourgeois, 1984; Massari & Parea, 1988; Hart & Plint, 1989). Logs of the same marine terrace were taken at different locations to compare with logs taken from the same topset. The correlations between logs and the comparison of the two correlations will determine if the case of lateral continuity within marine terrace levels is accurate in this area of active faulting and uplift. It is important to remember that the delta build-outs may cause lateral interference with longshore drift, distributary channels as well as breaks in terraces. A correlation is attempted between logs of T12 (logs 2, 7 and 8) as they represent clear distinct beach-shoreline features. The variations and similarities will be compared to those of a different kind of terrace, a depositional one of T11 (log 3 and log 4). The purpose of this is to examine the differences as the sedimentology and environment of the deposit may greatly affect its properties when thinking from an economic stand-point in the hydrocarbon industry or even water reservoirs.

6.1.1. Correlations

Logs used for correlation from left to right: Log 7, Log 8, Log 2 (marine terrace), Log 3 and Log 4 (topset).

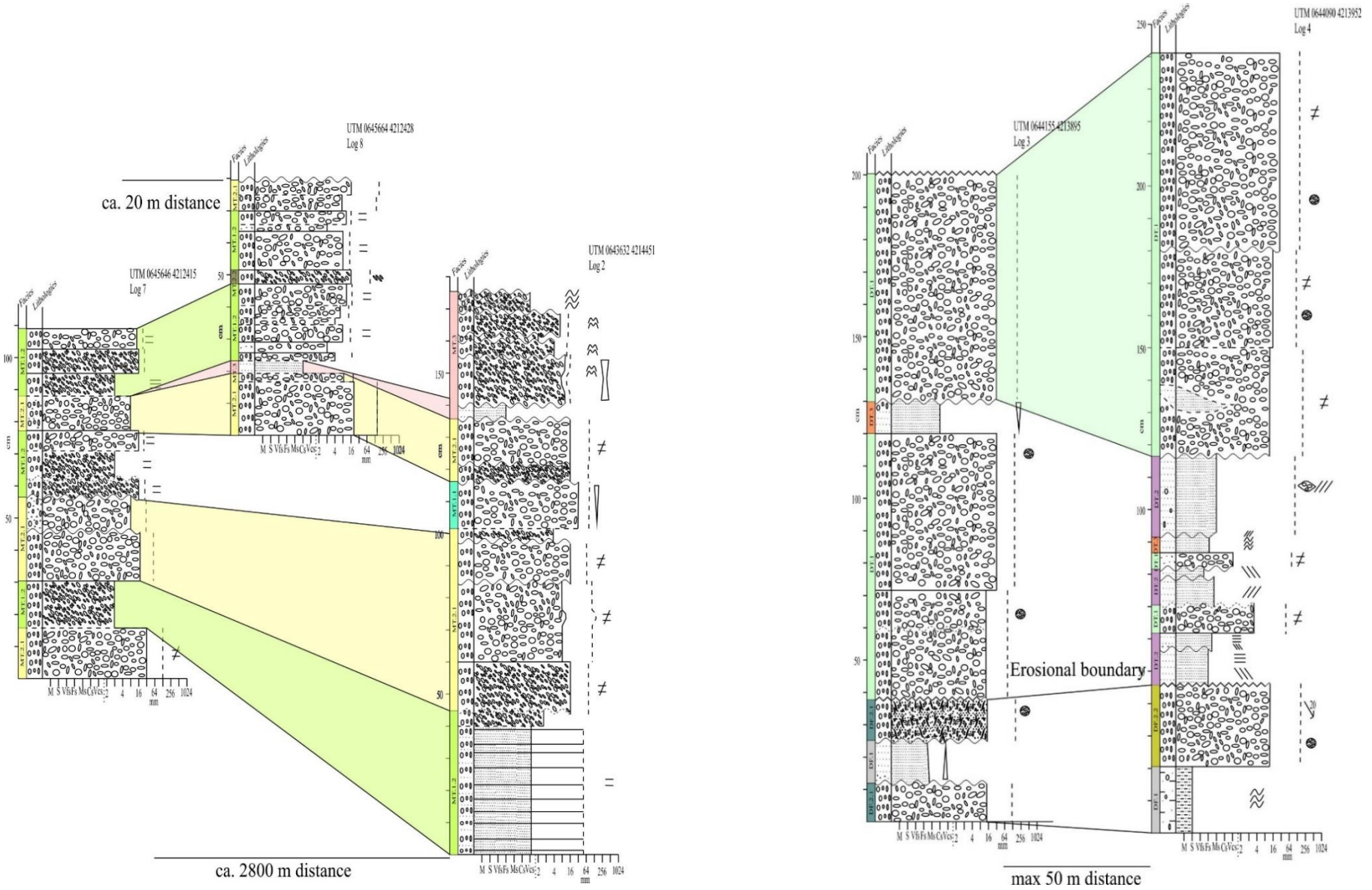

Figure 25. Correlation of logs, marine terrace logs to the left and to the rift delta topset logs. Note the difference in distance between logs, the deltas present in the area were small, therefore the short distance between topset logs.

Despite the distance between the logs (log 7 and 8 being from the same terrace area and not far apart unlike log 2), there are a few striking similarities such as the facies and thickness, given the 2.8 km distance between the outcrops. Log 2 has a better-preserved outcrop with a large, fresh surface to work from and, therefore, it may be more precise than log 7 and 8. The uppermost part of log 2 is missing in log 8 as well as log 7, this could either be due to erosion or a lack of preservation or alternatively, it never extended this far east. All three logs are expressing the similar facies as well as dominantly clast-supported or open framework conglomerates. Clast-size is slightly coarser in the west and this may be due to it being closer to a delta or clast source. As seen in figure 1 the shoreline in present day is very long and wave-dominated and all deltas are of very a small scale and have little influence on the shoreline, the present shoreline is a very good analogue for the past shoreline in this area.

As for the depositional terraces, even at a short distance the depositional terrace differs greatly, one expressing a lot of internal structural variations such as wavy laminations and inclined bedding, and the other appears generally structureless or the features are too indistinct. What they both share, however, is the presence of intraclasts.

The bounding surfaces below the marine terraces are frequently transgressive ravinement surfaces based on the lag and presence of intraclasts. However, this is not always the case, in some cases it would appear uplift is enough to create a sequence boundary and sub-aerial erosion morphologically changes the surface, e.g. a pinch out terrace like 6.1. Overall if one were to look at the shore from the rift centre, the marine terraces would have a straight bounding surface, unlike those of fluvial origin which would prove more difficult to traces. Additionally, some may even have a more incised outline, although the deltas in the area are generally small and the only large deltas follow a palaeovalley. There are a few isolated cases of incisions on Ridge 1, T6 in the Rehti-Dendro Formation which have been filled in by conglomerates of unknown origin. These are likely fluvial given the extent of small delta build-outs on Ridge 1 at this age. Beneath the terraces of fluvial origin, the foresets are commonly eroded by more recent topsets, unless the topset can be followed down to a clinothem in which case they are connected, and this is possible for some of the smaller deltas.

6.1.2. Significance for other studies

This knowledge can be implemented in other areas which have experienced similar rifting and likely formed terraces, e.g. in the North Sea and the Gulf of Suez (Ravnås & Steel, 1998; Gawthorpe & Leeder, 2000). The marine terraces show a lateral continuity unlike that of the topsets and this may be most beneficial when applied to resource geology. One issue which arises if implemented to

subsurface geology is the thinness of the beds, they would be difficult to distinguish on seismics. The difference in permeability and porosity is unlikely high enough if superposing a topset, although if superposing a foreset or similar formation to the Rehti-Dendro Formation, the boundary may be noticeable, as a change in acoustic impedance creating a surface. This surface may provide useful as a sequence boundary or other bounding surface, depending on surrounding beds and the nature of the surface, creating an understanding of the sequence stratigraphy in the subsurface.

6.2. Revised terraces, a comparison between small-scale mapping and large-scale mapping and the impact it has on sea-level trajectory

This study was done on a small scale and with a hands-on approach with traditional field mapping techniques as well as some modern drone footage from one rift edge. Previous mapping of the area has all been done as a part of a large-scale project with little to no outcrop studies, and so the sedimentology of the beds has been neglected until now. This part will focus on how the different scale mapping impacts the interpretation of the sea-level trajectories as well as the extent of terrace deposits.

6.2.1. Comparison of terraces

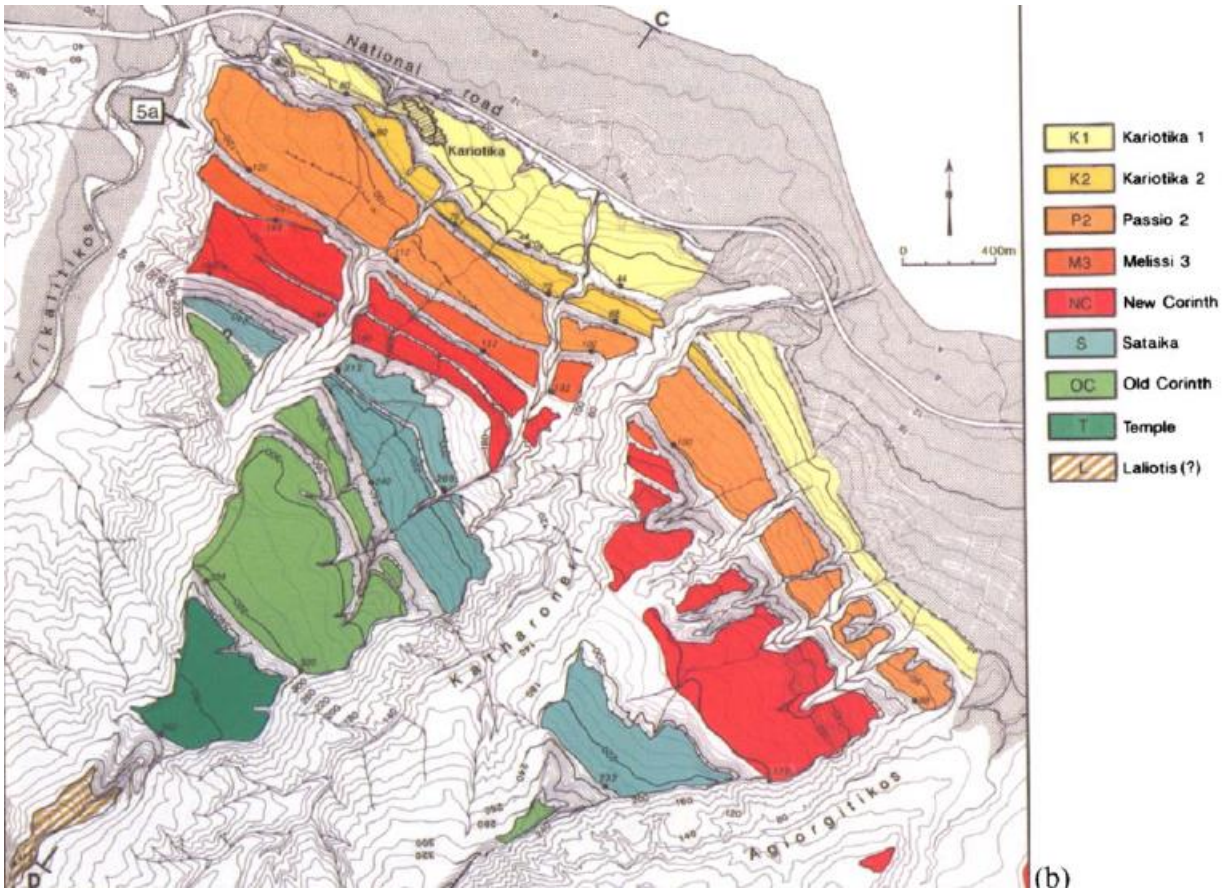

Figure 26a. Map of study area by Armijo et al. (1996).

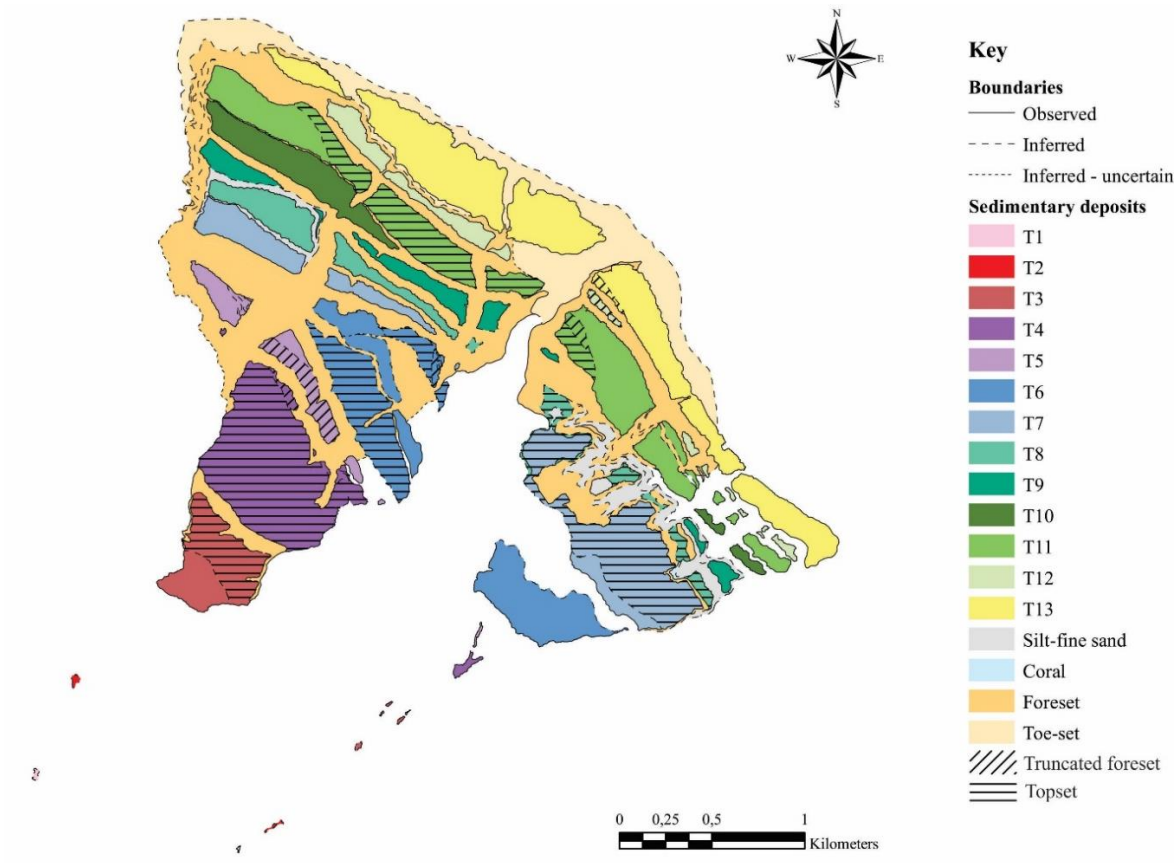

Figure 26b. Map generated for this paper repeated for ease of comparison, previously shown in larger scale in figure 14.

As seen in figure 26a and 26b, there are a lot of similarities, once depositional terraces and erosional terraces are both considered. The older terraces, T3 to T5 in this case, are similar in the map by Armijo *et al.* (1996) and the one generated by field data from this study. T1 is not included in the area studied by Armijo *et al.* (1996) and T2 is considered to be significantly smaller as the slope is rather steep and only a few outcrops were observed and mapped. Most variations lie within the deposits, whether they are marine terraces, topsets or truncated foresets. T3 appears the same and some variations to T4 and T5 (equivalent to the Old Corinth by Armijo *et al.*, 1996). Amongst the younger terraces, the main differences are found in T6 and T7 and their lateral continuity. Armijo *et al.* (1996) extends T6 all the way to the east, but as shown in chapter 5 with cross-section A and figure 20, no terrace deposit is present, neither topset or marine terrace. Therefore, in the version presented in this paper, the extent of T6 ends where last seen, in the middle of Ridge 1 in a mini-valley. T7, which is equivalent to the New Corinth (Armijo *et al.*, 1996), has been split up into sub terraces and also the size and extent has been reduced due to the lack of evidence of terrace deposits or extent. Terraces T8 to T13 do have a similar terrace extent, with main variations being sedimentological, which Armijo *et al.* (1996) did not map. The main issue created by these sedimentological differences occur when one attempts to create a sea-level trajectory or determine age of terraces as the sedimentological variations are important for the sequence stratigraphy, consequently impact the timing and age of deposition.

6.2.2. Impact on previous work

The main previous work for this area is that of Armijo *et al.* (1996) which does remain fairly accurate geomorphologically, with some adjustments. Albeit after close study of the sedimentology and sequence stratigraphy it became clear that transgression does occur and some terraces were generated by transgression, e.g. T3 and T7. Terraces mapped by De Gelder *et al.* (2018) provide a slightly better fit and an interesting take as it includes subdivisions of T6 (Sataika) and T3 (Temple), however, this research did not include the sedimentology or the sequence stratigraphy and focused on high resolution imagery and data, similarly to Armijo *et al.* (1996). In conclusion regarding the impact this study has on previous work, the previous theory regarding a constant uplift and a constant downstep does not work as evidence shown in the cross-sections, the trajectories and images indicate the presence of transgressive periods forming terraces and even cannibalising them before generating a new one.

6.3. Uplift and implications on sea-level curve

In this subsection, uplift rates are compared to terrace levels in order to determine the best fit uplift rate. This is done assuming a constant rate of uplift and the sea-level curve used is that of Spratt and Lisiecki (2016). Previous research in the area by Armijo *et al.* (1996) suggests that only uplift and regression take place in the area and does not include events of transgression which have been found to have taken place, see section 5.3 and 6.2. The regional sea-level fall is moderated due to the Rion Sill, which is a structural high. Implications of this mean the present-day elevation is –70 m to –60 m below sea level (Perissoratis *et al*., 1993; McNeill & Collier, 2004). Given the range of uplift in the area has been previously estimated to be between 1.3 to 1.6 mm/year (Armijo *et al.*, 1996), each profile will be analysed using two separate uplift interpretations, one being 1.3, and one being 1.6 in order to see which is the best fit, or alternatively neither is a great fit and the uplift may be something in-between, see figure 26. As the New Corinth has been positively dated in the Corinth Canal, and that particular bed corresponds to T7 used in this paper (Armijo *et al.*, 1996), that bed will be used as a correlative surface when calculating the uplift for the diagrams. Alternatively, Temple could also be used, however, the age of Temple (T3 in this paper) has been disputed from being referred to MIS 11 (Armijo *et al.*, 1996) to potentially corresponding to MIS 9e, leaving Laliotis (T2) to form during MIS 11 (De Gelder *et al.*, 2018), who also consider the Old Corinth to be part of MIS 7e due to U/Th coral dating (Collier *et al*., 1992; Dia *et al.*, 1997; Leeder *et al.*, 2005). Figure 28 provides a sea-level curve with the corresponding MIS which is sued for interpretation as well as a comparative sea-level curve.

6.3.1. Uplift models

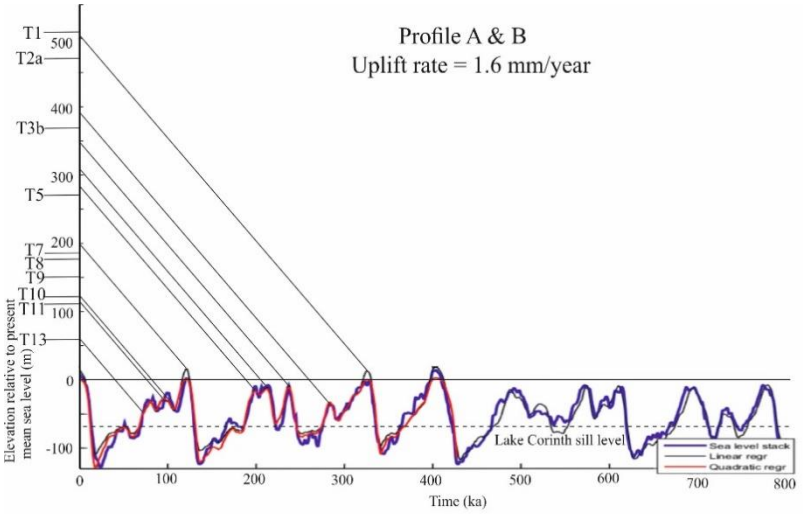
Profile A & B
Uplift rate = 1.6 mm/year
T1
T2a
T3b
T5
T7
T8
T9
T10
T11
T13
Elevation relative to present mean sea level (m)
Lake Corinth sill level
Sea level stack
Linear regr
Quadratic regr
Time (ka)

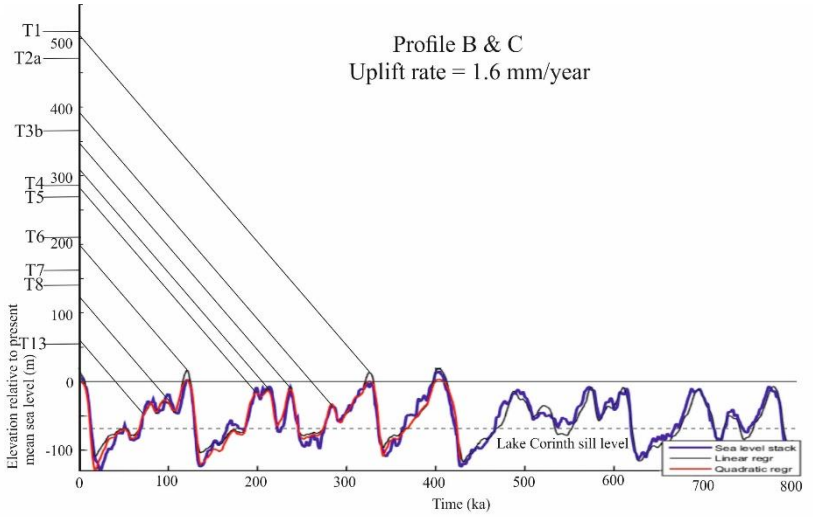
Profile B & C
Uplift rate = 1.6 mm/year
T1
T2a
T3b
T4
T5
T6
T7
T8
T13
Elevation relative to present mean sea level (m)
Lake Corinth sill level
Sea level stack
Linear regr
Quadratic regr
Time (ka)

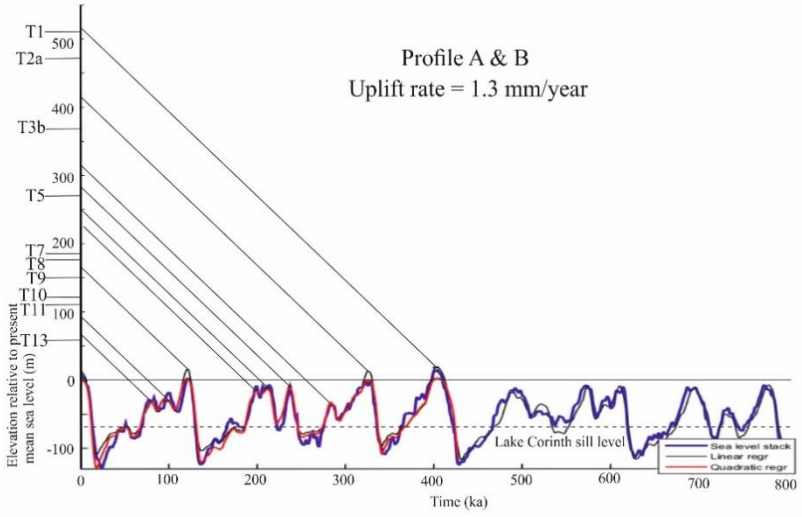
Profile A & B
Uplift rate = 1.3 mm/year
T1
T2a
T3b
T5
T7
T8
T9
T10
T11
T13
Elevation relative to present mean sea level (m)
Lake Corinth sill level
Sea level stack
Linear regr
Quadratic regr
Time (ka)

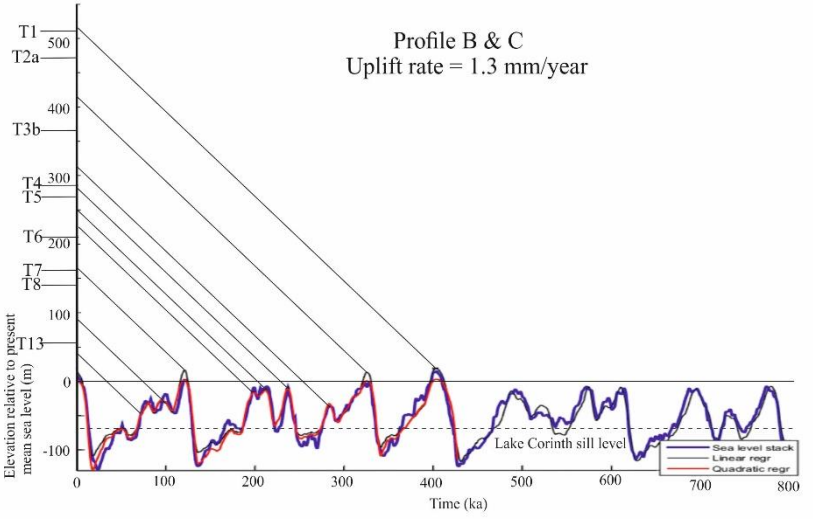
Profile B & C
Uplift rate = 1.3 mm/year
T1
T2a
T3b
T4
T5
T6
T7
T8
T13
Elevation relative to present mean sea level (m)
Lake Corinth sill level
Sea level stack
Linear regr
Quadratic regr
Time (ka)

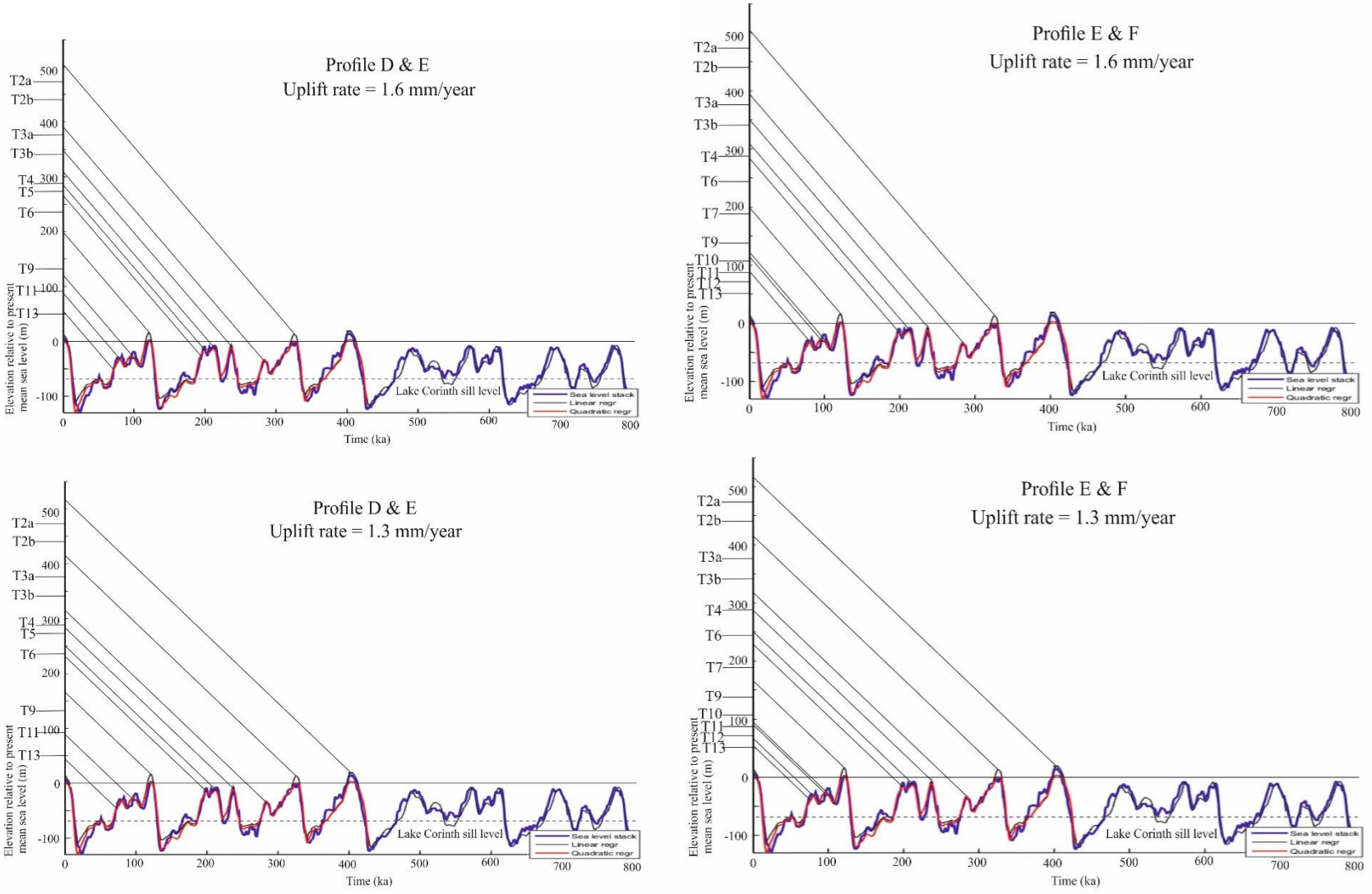

Figure 27. All four complete profiles with two uplift rates. The upper diagrams are always of a higher uplift rate (1.6 mm/year) and the lower is of an uplift rate of 1.3 mm/year.

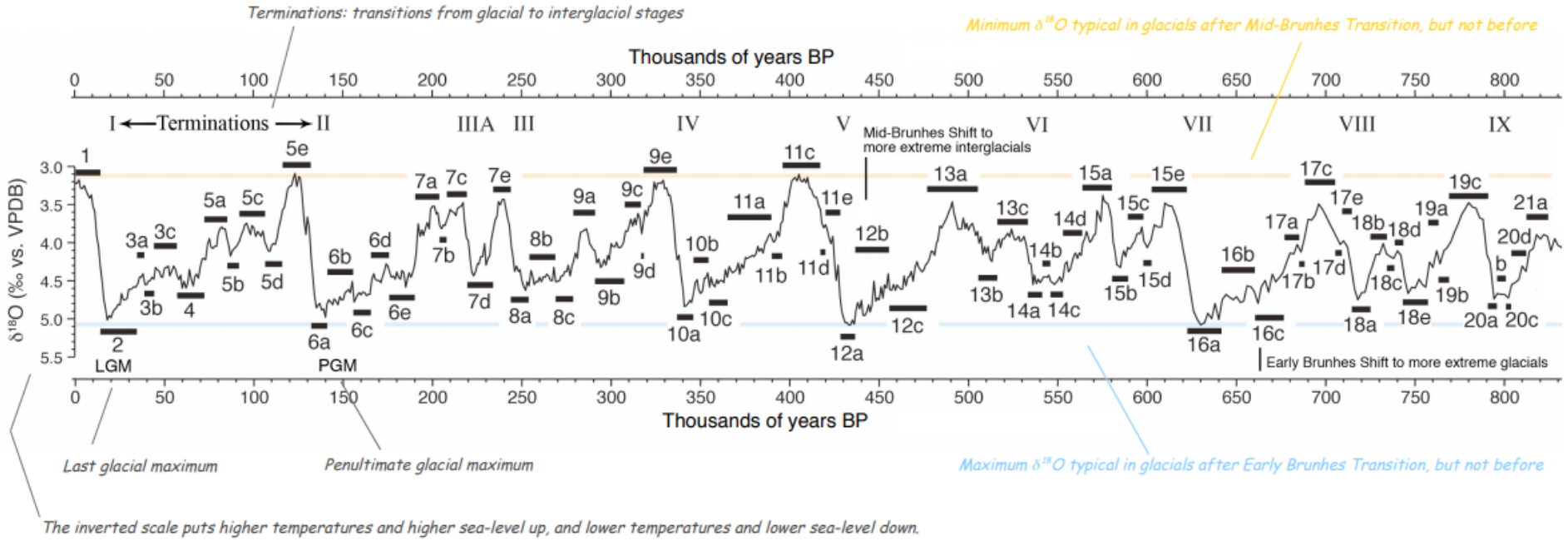

Figure 28. Eustatic sea-level curve with MIS marked out by Railbacks (2015).

Firstly, it should be noted that terraces in profile A&B are at a slightly higher elevation than their lateral counterparts. As to why this is the case is unknown, potentially due to the closeness of the Xylokastro fault. When comparing terrace levels to the uplift rate of 1.6 mm/year, of the older terraces T1 is a close fit from the profile A&B and B&C. T2 does not fit with any highstand and T3 sometimes appear to fit with MIS 7e. As for T4 and T5, either could fit with MIS 7a with a higher uplift rate. The terrace T6 never appear to have a good fit, which could explain the sloping nature of it on Ridge 1 where present, and lack thereof where not. However, there is a large deposit of it on Ridge 2, so this may indicate a terrace formation without a transgression. At a higher rate, T7 rarely appears to match up with MIS 5e even though it has been interpreted to by others e.g. Armijo *et al.* (1996). The only locality where it is remotely close is in the profile E&F. T10 may have formed during MIS 5c and T13 could correlate to a lower highstand during MIS 5a. These are all potential correlations if the uplift rate is as high as 1.6 mm/year and remains the same throughout. T4 correlate to MIS 7e throughout the area and there is a struggle to find a good correlation for T5, which may be due to it being formed by uplift rather than transgression. The following terrace, T6 seem to be either a good fit with MIS 7a or 7c depending on where it is observed, potentially both as in cross-section F, it is clear that there are two events to this terrace so potentially it was created during two highstands, the thinner upper part during 7c, followed by the main body during 7a. T7 fits exactly on the correlation for MIS 5e in profile B&C, however, laterally it does not fit nearly as well. T11 and T13 may correspond to MIS 5c and 5a respectively. Other terraces not mentioned did not show a great fit and may have been formed by uplift alone and not a highstand.

Alternatively, if a lower uplift rate is considered, 1.3 mm/year, T1 is almost a perfect fit with MIS 11c, T2 and T3 may then be formed dominantly by uplift, and potentially the increase in sea-level at MIS 9c created the erosion of T3b and the small in-terrace transgression (figure 15).

Overall as seen in figures above and described, uplift models with an uplift rate of 1.3 mm/year generally provide a closer fit, although given T7 is the terrace tied to dated corals and it is rarely a perfect fit, something like 1.4-1.5 mm/year might give a better fit, when considering a constant rate of uplift. Alternatively, one could consider variable rates throughout the time of uplift, but that would be very difficult to determine given the terraces do not provide an exact age, only an indication where the sea-level has been at some point in time.

6.3.2. Implications of this study

Uplift rates have been closely studied further to the west by McNeill & Collier (2004) and by the Corinth Canal in the east by Leeder *et al.* (2003), and the most recent study of uplift rates in the Xylokastro area was done by Armijo *et al.* (1996), which was a very broad study covering a large area. With the detailed mapping of terraces and the sequence stratigraphical data taken into account when comparing terraces to uplift rates, it becomes clear that either (a) they are formed by different events, some uplift and some during a highstand, and/or (b) the uplift rate varies laterally even within such a small area or alternatively the uplift rate is slightly higher than 1.3 mm/year. These are the conclusions when considering a constant uplift rate as there are no current constraints usable to determine a non-linear uplift rate. Most likely it is a combination of (a) and (b), where there are different types of terraces (uplift-derived and transgressive terraces) as well as a different or multiple different uplift rates. Given the higher altitude of the terraces by the Sythas Valley near Xylokastro, it can also be assumed that the closeness to the fault impacts this as it has been shown to do in other parts of the Corinth Rift (e.g. Armijo *et al.*, 1996; McNeill & Collier, 2004).

7. Conclusion

With the aid of traditional mapping methods as well as drone photometry, the sedimentology and the sequence stratigraphy of the area has been described and interpreted. With the aid of the cross-sections and the trajectory built from them, a general vertical succession was generated, and this knowledge was used when fulfilling the aims by linking current marine terrace levels with constant uplift rates in order to find a best-fit age constraint.

- A differentiation was made between terraces of depositional (topsets) and erosional (marine) origin, a map was made accordingly.
- At least 13 marine terraces were mapped and described sedimentologically, many of them logged in detail and a few were logged laterally in order for a correlation to be made to determine the lateral continuity of marine terraces, which was shown to be very high compared to terraces of fluvial origin.
- The marine terraces are predominantly of beachface facies, with some shoreface deposits present in a few marine terraces.
- Trajectories made indicated transgressive events within terraces have occurred, where the original terrace was cannibalised and then re-deposited at a slightly higher elevation.

Transgression between terraces is a possibility, but no clear evidence of such events was found.

- Armijos method does not work as it does not take into account small-scale sea-level changes and may overlook transgressive events. In a broad spectrum, yes, the large-scale mapping Armijo *et al.* (1996) generated works, however, it is not entirely accurate as it overlooks sedimentological variations as well as sequence stratigraphic variations and thusly can leave a large margin for error when implicating this model for e.g. the subsurface.
- Correlations between marine terrace elevations with uplift rates have suggested that not all terraces are generated by highstands, in some cases uplift appears to be enough. Correlations further indicate that an uplift rate of 1.3 mm/year or slightly higher may be appropriate in this area as 1.6 mm/year did not provide the best fit, however, this is when assuming a constant uplift rate.

It would be very interesting if this area was continuously studied, especially the silt-fine sand sediment which appears to be localised in a few areas. The deposits were not of direct relevance for the marine terraces and were therefore not extensively studied, although from a sequence stratigraphic viewpoint they are most interesting. Furthermore, a study following the terraces laterally, whether the depositional terraces or the marine terraces dominate and what impact they would have on a reservoir would be intriguing as well as beneficial from an economic stand-point. Another potential study would be to investigate if there is a way to determine if a terrace is formed by uplift or by transgression.

References

Anderson, R. S., Densmore, A. L. and Ellis, M. A. (1999). The generation and degradation of marine terraces. *Basin Research*, **11(1)**, pp. 7-19.

Armijo, R., Meyer, B., King, G., Rigo, A. and Papanastassiou, D. (1996). Quaternary evolution of the Corinth Rift and its implications for the Late Cenozoic evolution of the Aegean. *Geophysical Journal International*, **126(1)**, pp.11-53.

Armijo, R., Meyer, B., Hubert, A. and Barka, A. (1999). Westward propagation of the north Anatolian into the northern Aegean: timing and kinematics. *Geology*, **27(3)**, pp. 267-270.

Avallone, A., Briole, P., Agatza-Balodimou, A.M., Billiris, H., Charade, O., Mitsakaki, C., Nercessian, A., Papazissi, K., Paradissis, D., Veis, G., (2004). Analysis of eleven years of deformation measured by GPS in the Corinth Rift Laboratory area. *Comptes Rendus Geosciences*, **336(4)**, pp. 301-311.

Backert, N., Ford, M. and Malartre, F. (2010). Architecture and sedimentology of the Kerinitis Gilbert-type fan delta, Corinth Rift, Greece. *Sedimentology*, **57(2)**, pp. 543-586.

Bardaji, T., Dabrio, C. J., Goy, J. L., Somoza, L. and Zazo, C. (1990). Pleistocene fan deltas in southeastern Iberian peninsula: sedimentary controls and sea-level changes. In: Colella, A. and Prior. D. B. (Eds.), *Coarse-Grained Deltas.* Blackwell Publishing Ltd., Oxford, UK, pp. 129-151.

Bell, R. E., McNeill, L. C., Bull, J. M., and Henstock, T. J. (2008). Evolution of the offshore western Gulf of Corinth, *Geological Society of America Bulletin*, **120(1-2)**, pp. 156–178.

Bergman, K. M. and Walker, R. G. (1987). The importance of sea-level fluctuations in the formation of linear conglomerate bodies; Carrot Creek Member of the Cardium Formation, Cretaceous Western Interior Seaway, Alberta, Canada. *Journal of Sedimentary Research*, **57(4)**, pp. 651-665.

Bernard, P., Lyon-Caen, H., Briole, P., Deschamps, A., Boudin, F., Makropoulos, K., Papadimitriou, P., Lemeille, F., Patau, G., Billiris, H., Paradissis, D., Papazissi, K., Castarède, H., Charade, O., Nercessian, A., Avallone, A., Pacchiani, F., Zahradnik, J., Sacks, S., Linde, A. (2006). Seismicity, deformation and seismic hazard in the western rift of Corinth: new insights from the Corinth Rift Laboratory (CRL), *Tectonophysics*, **426(1-2)**, pp. 7-30.

Breda, A., Mellere, D. and Massari, F. (2007). Facies and processes in a Gilbert-delta-filled incised valley (Pliocene of Ventimigli, NW Italy). *Sedimentary Geology*, **200(1)**, pp. 31-55.

Briole, P., Rigo, A., Lyon-Caen, H., Ruegg, J., Papazissi, K., Mistakaki, C., Balodimou, A., Veis, G., Hatzfeld, D. and Deschamps, A. (2000). Active deformation, of the Gulf of Korinthos, Greece: results from repeated GPS surveys between 1990 and 1995, *Journal of Geophysics Research*, **105(11)**, pp. 25605-25625.

Chappell, J. (1974). Geology of coral terraces, Huon Peninsula, New Guinea: a study of Quaternary tectonic movements and sea-level changes. *Geological Society of America Bulletin*, **85(4)**, pp. 553-570.

Clarke, P. J., Davies, R. R., England, P. C., Parsons, B., Billiris, H., Paradissis, D., Veis, G., Cross, P. A., Denys, P. H., Ashkenazi, V., Bingley, R., Kahle, H. G., Muller, M. V. and Briole, P (1998). Crustal strain in central Greece from repeated GPS measurements in the interval 1989-1997, *Geophysical Journal International*, **135(1)**, pp. 195-214.

Clifton, H. E. (1973). Pebble segregation and bed lenticularity in wave-worked versus alluvial gravel. *Sedimentology*, **20(2)**, pp. 173-187.

Collier, R. E. LL. (1990). Eustatic and tectonic controls upon the Quaternary coastal sedimentation in the Corinth Basin, Greece. *Journal of the Geological Society, London*, **147(2)**, pp. 301-314.

Collier, R. E. LL., Leeder, M. R., Rowe, P. J. & Atkinson, T. C. (1992). Rates of tectonic uplift in the Corinth and Megara Basins, central Greece. *Tectonics*, **11(6)**, pp. 1159–1167.

De Gelder, G., Fernández-Blanco, D., Lacassin, R., Armijo, R., Delorme, A., Jara-Muñoz, J. and Melnick, D. (2015). Corinth terraces re-visited: Improved paleoshoreline determination using Pleiades-DEMs. *Geotectonic Research*, **97(1)**, pp. 12-14.

De Gelder, G., Fernández-Blanco, D., Melnick, D., Duclaux, G., Bell, R. E., Jara-Muñoz, J., Armijo, R. and Lacassin, R. (2018). Fault flexure and lithospheric rheology set from climate cycles in the Corinth Rift, To be published in: *Geology*.

Demoulin, A., Beckers, A. and Hubert-Ferrari, A. (2015). Patterns of Quaternary uplift of the Corinth rift southern border (N Peloponnese, Greece) revealed by fluvial landscape morphometry. *Geomorphology*, **246**, pp. 188-204.

Depéret, C. (1913). Observations sur l'histoire géologique pliocène et quaternaire du golfe et de l'isthme de Corinthe, *Comptes rendus hebdomadaires des séances de l'Académie des Sciences*, **156**, pp. 427-431, 659-663, 1048-1052.

Dia, A. N., Cohen, A. S., O'Nions, R. K. and Jackson, J. A. (1997). Rates of uplift investigated through 230Th dating in the Gulf of Corinth (Greece). *Chemical Geology*, **138(3-4)**, pp. 171–184.

Doutsos, T., Kontopoulos, N. and Poulimenos, G. (1988). The Corinth-Patras rift as the initial stage of continental fragmentation behind an active island arc (Greece), *Basin Research*, **1**, pp. 177-190.

Doutsos, T. and Piper, D. J. E. (1990). Listric faulting, sedimentation, and morphological evolution of the Quaternary eastern Corinth rift, Greece: first stages of continental rifting. *Geological Society of America Bulletin*, **102(6)**, pp. 812-829.

Dufaure, J. J. and Zamanis, A. (1980). Styles neotectoniques et etagements de niveaux marins sur un segment d'arc insulaire, le Peloponntse. In: *Proc. Conf. Niueaux marins et Tectonique Quaternaire dans l'Aire Méditerranéenne*, CNRS, Paris, France, pp. 77-107.

Dupré, W. R., Clifton, H. E. and Hunter, R. A. (1980). Modern sedimentary facies of the open Pacific Coast and Pleistocene analogs from Monterey Bay, California. In: Field, M. E. *et al.* (Eds.), *Quaternary Depositional Environments of the Pacific Coast*, Society of Economic Paleontologists and Mineralogists Pacific section, Tulsa, pp. 105-120.

El-Hames, A. S. and Richards, K. S. (1994). Progress in arid-lands rainfall-runoff modelling. *Progress in Physical Geography*, **18(3)**, pp. 343-365.

Emery, K. O. (1955). Grain size of marine beach gravels. *Journal of Geology*, **63(1)**, pp. 39-49.

Ford, M., Rohais, S.,Williams, E., Bourlange, S., Jousselin, D., Backert, N., Malartre, F. (2013). Tectono-sedimentary evolution of the western Corinth rift (Central Greece). *Basin Research*, **25(1)**, pp. 3–25.

Frébourg, G., Hasler, C. A., Davaud, E. (2012). Uplifted marine terraces of the Akamas Peninsula (Cyprus): evidence of climatic conditions during the Late Quaternary highstands. *Sedimentology*, **59(5)**, pp. 1409-1425.

Freyberg, B. (1973) Geologie des Isthmus von Korinth. *Erlanger Geologische Abhandlungen*, **95**, pp. 1-183.

Gawthorpe, R. L. and Leeder, M. R. (2000). Tectono-sedimentary evolution of active extentional basins, *Basin Research*, **12**, pp. 196-218.

Gawthorpe, R. L., Leeder, M., Kranis, H., Skourtsos, E., Andrews, J., Henstra, G., Mack, G., Muravchik, M., Turner, J. and Stamatakis, M. (2017). Tectono-sedimentary evolution of the Plio-Pleistocene Corinth rift, Greece. *Basin Research*, **30(3)**, pp. 448-479.

Gobo, K., Ghinassi, M. and Nemec, W. (2014). Reciprocal changes in foreset to bottomset facies in a Gilbert-type delta: response to short-term changes in base level. *Journal of Sedimentary Research*, **84(11)**, pp. 1079-1095.

Gobo, K., Ghinassi, M. and Nemec, W. (2015). Gilbert-type deltas recording short-term base-level changes: Delta-brink morphodynamics and related foreset facies. *Sedimentology*, **62(7)**, pp. 1923-1949.

Hart, B. S. and Plint, A. G. (1989). Gravelly shoreface deposits: a comparison of modern and ancient facies sequences. *Sedimentology*, **36(4)**, pp. 551-557.

Hart, B. S. and Plint, A. G. (1995). Gravelly Shoreface and beachface deposits. In: Guy Plint, A. (Eds.), *Sedimentary Facies Analysis*, 1st ed., Blackwell Science, Oxford, UK.

Helland-Hansen, W. and Martinsen, O. J. (1996). Shoreline trajectories and sequences: description of variable depositional-dip scenarios. *Journal of Sedimentary Research*, **66(4)**, pp. 670-688.

Horrillo-Caraballo, J. and Reeve, D. (2010). An investigation of the performance of a data-driven model on sand and shingle beaches. *Marine Geology*, **274(1-4)**, pp. 120-134.

Hågenvik, A. (2018). *Forced regression in rift shoulder derived deltas*. MSc, University of Bergen, Bergen.

Jackson, J. A., Gagnepain, J., Houseman, G., King, G. C. P., Papadimitriou, P., Soufleris, C. and Virieux, J. (1982). Seismicity, normal faulting, and the geomorphological development of the Gulf of Corinth (Greece): the Corinth earthquakes of February and March 1981- *Earth and Planetary Science Letter*, **57(2)**, pp. 377-397.

Jennings, R. and Shulmeister, J. (2002). A field based classification scheme for gravel beaches. *Marine Geology*, **186(3-4)**, pp. 211-228.

Johnson, H. D. and Baldwin, C. T. (1996). Shallow clastic seas. In: Reading, H. (Eds.), *Sedimentary Environments: Processes, Facies and Stratigraphy*, 3rd ed., Blackwell Science, Oxford, UK.

Karp, S. and Stotts, L. B. (2013). *Fundamentals of electro-optic systems design: communications, lidar, and imaging.* Cambridge University Press, Cambridge, UK.

Keraudren, B. and Sorel, D. (1987). The terraces of Corinth (Greece) – A detailed record of eustatic sea-level variations during the last 500,000 years. *Marine Geology*, **77(1-2)**, pp. 99-107.

Kershaw, S., Li Guo, L. and Braga, J. C. (2005). A Holocene coral-algal reef at Mavra Litharia, Gulf of Corinth, Greece: structure, history, and applications in relative sea-level change, *Marine Geology*, **215(3-4)**, pp.171-192.

Kirk, R. M. (1980). Mixed sand and gravel beaches: morphology, processes and sediments. *Progress in Physical Geography*, **4(2)**, pp. 189-210.

Komar, P. D. (2005). Hawke's Bay: Environmental Change, Shoreline Erosion & Management Issues. HBRC Plan number 3839. Asset Management Group Technical Report. Napier. ISSN 1174 3085.

Lajoie, K. R. (1986). Coastal tectonics. In: *Active Tectonics*. National Academic Press, Washington, DC, USA, pp. 95-124.

Leeder, M. R., McNeill, L. C., Portman C., Rowe, P. J. and Andrews, J. E. (2003). Corinth rift margin uplift: New evidence from Late Quaternary marine shorelines. *Geophysical Research Letters*, **30(12)**, pp. 131-134.

Leeder, M. R., Portman, C., Andrews, J. E., Collier, R. E. LL., Finch, E., Gawthorpe, R. L., McNeill, L. C., Pèrez-Arlucea, M. and Rowe, P. (2005). Normal faulting and crustal deformation, Alkyonides Gulf and Perachora peninsula, eastern Gulf of Corinth rift, Greece. *Journal of the Geological Society, London*, **162**, pp. 549–561.

Leithold, E. L. and Bourgeois, J. (1984). Characteristics of coarse-grained sequences deposited in nearshore, wave-dominated environments-example from the Miocene of south-west Oregon. *Sedimentology*, **31(6)**, pp. 749-775.

Leszczyński, S. and Nemec, W. (2014). Dynamic stratigraphy of composite peripheral unconformity in a foredeep basin. *Sedimentology*, **62(3)**, pp. 645-680.

Lowe, D. R. (1982). Sediment gravity flows, II. Depositional models with special reference to the deposits of high-density turbidity currents. *Journal of Sedimentary Research*, **52(1)**, pp. 279-297.

Maejima, W. (1982). Texture and stratification of gravelly beach sediments, Enju Beach, Kii Peninsula, Japan. *Journal of Geocience. Osaka City University*, **25**, pp. 35-51.

Massari, F. and Parea, G. C. (1988). Progradational gravel beach sequences in a moderate- to high-energy, microtidal marine environment. *Sedimentology*, **35(6)**, pp.881-913.

Massari, F. and Parea, G. C. (1990). Wave-dominated Gilbert-type gravel deltas in the hinterland of the Gulf of Taranto (Pleistocene, southern Italy). In: Colella, A. and Prior. D. B. (Eds.), *Coarse-Grained Deltas*. Blackwell Publishing Ltd., Oxford, UK, pp. 311-331.

McMurray, L. and Gawthorpe, R. (2000). Along-strike variability of forced regressive deposits: late Quaternary, northern Peloponnesos, Greece. In: Hunt, D. and Gawthorpe, R. (Eds.), *Sedimentary Responses to Forced Regressions*, 1st ed., The Geological Society of London, Oxford, UK

McNeill, L. C. and Collier R. E. LL. (2004). Uplift and slip rates of the eastern Eliki fault segment, Gulf of Corinth, Greece, inferred from Holocene and Pleistocene terraces. *Journal of Geological Society, London*, **161(1)**, pp. 81-92.

Nixon, C. W., McNeill, L. C., Bull, J. M., Bell, R. E., Gawthorpe, R. L., Henstock, T. J., Christodoulou, D., Ford, M., Taylor, B., Sakellariou, D., Ferentinos, G., Papatheodorou, G., Leeder, M. R., Collier, R. E. LL., Goodliffe, A. M., Sachpazi, M. and Kranis, H. (2016). Rapid

spatiotemporal variations in rift structure during development of the Corinth Rift, central Greece. *Tectonics*, **35(5)**, pp. 1225–1248.

Nyst, M. and Thatcher, W. (2004). New constraints on the active tectonic deformation of the Aegean, *Journal of Geophysical Research*, **109**, B11406, epub. doi: 10.1029/2003JB002830.

Ori, G. G. (1989). Geological history of the extensional basin of the Gulf of Corinth (?Miocene-Pleistocene), Greece. *Geology*, **17**, pp. 918-921.

Perissoratis, C., Piper, D. J. W. and Lykousis, V. (1993). Late Quaternary sedimentation in the Gulf of Corinth: the effects of marine-lake fluctuations driven by eustatic sea level changes. In: *Special Publications of the Technical University of Athens*, pp. 693-744.

Pirazzoli, P. A., Stiros, S. C., Fontugne, M. and Arnold, M. (2004). Holocene and Quaternary uplift in the central part of the southern coast of the Corinth Gulf (Greece), *Marine Geology*, **212(1-4)**, pp. 35-44.

Postma, G. (1984a). Slumps and their deposits in fan delta front and slope. *Geology*, **12(1)**, pp. 27-30.

Postma, G. (1984b). Mass-flow conglomerate I a submarine canyon: Abrioja fan delta, Pliocene, southeast Spain. In: Koster, E. H. and Steel, R. J. (Eds.), *Sedimentology of Gravels and Conglomerates*, Canadian Society of Petroleum Geologists, **10**, pp. 237-258.

Postma, G. and Roep, Th. B. (1985). Resedimented conglomerates in the bottomset of a Gilbert type gravel delta. *Journal of Sedimentary Petrology*, **55(6)**, pp. 874-885.

Poulimenos, G. (1993). Tectonics and sedimentation in the western Corinth graben, Greece. *Neues Jahrbuch für Geologie und Paläontologie*, **H10**, pp. 607-630.

Ravnås, R. and Steel, R. J. (1998). Architecture of Marine Rift-Basin Successions, *American Association of Petroleum Geologists*, **82(1)**, pp. 110-146.

Reading, H. and Collinson, J. (1996). Clastic Coasts. In: Reading, H. (Eds.), *Sedimentary Environments: Processes, Facies and Stratigraphy*, 3rd ed., Blackwell Science, Oxford, UK.

Rohais, S., Eschard, R., Ford, M., Guillocheau, F. and Moretti, I. (2007a). Stratigraphic architecture of the Plio-Pleistocene infill of the Corinth Rift: Implications for its structural evolution. *Tectonophysics*, **440(1)**, pp. 5-28.

Rohais, S., Joannin, S., Colin, J. P., Suc, J. P., Guillocheau, F. and Eschard, R. (2007b). Age and environmental evolution of the syn-rift fill of the southern coast of the gulf of Corinth (Akrata-Derveni region, Greece). *Bulletin de la Societe Geologique de France*, **178(3)**, pp. 231-243.

Rohais, S., Eschard, R. and Guillocheau, F. (2008). Depositional model and stratigraphic architecture of rift climax Gilbert-type fan deltas (Gulf of Corinth, Greece). *Sedimentary Geology*, **210**, pp. 132-145.

Schrøder, B. (1975). Bemerkungnen zu marinen Terrassen des Quatars im NE-Peloponnes, Griechenland, *Neues Jahrbuch für Geologie und Paläontologie*, **149**, pp. 148-161.

Sébrier, M. (1977). Tectonique récente d'une transversal à l'Arc Egéen: le Golfe de Corinthe et ses regions périphériques, *Thèse 3ème cycle*, Univ. Paris-Sud, France.

Short, A. D. (1984). Beach and nearshore facies: southeast Australia. *Marine Geology*, **60(1-4)**, pp. 261-282.

Siddall, M., Rohling, E. J., Almogi-Labin, A., Hemleben, C., Meischner, D., Schmelzer, L. and Smeed, D. A. (2003). Sea-level fluctuations during the last glacial cycle. *Nature*, **423(6942)**, pp. 853-858.

Skourtsos, E. and Kranis, H. (2009). Structure and evolution of the western Corinth Rift, through new field data from the Northern Peloponnesus. *Geological Society of London Special Publications*, **321(1)**, pp. 119-138.

Spratt, R. M. and Lisiecki, L. E. (2016). A Late Pleistocene sea level stack. *Climate of the Past*, **12(4)**, pp. 1079-1092.

Stewart, I. (1996). Holocene uplift and palaeoseismicity on the Eliki fault, Western Gulf of Corinth, Greece. *Annali di Geofisica*, **39(3)**, pp. 575-588.

Taylor, B., Weiss, J., Goodliffe, A., Sachpazi, M., Laigle, M. and Hirn, A. (2011). The structures, stratigraphy and evolution of the Gulf of Corinth rift, Greece. *Geophysical Journal International*, **185(3)**, pp. 1189-1219.

Tucker, M. E. (2011). *Sedimentary rocks in the field*. 4th ed., Wiley-Blackwell, Chichester, UK.

Turner, J. A., Leeder, M. R., Andrews, J. E., Rowe, P. J., Van Calsteren, P. and Thomas, L. (2010). Testing rival tectonic uplift models for the Lechaion Gulf in the Gulf of Corinth rift. *Journal of the Geological Society, London*, **167(6)**, pp. 1237-1250.

Zelilidis, A. and Kontopoulos, N. (1996). Significance of fan deltas without toe-sets within rift and piggy-back basins: examples from the Corinth graben and the Meso-Hellenic through, Central Greece. *Sedimentology*, **43(2)**, pp. 253-262.

Zenkovitch, V. P. (1967). *Processes of Coastal Development*. Oliver and Boyd, London, UK.

Online:

Railbacks, L. B. (2015). Marine Isotope Stages and Substages. Available at: http://www.gly.uga.edu/railsback/Fundamentals/SFMGSubstages01.pdf [Accessed 15/10/2018].

Appendix

Contents as following:

Maps

- Map with strike-dip taken from terraces
- Map superposed onto a slope map
- Map with contour-lines, 6 m apart
- Map superposed onto GoogleEarth map of area
- Map with log locations highlighted

Logs

- Key
- Log 1
- Log 2
- Log 3
- Log 4
- Log 5
- Log 6
- Log 7
- Log 8
- Log 9
- Log 10
- Log 11
- Log 12
- Log 13
- Log 14
- Log 15
- Log 16
- Log 17
- Log 18
- Log 19
- Log 20
- Log 21

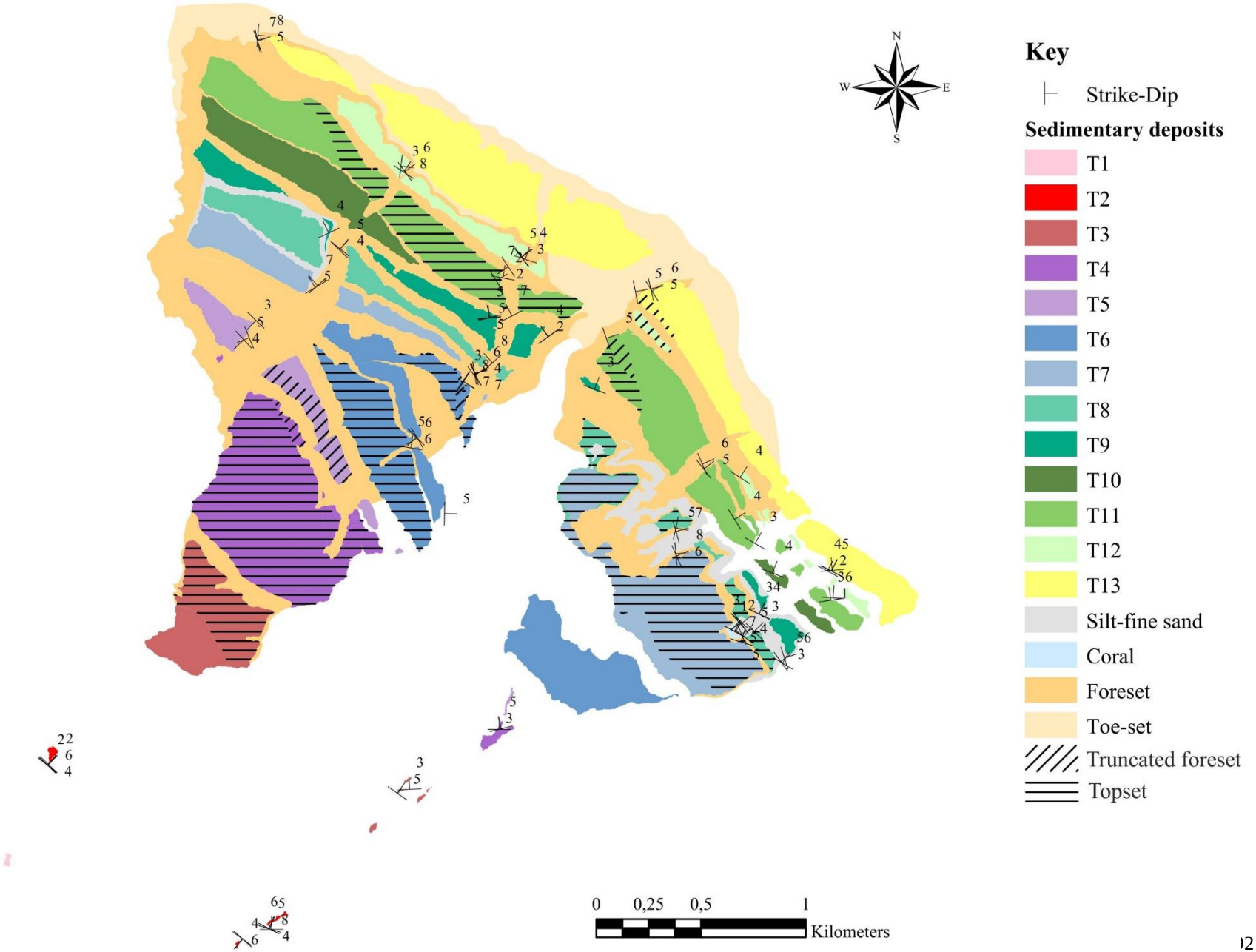
N
W
E
S
Key
Strike-Dip
Sedimentary deposits
T1
T2
T3
T4
T5
T6
T7
T8
T9
T10
T11
T12
T13
Silt-fine sand
Coral
Foreset
Toe-set
Truncated foreset
Topset
0
0,25
0,5
1
Kilometers

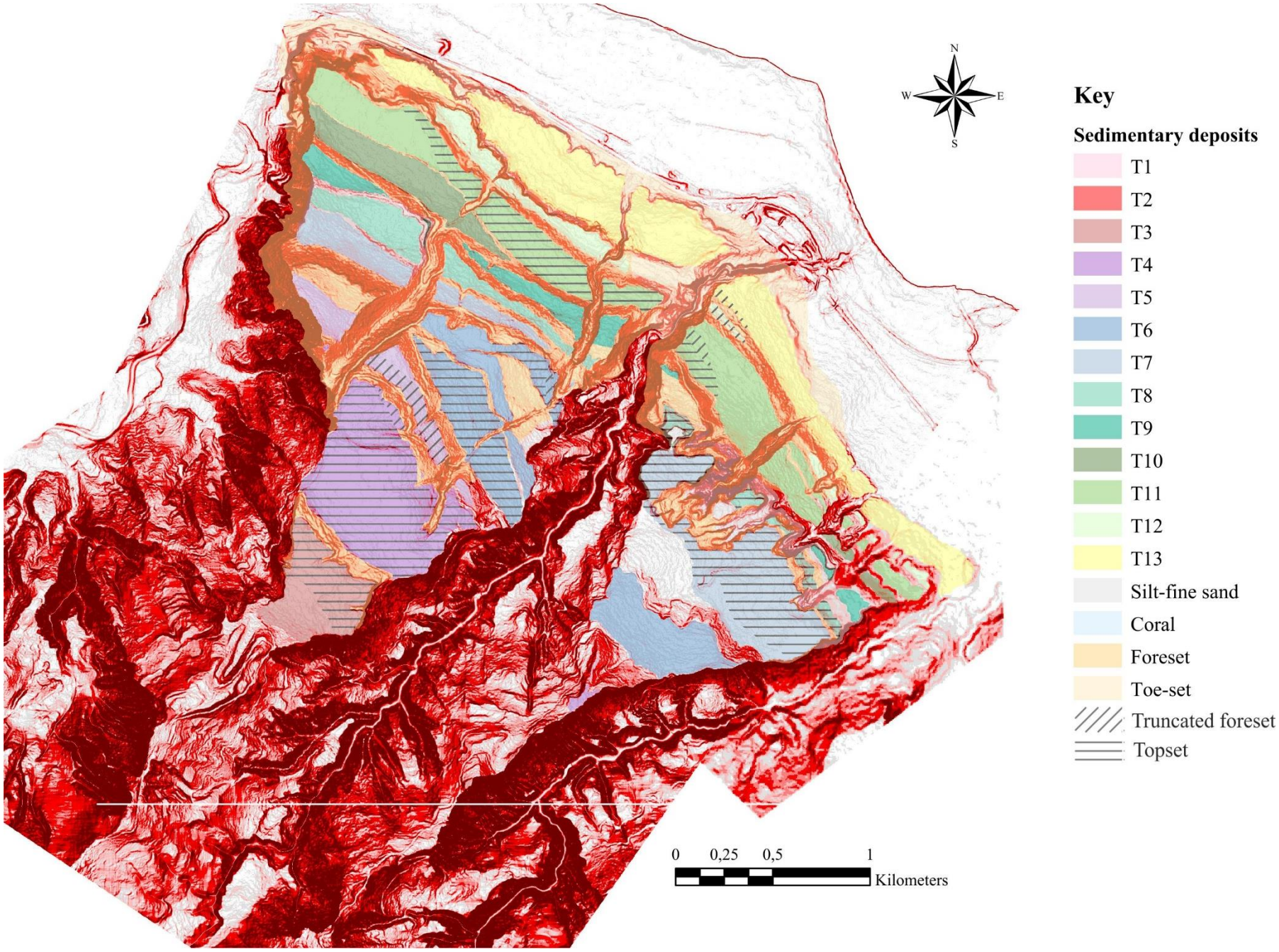
N
W
E
S
Key
Sedimentary deposits
T1
T2
T3
T4
T5
T6
T7
T8
T9
T10
T11
T12
T13
Silt-fine sand
Coral
Foreset
Toe-set
Truncated foreset
Topset
0
0,25
0,5
1
Kilometers

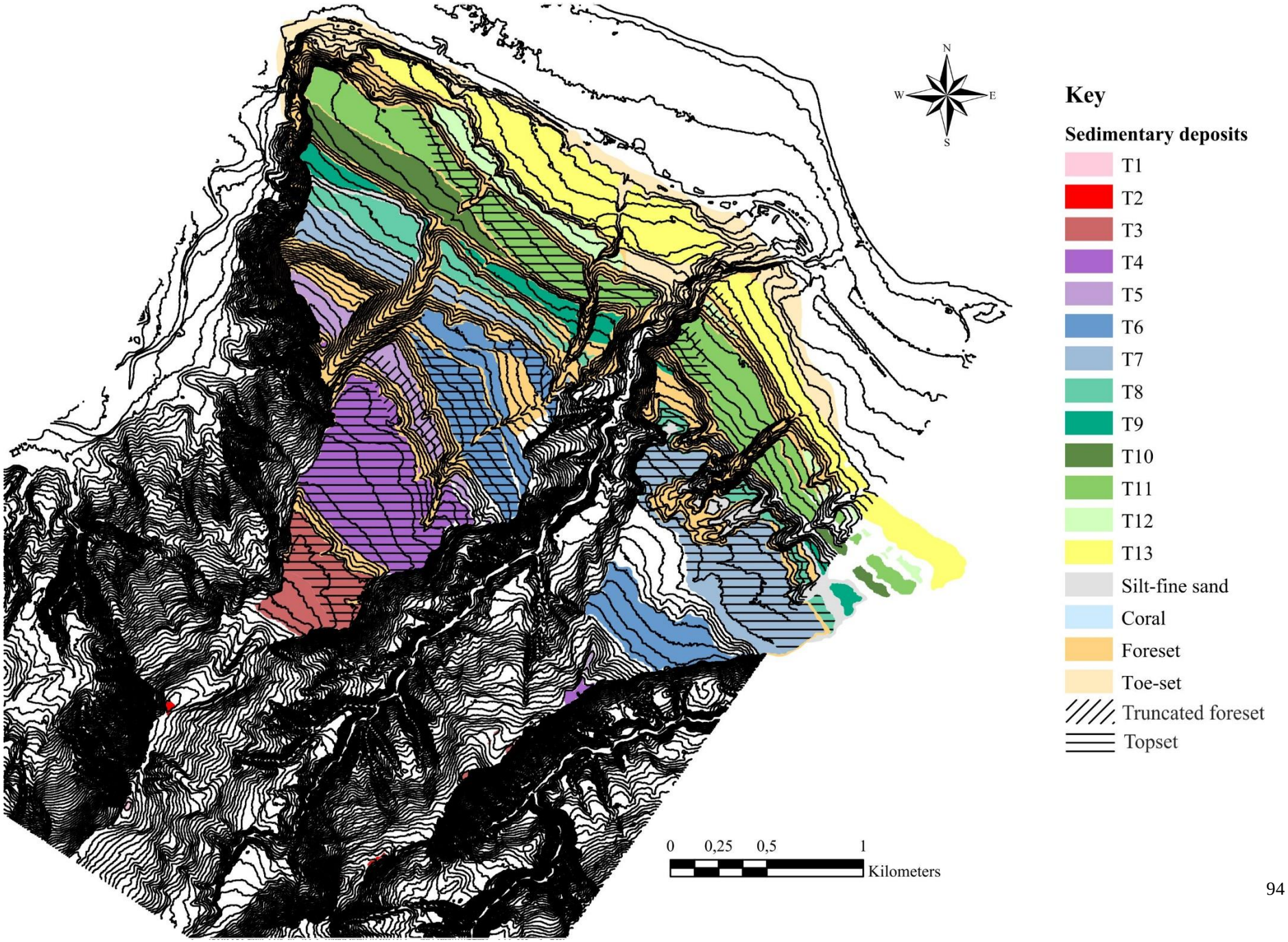
N
W
E
S
Key
Sedimentary deposits
T1
T2
T3
T4
T5
T6
T7
T8
T9
T10
T11
T12
T13
Silt-fine sand
Coral
Foreset
Toe-set
Truncated foreset
Topset
0
0,25
0,5
1
Kilometers

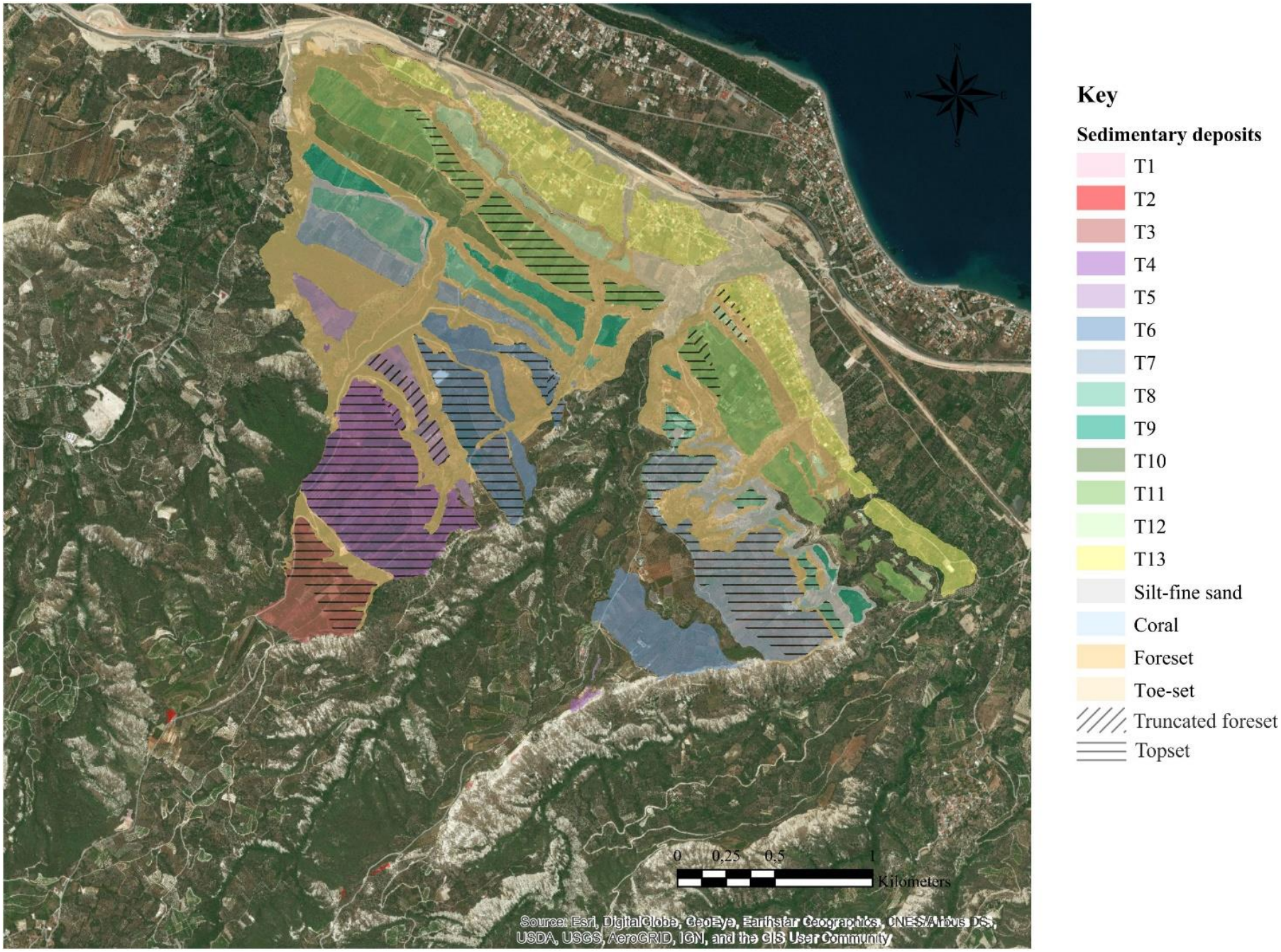
Key
Sedimentary deposits
T1
T2
T3
T4
T5
T6
T7
T8
T9
T10
T11
T12
T13
Silt-fine sand
Coral
Foreset
Toe-set
Truncated foreset
Topset
0
0,25
0,5
1
Kilometers
Source: Esri, DigitalGlobe, GeoEye, Earthstar Geographics, CNES/Airbus DS, USDA, USGS, AeroGRID, IGN, and the GIS User Community

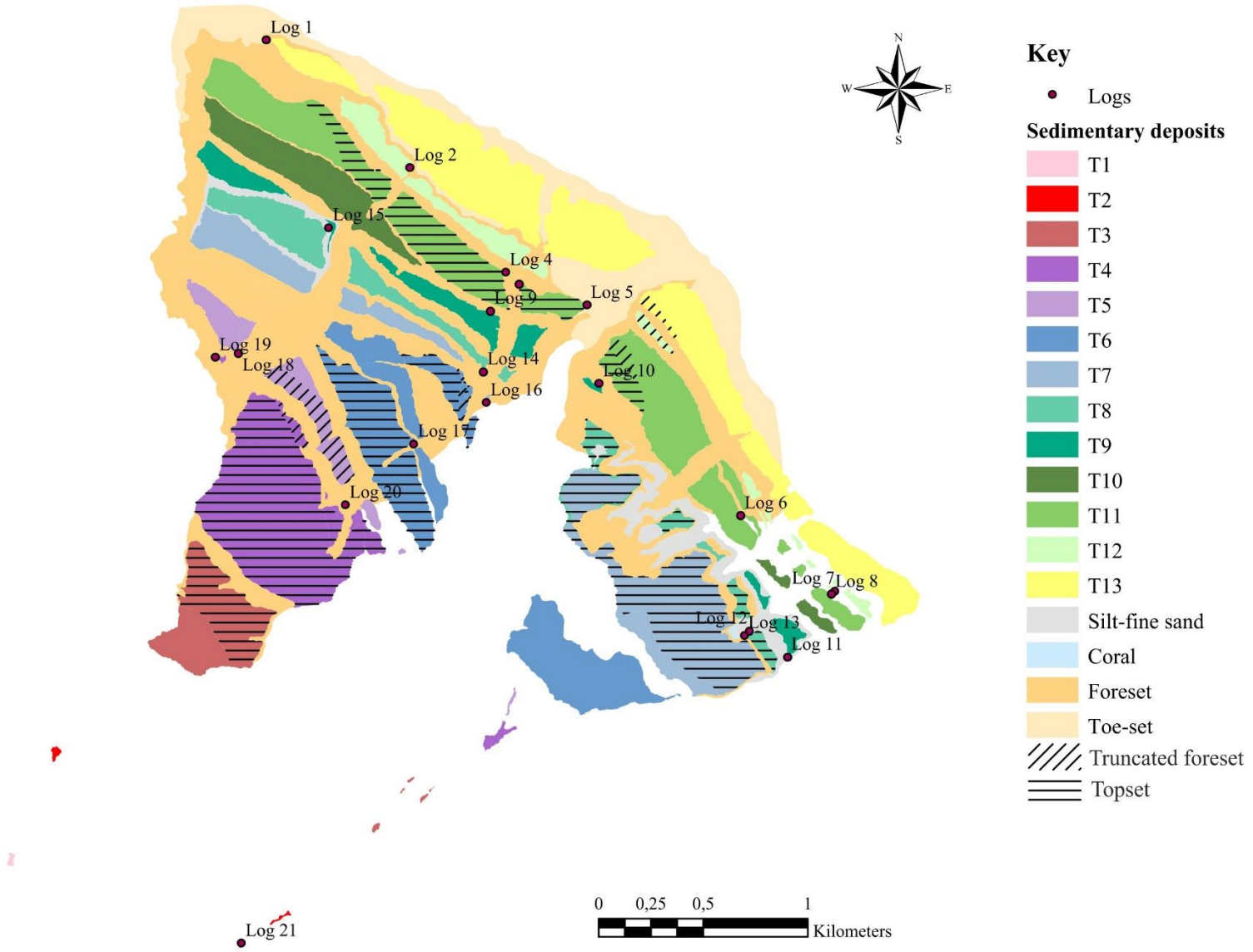
Log 1
Log 2
Log 15
Log 4
Log 9
Log 5
Log 19
Log 18
Log 14
Log 10
Log 16
Log 17
Log 20
Log 6
Log 7
Log 8
Log 12
Log 13
Log 11
Log 21
N
W
E
S
0
0,25
0,5
1
Kilometers
Key
Logs
Sedimentary deposits
T1
T2
T3
T4
T5
T6
T7
T8
T9
T10
T11
T12
T13
Silt-fine sand
Coral
Foreset
Toe-set
Truncated foreset
Topset

Log Key

Lithologies

- Clast-supported conglomerate
- Open-work conglomerate
- Matrix-supported conglomerate
- Sand
- Silt

Qualifiers

- Pebbly
- Granule
- Sandy
- Silty
- Intraclasts
- Calcitic

Bed Contacts

- Planar, sharp
- Planar, gradational
- Irregular, sharp
- Irregular, gradational
- Erosive
- Not visible

Fossils

- Corals
- Bivalve
- Fossil fragment

Biogenic

- Bioturbation

Depositional

- Planar bedding
- Planar lamination
- Wavy bedding
- Wavy lamination
- Inclined bedding
- Structureless
- tr Trough cross-bedding
- Symmetrical ripples
- Imbrication
- Lenses
- 20 Dip
- Normal grading
- Reverse grading
- Normal-reverse grading
- Ct Coarse-tail normal grading
- Ct Coarse-tail reverse grading
- Repeated grading of individual structures
- Channel feature

Other

- Max clast size
- M Mud
- S Silt
- Vfs Very fine sand
- Fs Fine sand
- Ms Medium sand
- Cs Coarse sand
- Vcs Very coarse sand

Facies colour

- MT.1.1
- MT.1.2
- MT.2.1
- MT.2.2
- MT.3
- MT.4
- DT.1
- DT.2
- DT.3
- DF.1
- DF.2.1
- DF.2.2
- C

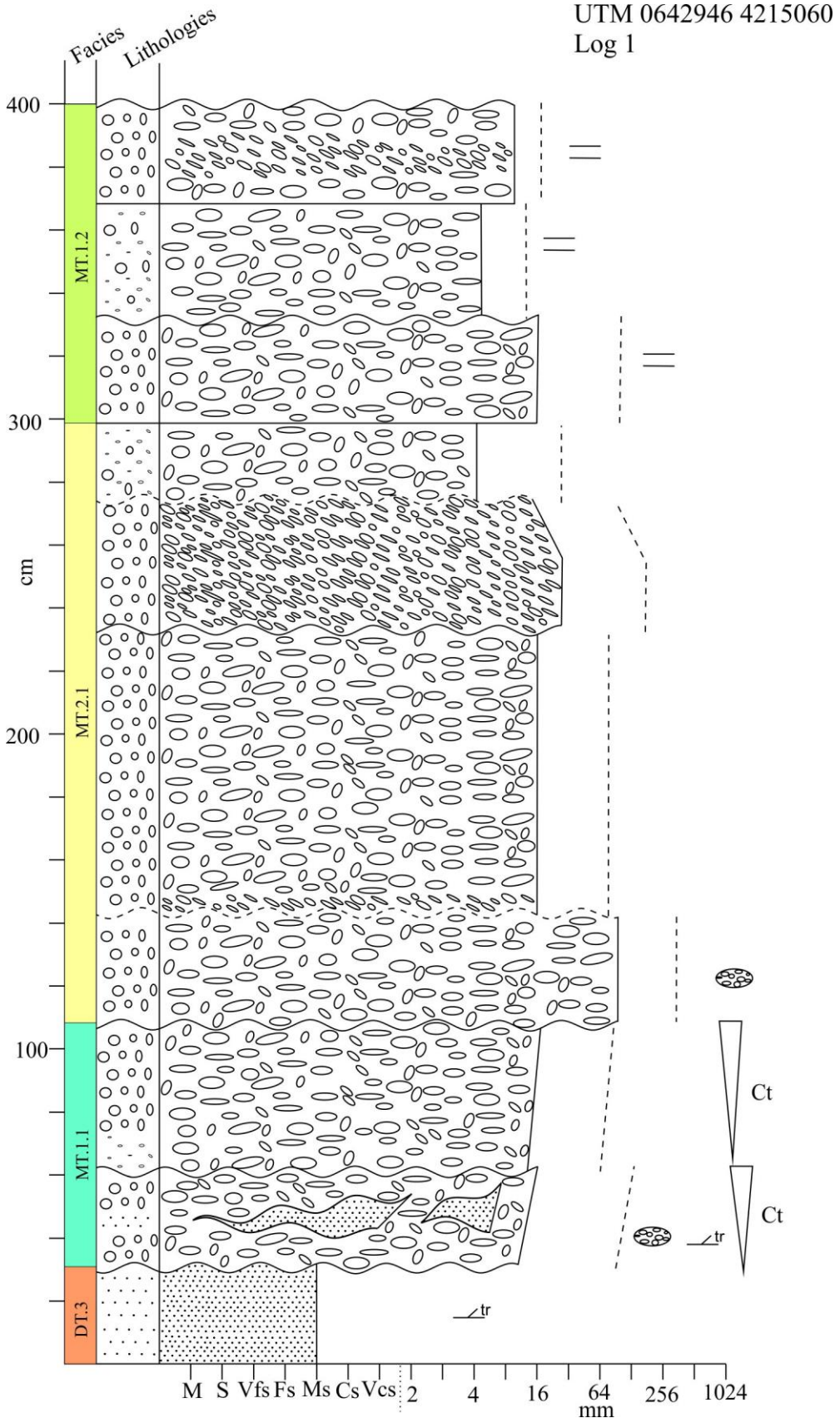
UTM 0642946 4215060
Log 1
Facies
Lithologies
400
300
200
100
cm
MT.1.2
MT.2.1
MT.1.1
DT.3
Ct
Ct
tr
tr
M S Vfs Fs Ms Cs Vcs
2
4
16
64
256
1024
mm

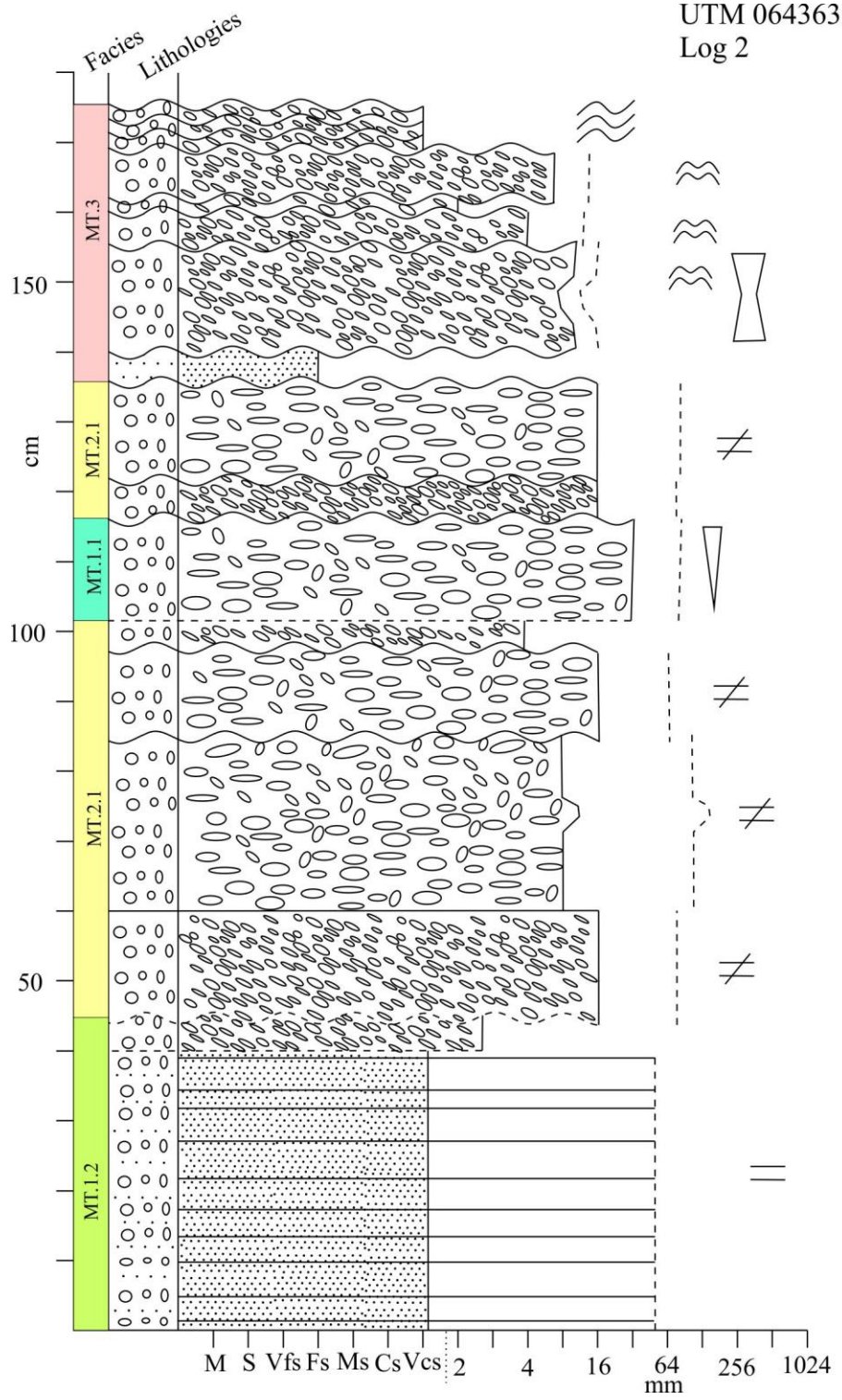
UTM 0643632 4214451
Log 2
Facies
Lithologies
MT.3
MT.2.1
MT.1.1
MT.2.1
MT.1.2
150
100
50
cm
M S Vfs Fs Ms Cs Vcs
2 4 16 64 256 1024
mm

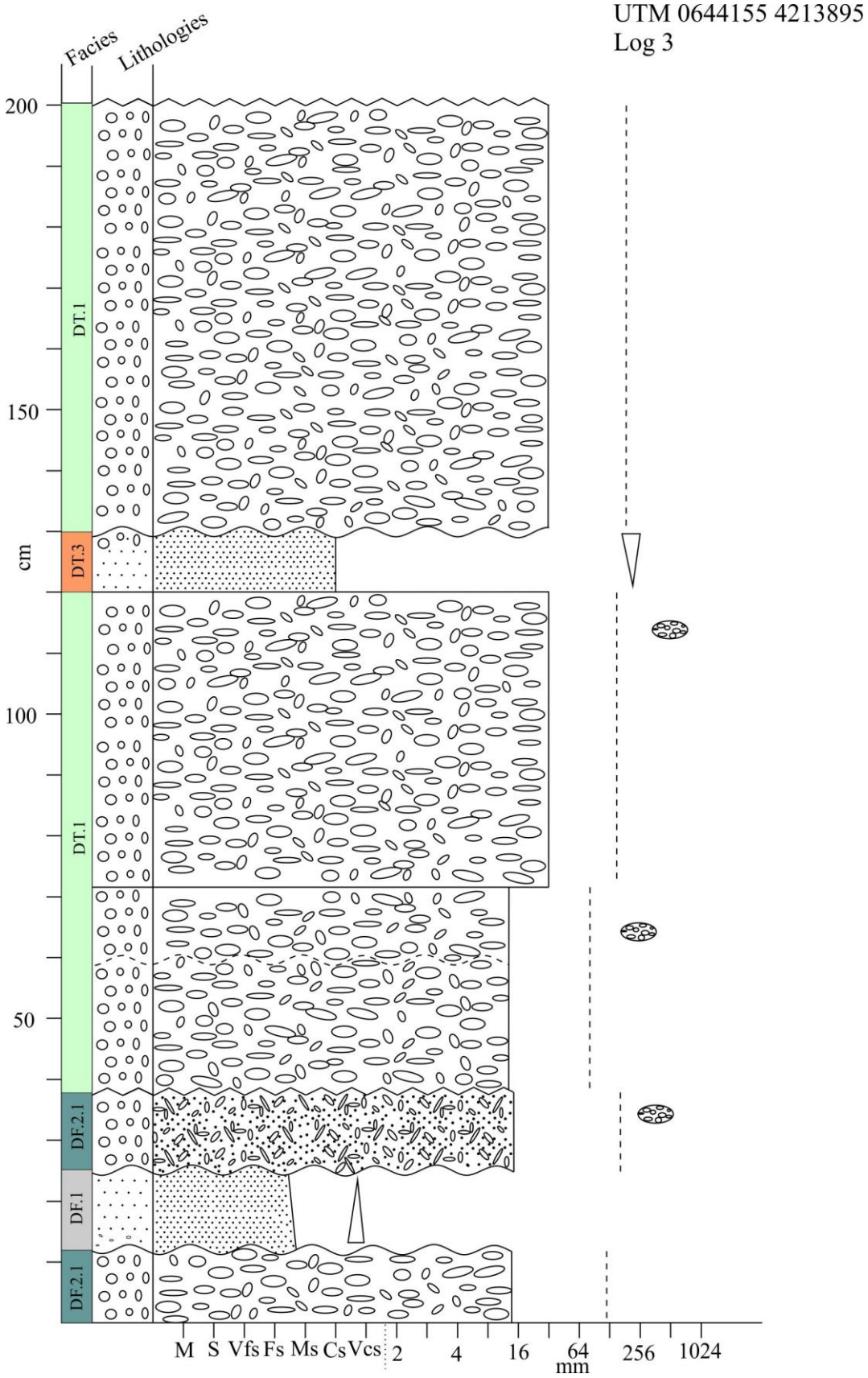
UTM 0644155 4213895
Log 3
Facies
Lithologies
200
150
100
50
cm
DT.1
DT.3
DT.1
DF.2.1
DF.1
DF.2.1
M S Vfs Fs Ms Cs Vcs 2 4 16 64 256 1024
mm

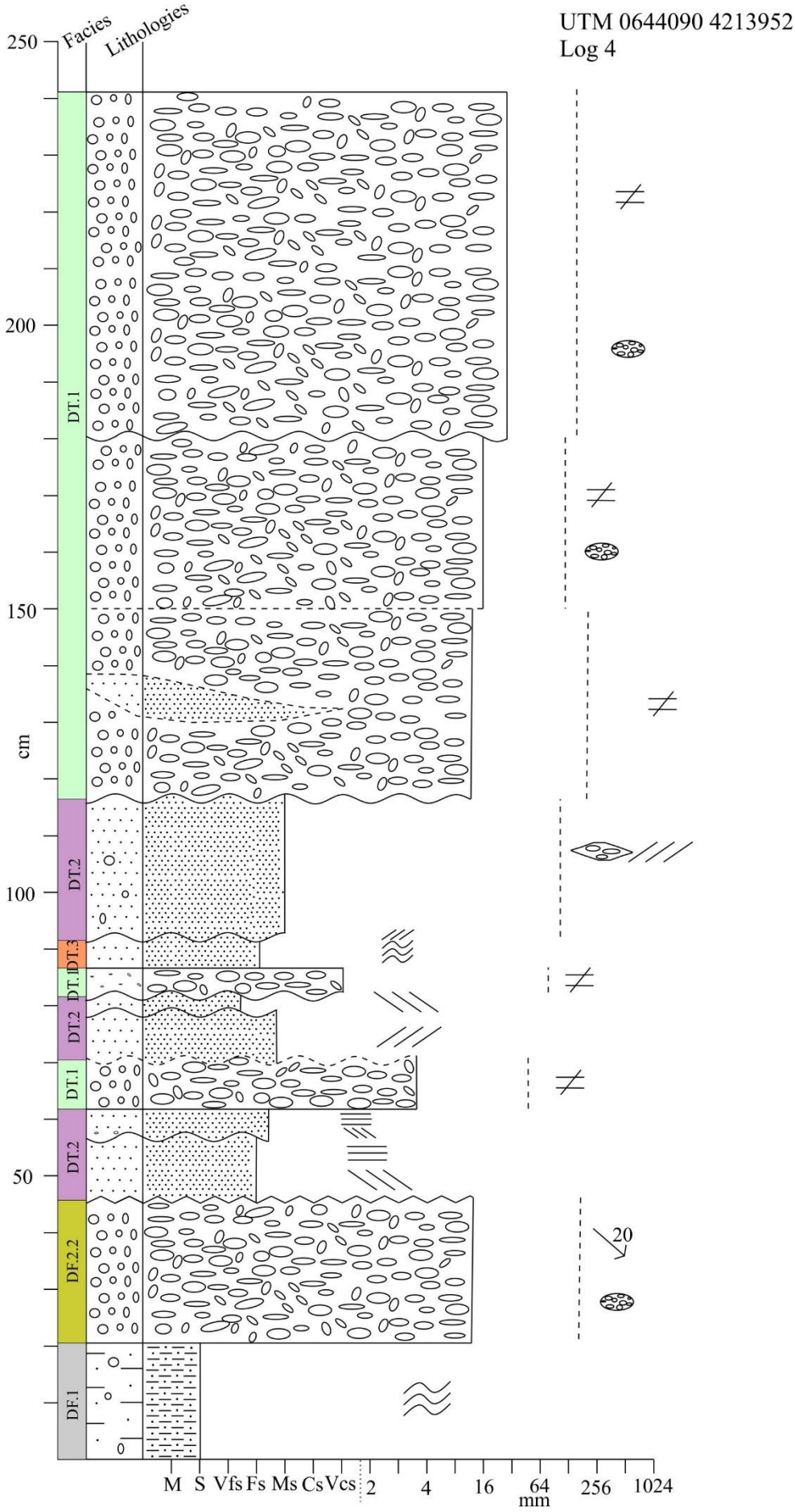
UTM 0644090 4213952
Log 4
Facies
Lithologies
250
200
150
100
50
cm
DT.1
DT.2
DT.3
DT.1
DT.2
DT.1
DT.2
DF.2.2
DF.1
20
M S Vfs Fs Ms Cs Vcs 2 4 16 64 256 1024
mm

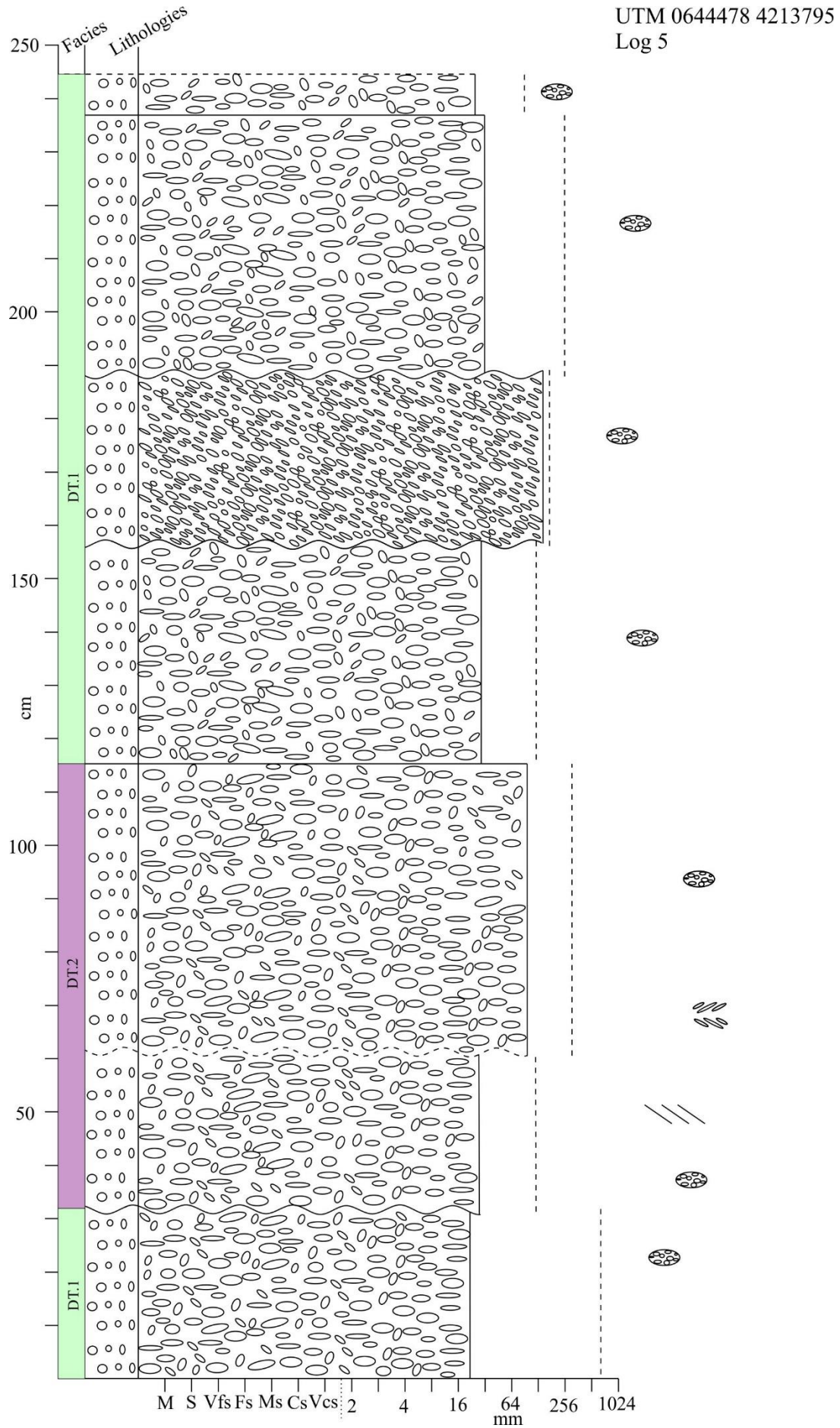
UTM 0644478 4213795
Log 5
Facies
Lithologies
250
200
150
100
50
cm
DT.1
DT.2
DT.1
M S Vfs Fs Ms Cs Vcs 2 4 16 64 256 1024
mm

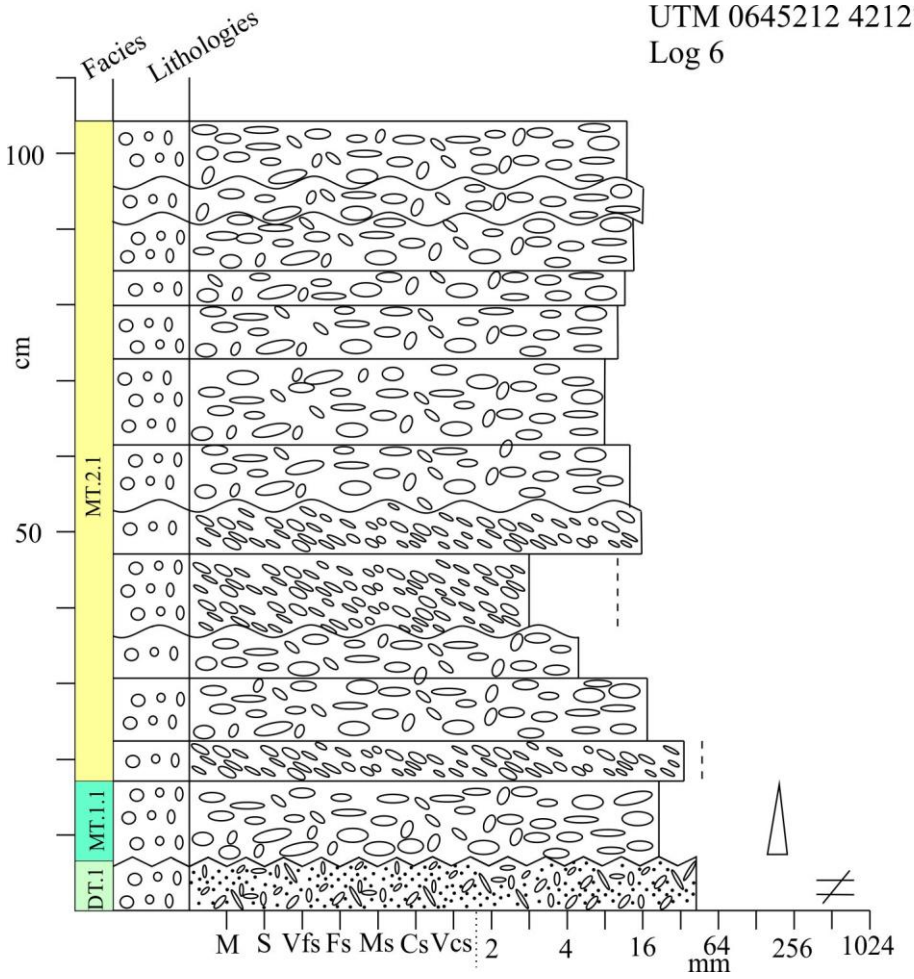
UTM 0645212 4212789
Log 6
Facies
Lithologies
100
50
cm
MT.2.1
MT.1.1
DT.1
M S Vfs Fs Ms Cs Vcs 2 4 16 64 256 1024
mm

UTM 0645646 4212415
Log 7

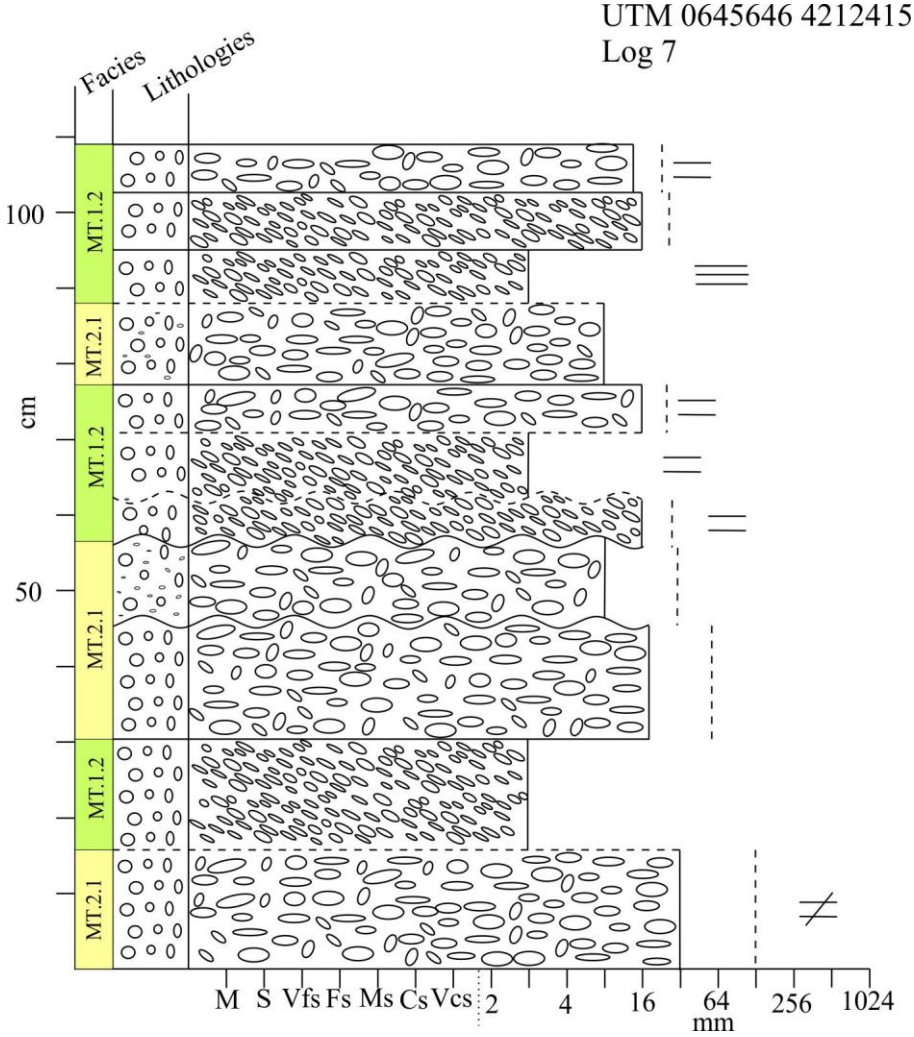

UTM 0645664 4212428
Log 8

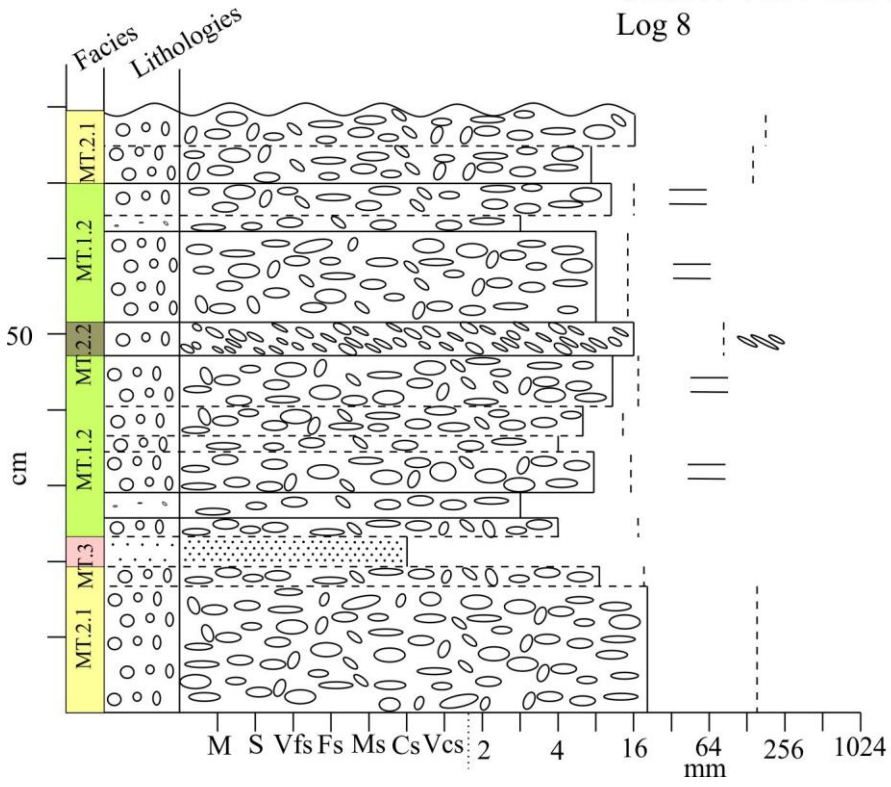

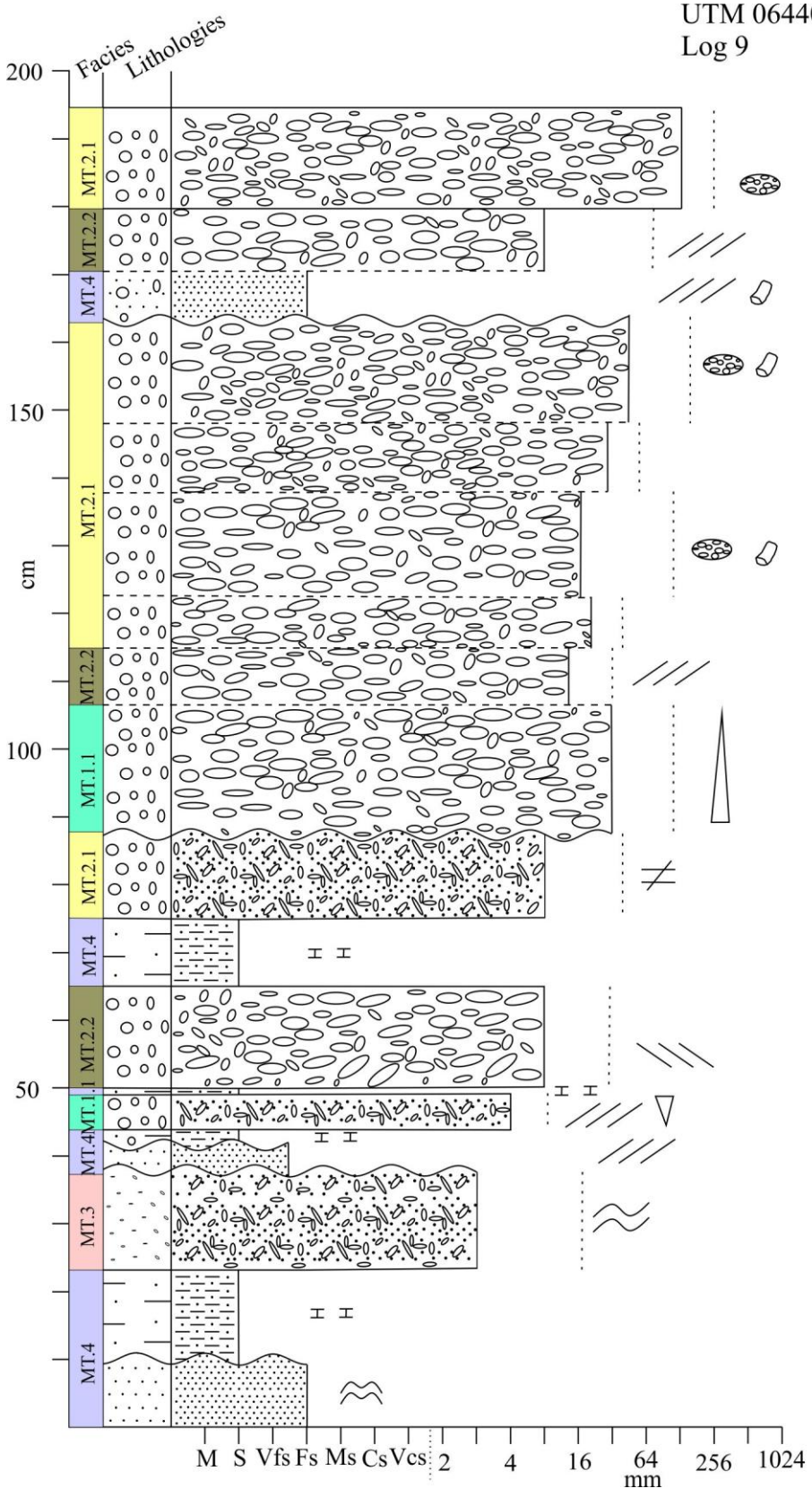
UTM 0644016 4213766
Log 9
Facies
Lithologies
200
150
100
50
cm
MT.2.1
MT.2.2
MT.4
MT.2.1
MT.2.2
MT.1.1
MT.2.1
MT.4
MT.2.2
MT.1.1
MT.4
MT.3
MT.4
M S Vfs Fs Ms Cs Vcs 2 4 16 64 256 1024
mm

UTM 0644536 4213420
Log 10

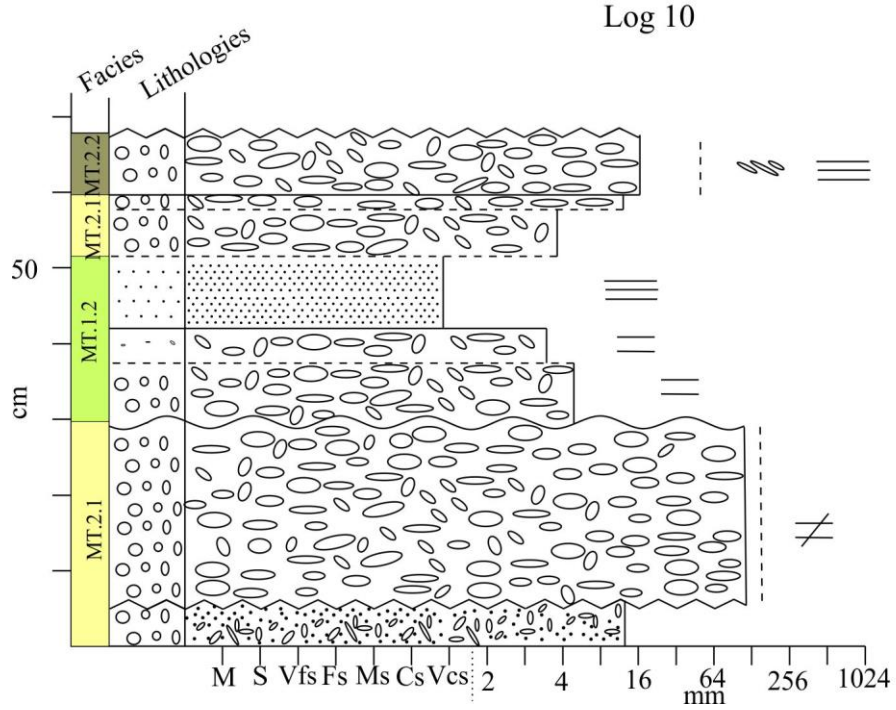

UTM 0645438 4212113
Log 11

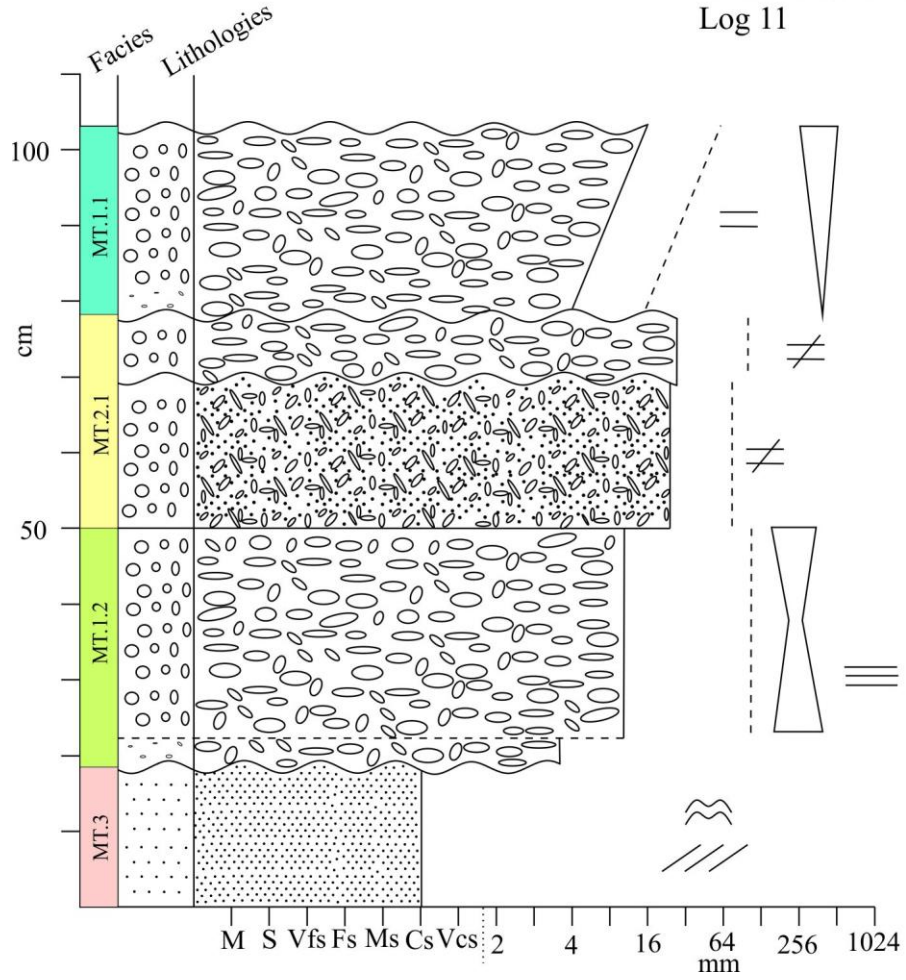

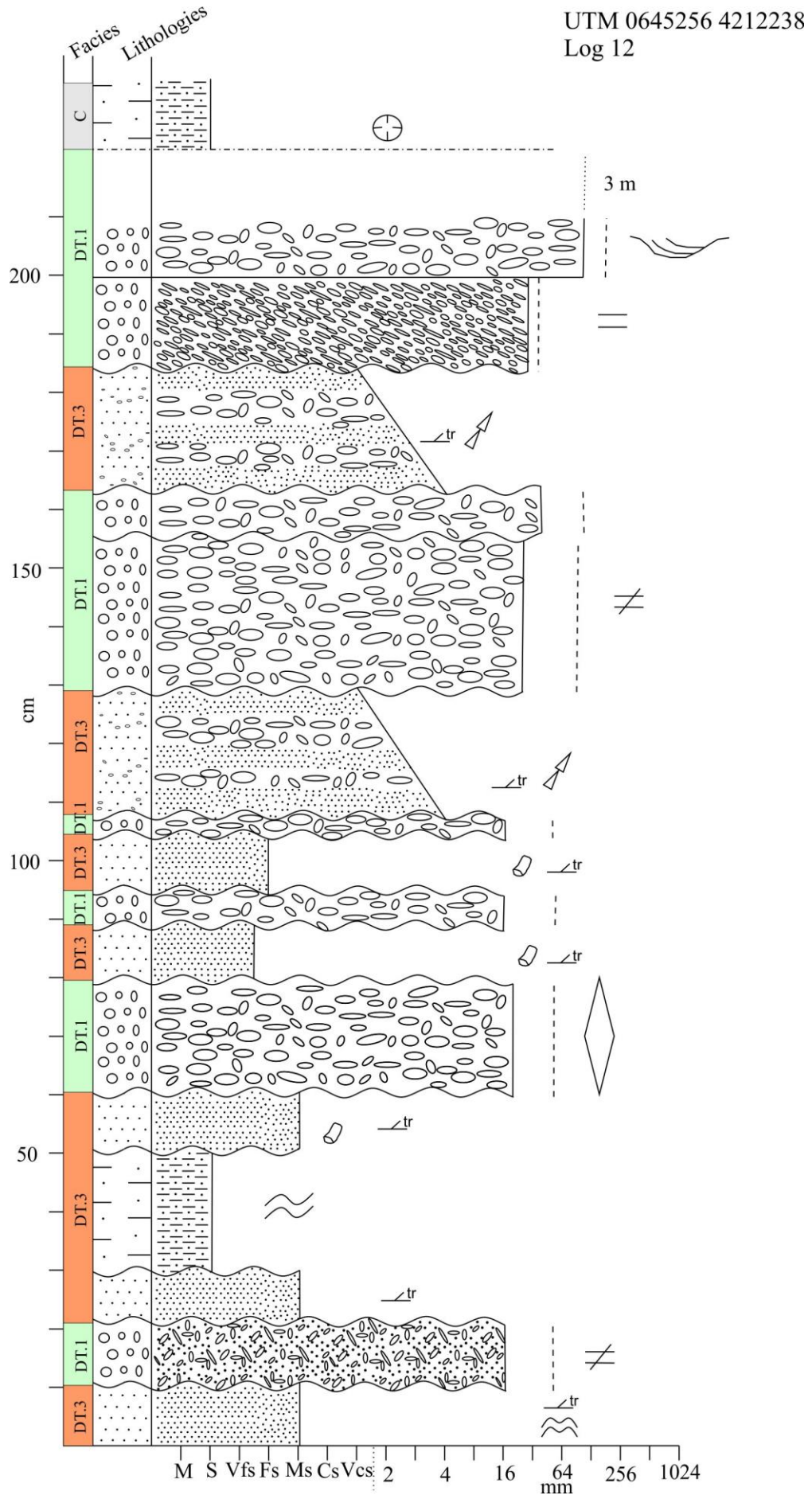
UTM 0645256 4212238
Log 12
Facies
Lithologies
C
DT.1
DT.3
3 m
200
150
100
50
cm
tr
M S Vfs Fs Ms Cs Vcs 2 4 16 64 256 1024
mm

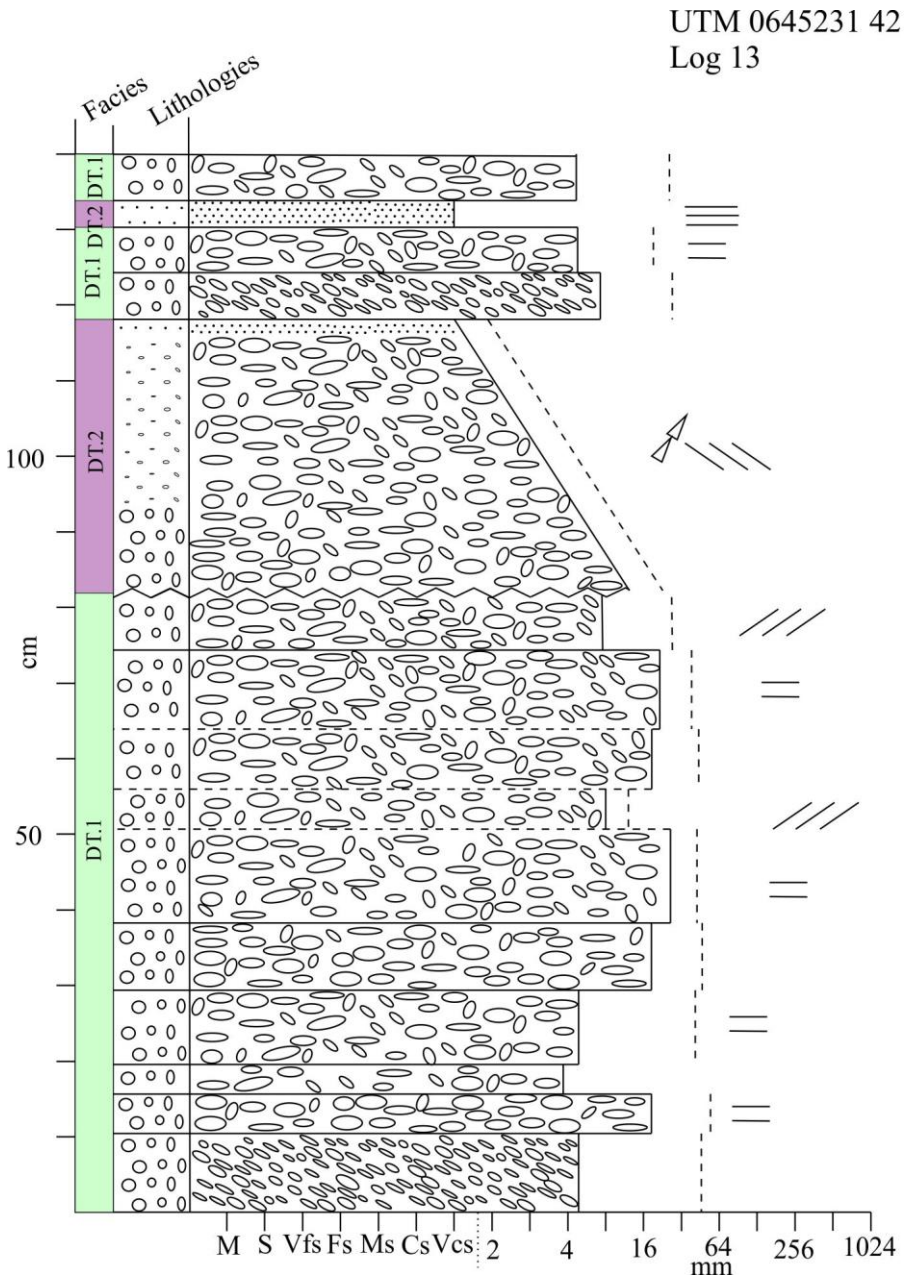
UTM 0645231 4212217
Log 13
Facies
Lithologies
DT.1
DT.2
DT.1 DT.2
DT.2
DT.1
100
50
cm
M S Vfs Fs Ms Cs Vcs 2 4 16 64 256 1024
mm

UTM 0643983 4213476
Log 14

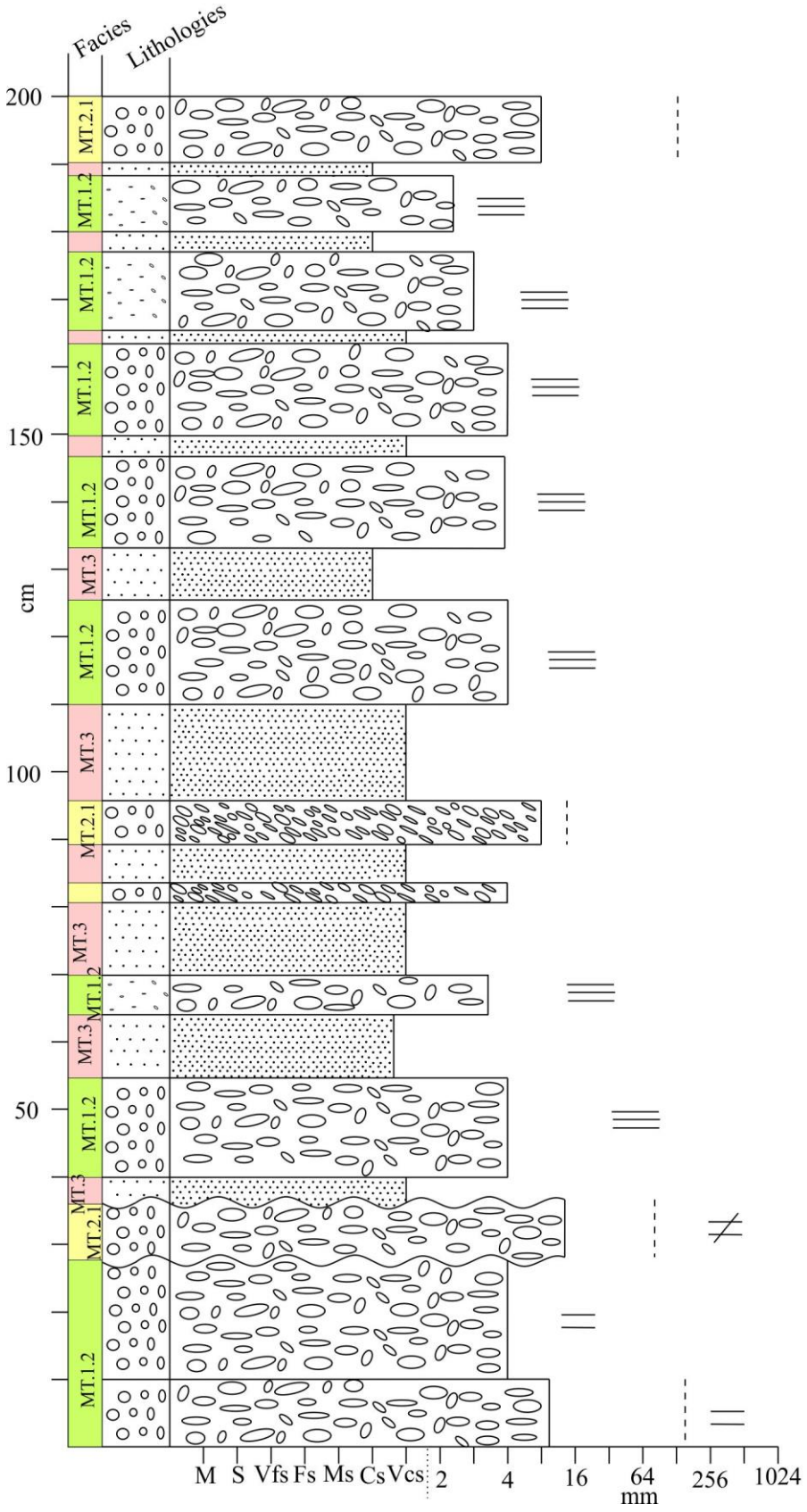

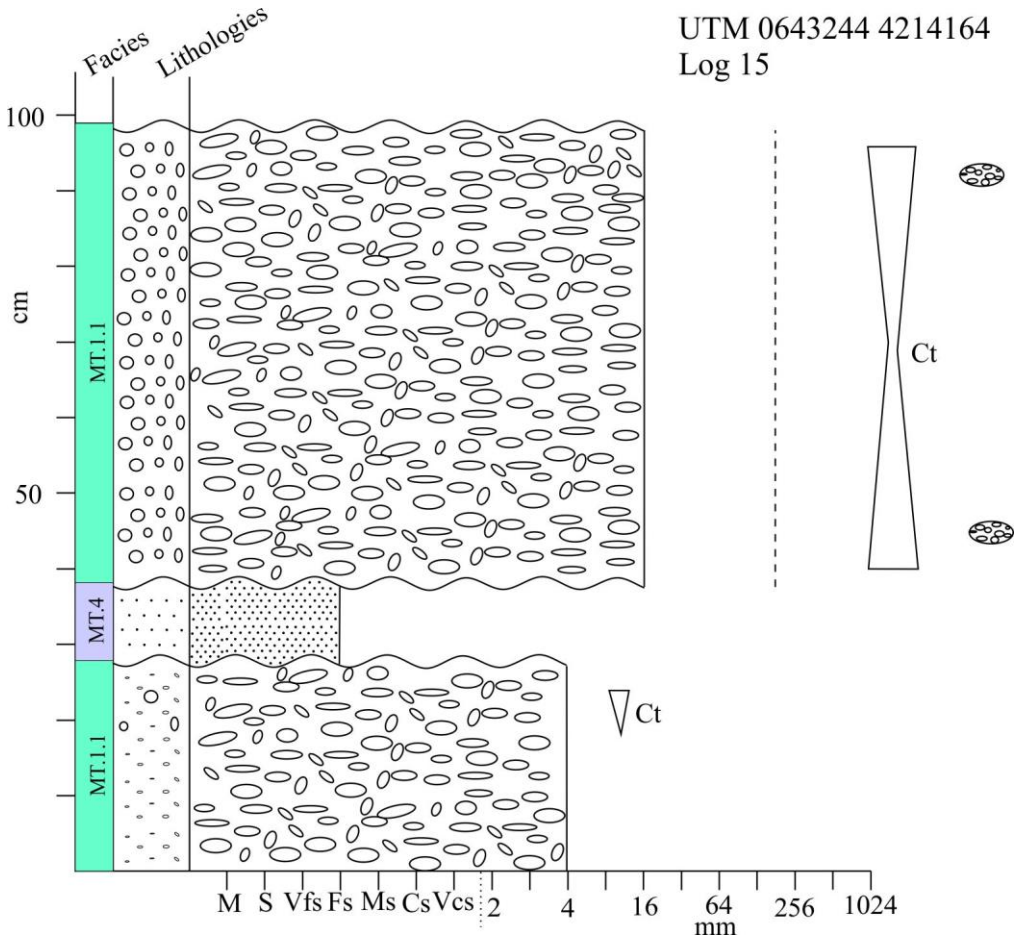
UTM 0643244 4214164
Log 15
Facies
Lithologies
100
50
cm
MT.1.1
MT.4
MT.1.1
Ct
Ct
M S Vfs Fs Ms Cs Vcs 2 4 16 64 256 1024
mm

UTM 0643998 4213329
Log 16

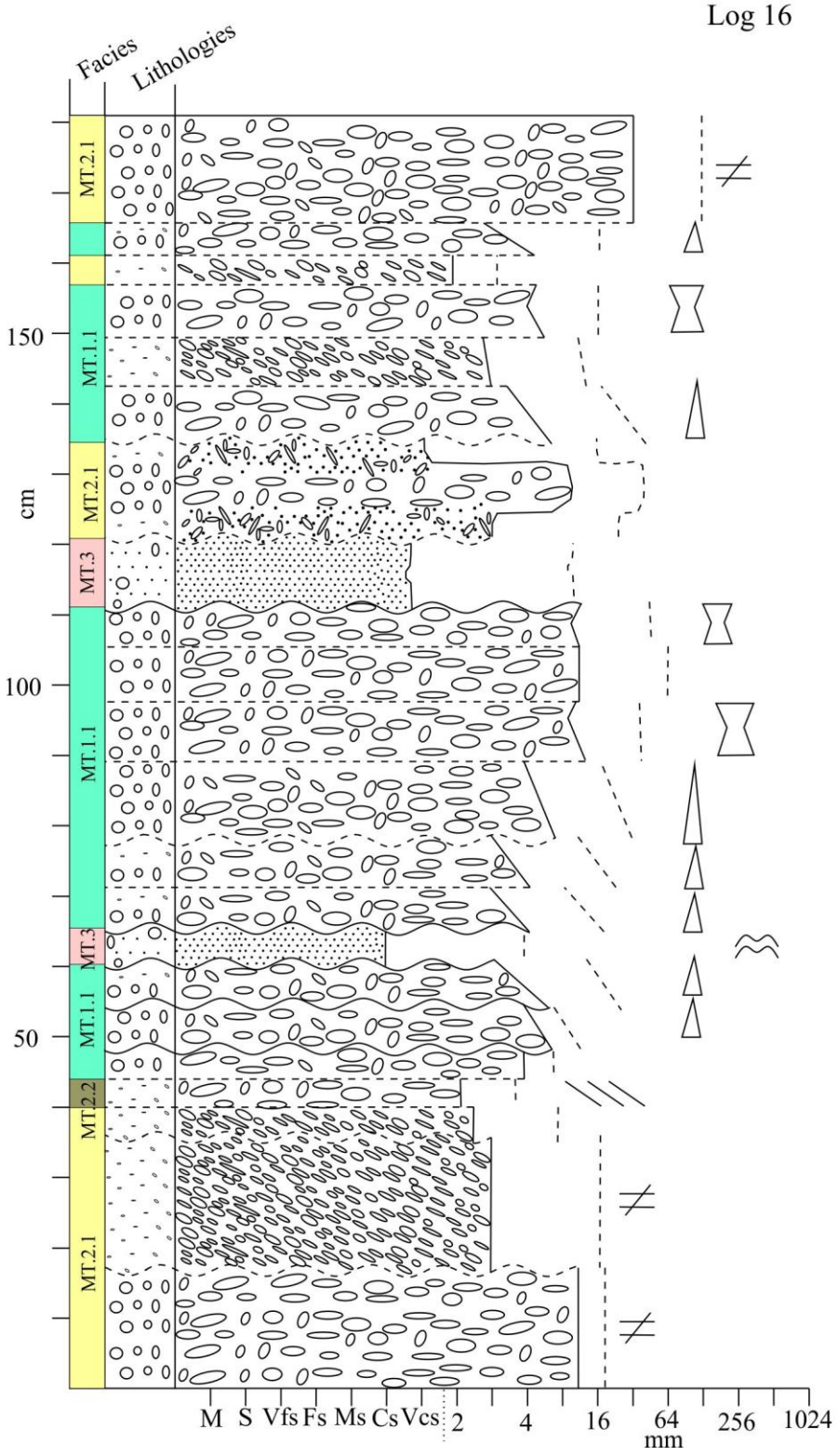

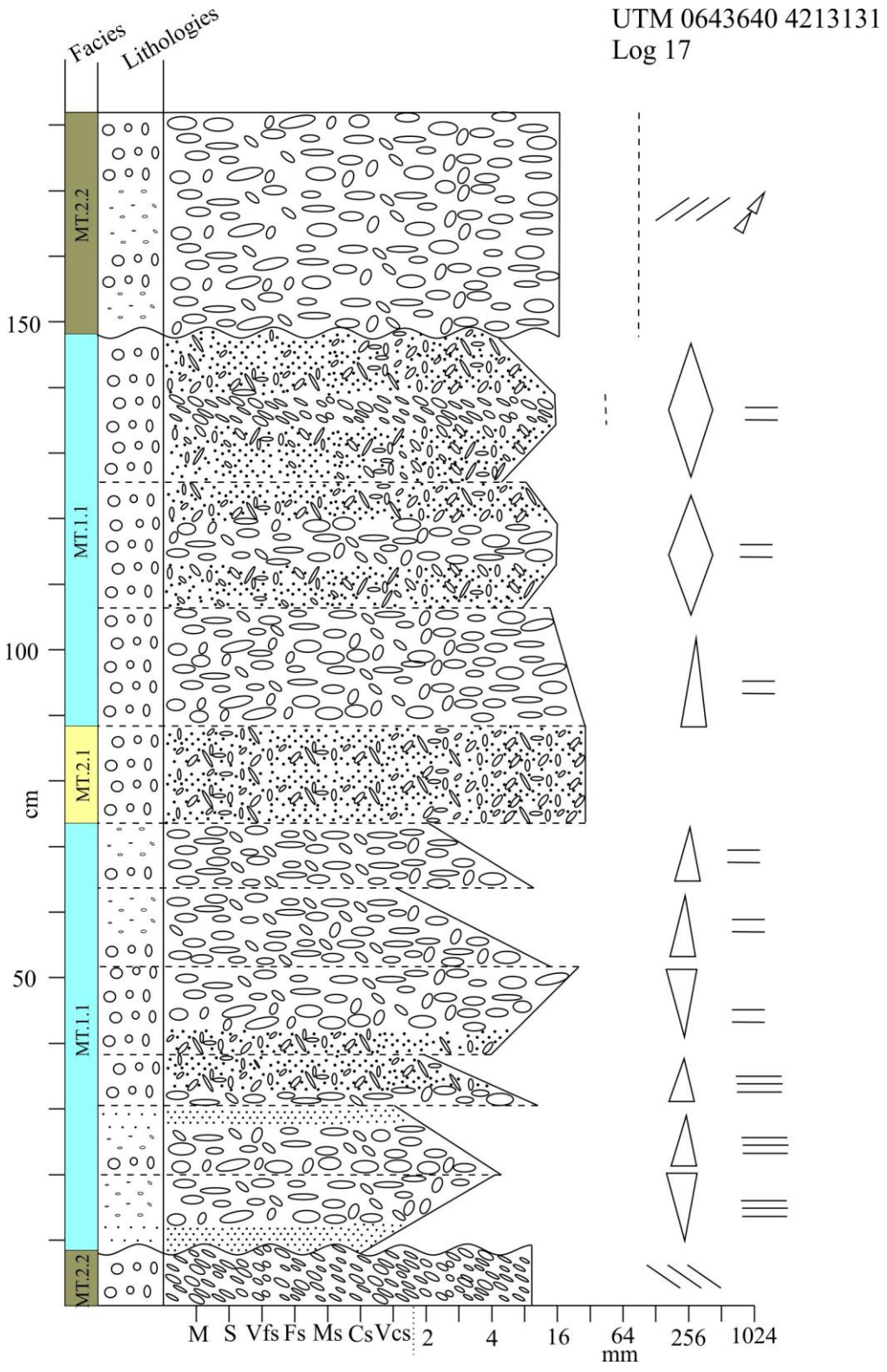
UTM 0643640 4213131
Log 17
Facies
Lithologies
MT.2.2
MT.1.1
MT.2.1
MT.1.1
MT.2.2
150
100
50
cm
M S Vfs Fs Ms Cs Vcs 2 4 16 64 256 1024
mm

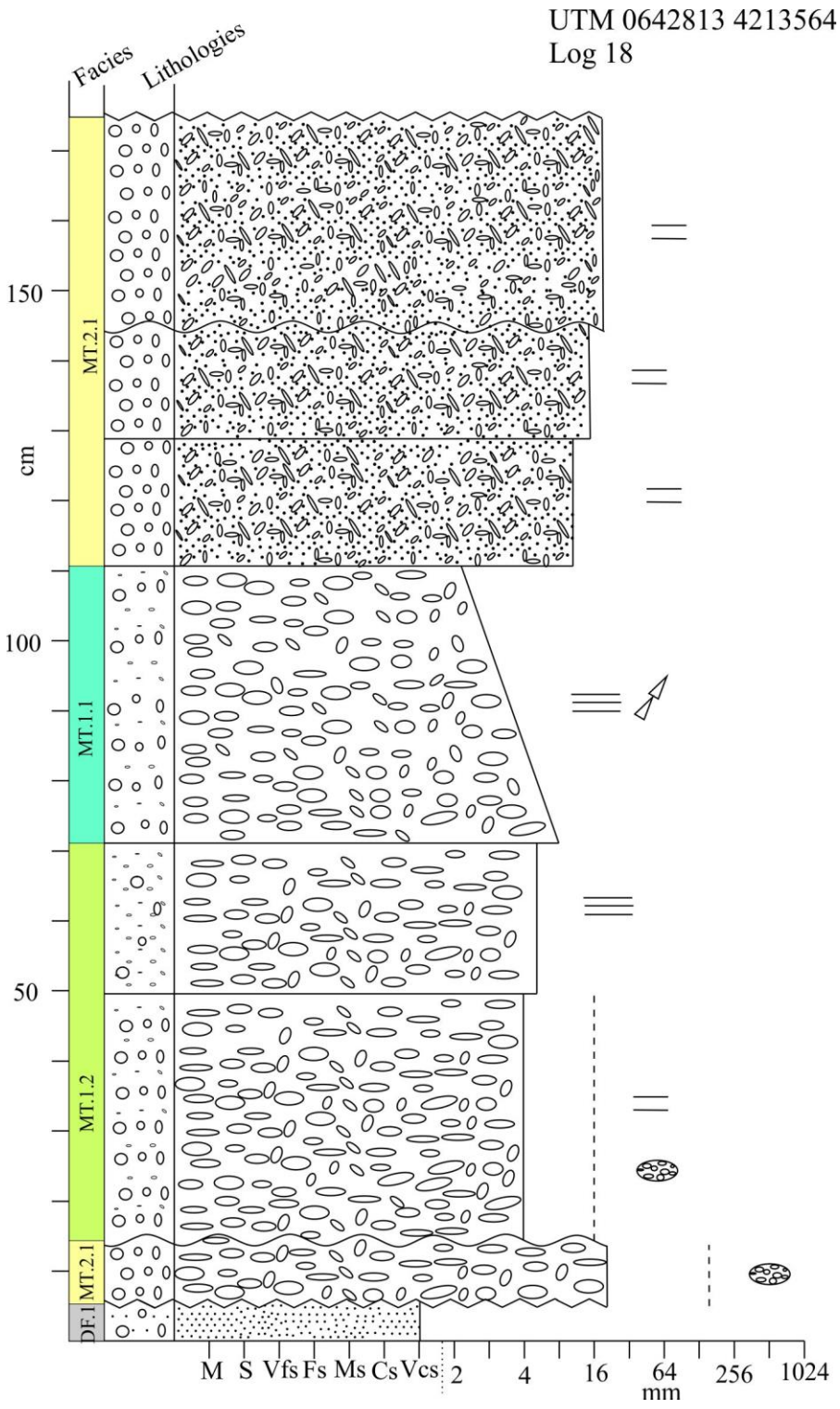
UTM 0642813 4213564
Log 18
Facies
Lithologies
150
cm
100
50
MT.2.1
MT.1.1
MT.1.2
MT.2.1
DF.1
M S Vfs Fs Ms Cs Vcs 2 4 16 64 256 1024
mm

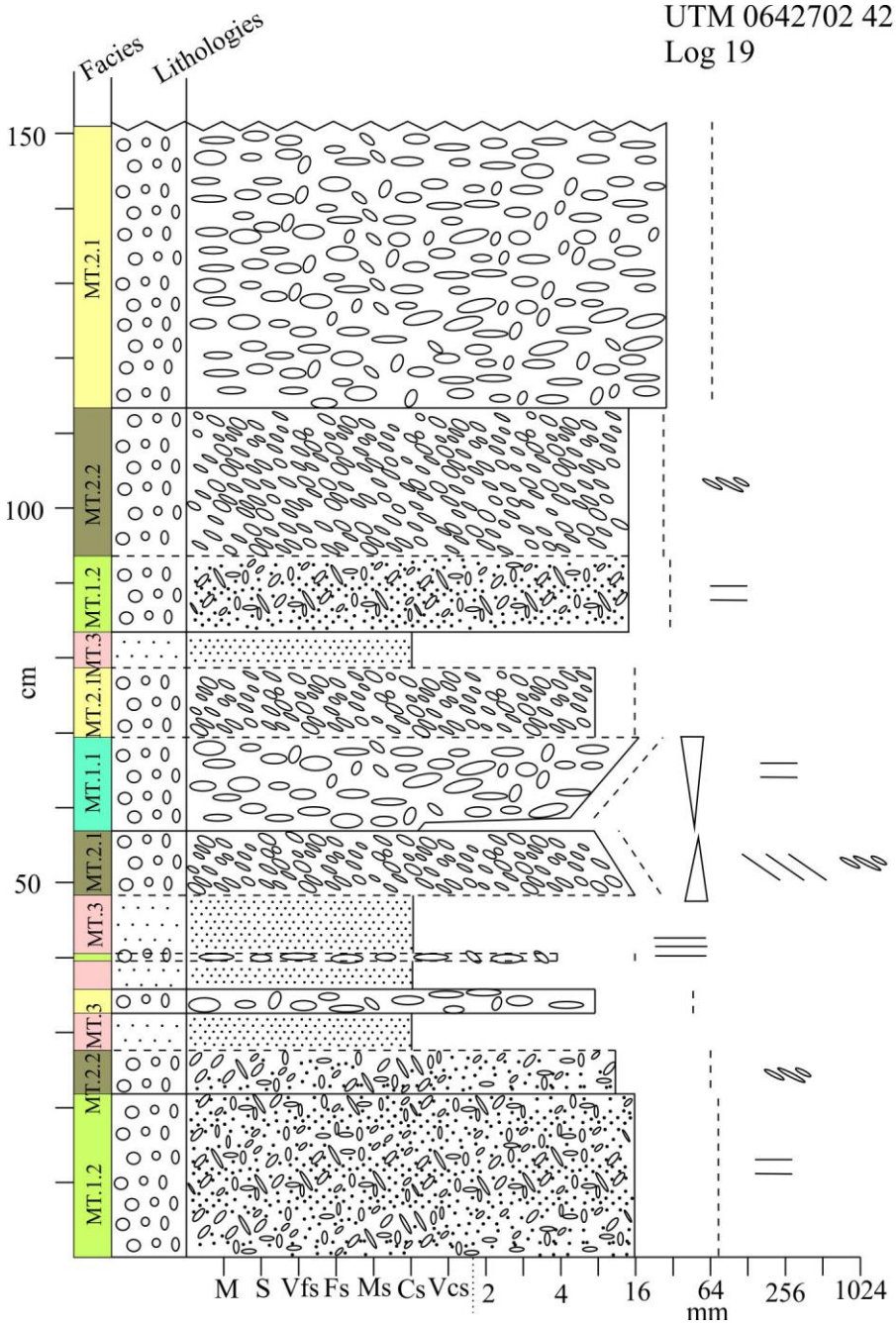
UTM 0642702 4213545
Log 19
Facies
Lithologies
150
100
50
cm
MT.2.1
MT.2.2
MT.1.2
MT.3
MT.2.1
MT.1.1
MT.2.1
MT.3
MT.3
MT.2.2
MT.1.2
M S Vfs Fs Ms Cs Vcs 2 4 16 64 256 1024
mm

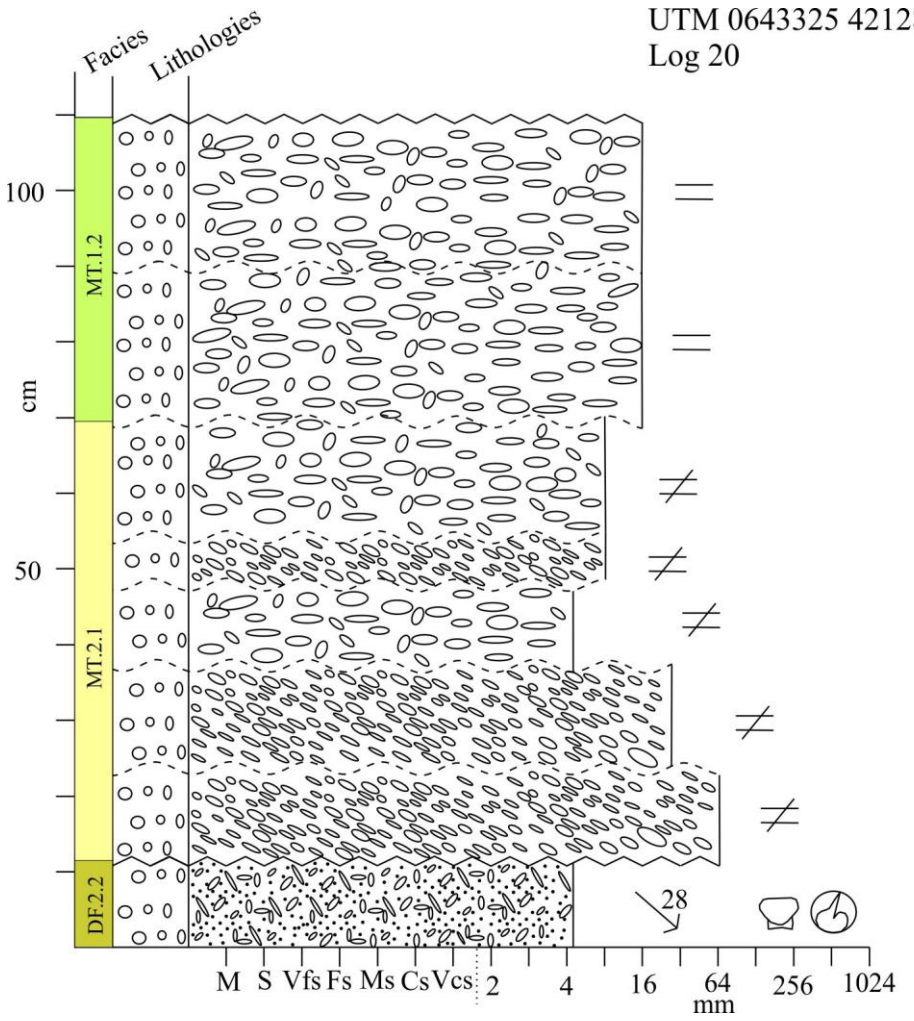
UTM 0643325 4212840
Log 20
Facies
Lithologies
100
50
cm
MT.1.2
MT.2.1
DF.2.2
28
M S Vfs Fs Ms Cs Vcs 2 4 16 64 256 1024
mm

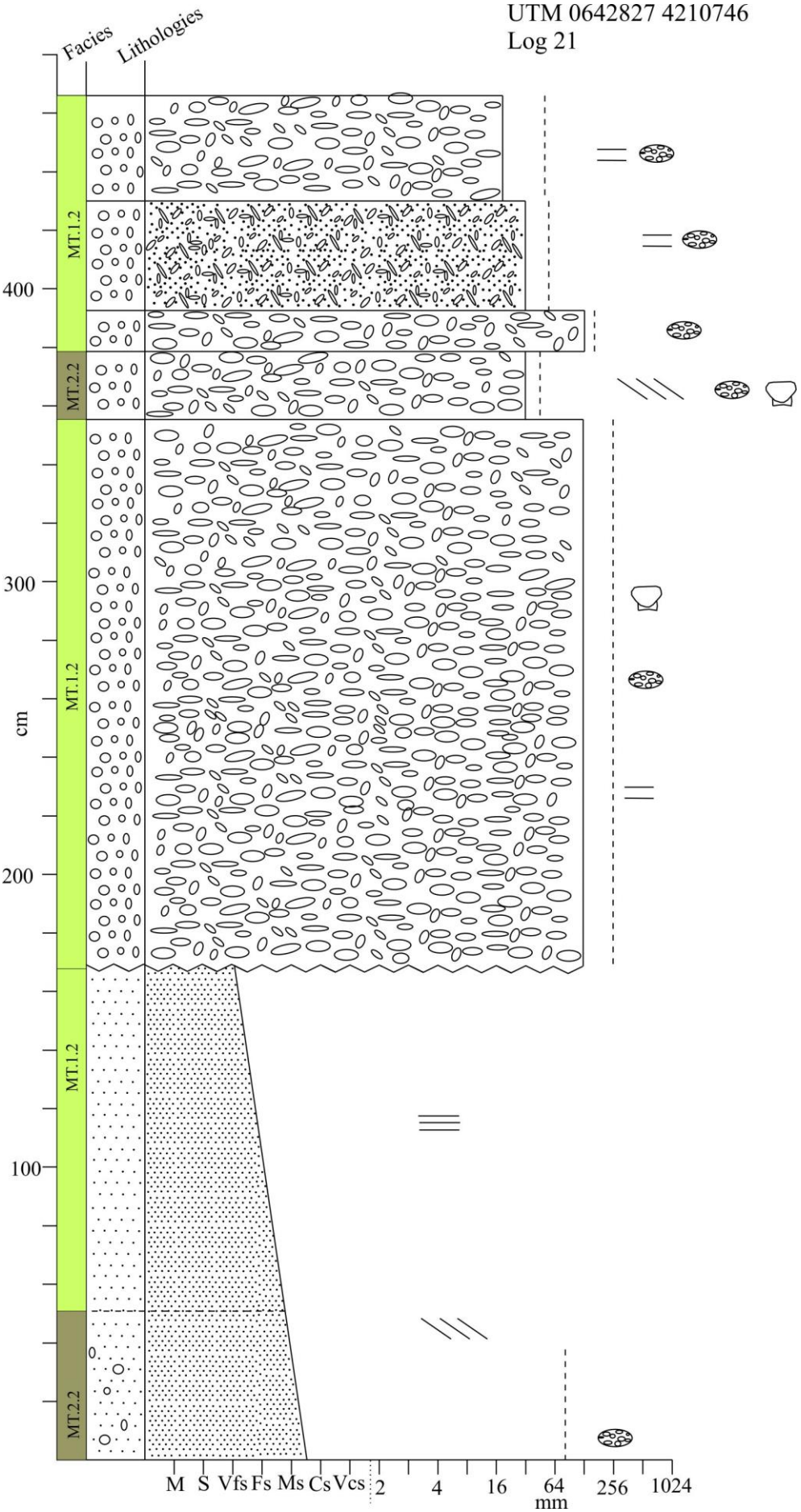
UTM 0642827 4210746
Log 21
Facies
Lithologies
MT.1.2
MT.2.2
MT.1.2
MT.1.2
MT.2.2
400
300
200
100
cm
M S Vfs Fs Ms Cs Vcs 2 4 16 64 256 1024
mm